

Editorial

Dear Readers,

Welcome to the second issue of Nijmegen CNS, the Proceedings of the Cognitive Neuroscience Master of the Radboud University. This journal, run entirely by students, was set up two years ago, leading to publication of the first issue in March 2006. The journal is an integral part of the Master's programme in Cognitive Neuroscience of the Radboud University Nijmegen, and reflects the research carried out by its students. The journal offers the students involved the opportunity to gain experience in writing, reviewing, editing and publishing. Furthermore, the journal, consisting of a hardcopy edition combined with an online version, functions as an archive of all theses written by the students enrolled in the Master's programme.



A new generation of Master's students was responsible for running and creating the journal you now see before you, thereby taking over from the previous editorial board. We highly appreciate the work done by our predecessors: the first board, headed by Jochen Hempleman and Jan Scholz, and advised by Peter Desain. We have learned a lot from these 'pioneers' and strive to continue the work they started.

The current issue contains four theses from recently graduated students. As the number of students within the programme grows, so does the number of submitted theses. After an extensive review and editing process, a selection was made from among the submitted theses for publication in the printed version of the journal. This selection was based on originality, quality and significance, and aims at reflecting the diversity of projects undertaken by our fellow students. Abstracts of all other theses can be found at the end of this printed edition. Furthermore, all theses, as well as the previous issue of this journal, can be found on our website: <http://www.cns.ru.nl/nijmegencns>.

Thank you for your interest in our work, and we hope you will enjoy reading this journal.

Best regards,

*Saskia Haegens
Editor-in-Chief*



From the Programme Director



It is a pleasure to introduce the second issue of Nijmegen CNS, the Proceedings of the Cognitive Neuroscience Master of the Radboud University. This archive of high-quality Master's theses reports the results of the research activities of Nijmegen CNS students following a critical reviewing process organized by the students themselves.

Cognitive Neuroscience is a fast-growing research domain encompassing many different disciplines. The papers published in the CNS reflect this multidisciplinary nature by covering areas such as biophysics, cognitive psychology, electrophysiology, neuroanatomy and psycholinguistics.

Another typical feature of the field is that a wide range of brain-imaging techniques is exploited in rigorous experimentation. The contributions in the present journal issue are indicative of that as well. The first study that is presented explores the potential of fibre-tracking techniques to capture visuomotor networks involved in eye-movement control. Given the limitations in either temporal or spatial accuracy of the currently available research methods in cognitive neuroscience, this is a vital development. In a second paper, functional-connectivity analyses are exploited to investigate the nature of verbal hallucinations in healthy people. It is interesting to see how neuroscientific research addresses such an intriguing clinical phenomenon in a straightforward manner. The third contribution reports the results of systematic analyses of event-related brain potentials (ERPs) in language comprehension in bilinguals. The report convincingly delineates the effects of semantic incongruencies when listening to one's native or an acquired language. The fourth paper that met the strict criteria for publication in this original student journal enters the field of social cognitive neuroscience. It examines the nature of ERPs that occur when two actors are engaged in a collaborative go/no-go reaction-time task. The study touches upon the intriguing question of how the other's behaviour is internally represented during this collaborative effort in comparison to the representation one forms when competing with one another.

This second issue of the Nijmegen CNS student journal clearly reflects the enthusiasm and professionalism of the student team running the journal and thus sets the standards for future research in the programme at a commendable level.

Dr. Ruud Meulenbroek

Programme Director of the Master's Programme of Cognitive Neuroscience

Table of Contents

About us.....	7
<i>Jan Scholz</i> DTI-based fibre tracking in the examination of visuomotor networks.....	9
<i>Kelly Diederer</i> Functional connectivity in healthy subjects with auditory verbal hallucinations.....	31
<i>Ian FitzPatrick</i> Effects of sentence context in L2 natural speech comprehension.....	43
<i>Stephan Miedl</i> The faster one has blinkers on: The role of co-representation in response inhibition and error detection.....	57
Abstracts.....	67
Institutes associated with the Master's Programme in Cognitive Neuroscience.....	72

Nijmegen CNS

Proceedings of the Cognitive Neuroscience Master of the Radboud University

Editorial Board

Editor-in-Chief

Saskia Haegens

Section Editor Perception & Action

Iris Grothe

Section Editors Neurocognition

Yaël Reymer

Henk Cremers

Section Editors Psycholinguistics

Kirsten Weber

Giovanni Piantoni

Layout

Xu Lu

Webmaster

Jeroen Geuze

Finances

Peter Hendrix

Assistant Editors

Sasha Ondobaka

Vivian Eijssink

Bernard Bloem

Christina Pawliczek

Assistant Layout

Anne van der Kant

Assistant Webmaster

Marlieke van Kesteren

Programme Director: **Ruud Meulenbroek**

Senior Advisors: **Peter Desain & Ben Maassen**

Journal Logo by: **Guido Cavalini & Iris Grothe**

DTI-based fibre tracking in the examination of visuomotor networks

Jan Scholz¹

Supervisors: Pieter Medendorp¹, David Norris¹

¹*F.C. Donders Centre for Cognitive Neuroimaging, Nijmegen, The Netherlands*

The ability to follow axonal tracts in white matter using diffusion tensor imaging (DTI) has existed for some years. Only very recently have research groups attempted to combine functional magnetic resonance data (fMRI) with tractographic data obtained with DTI. In this project we assessed the utility of DTI-based fibre-tracking for examining visuomotor networks in healthy human adults. We hypothesized that cortical pathways for oculomotor control can be mapped using a combined DTI-fMRI approach. We used a delayed-saccade task to map the topographic organization of the frontoparietal oculomotor system. Varying the polar angle of the peripheral target for a delayed saccade in a systematic fashion revealed several topographically organized areas in parietal and frontal cortices. Subsequently we attempted to determine anatomical connectivity of these regions, in particular the connections between the human analogues of monkey areas FEF and LIP, with several DTI-based fibre-tracking approaches. Each approach met with limited success.

Keywords: FEF, IPS, oculomotor system, saccades, fibre-tracking

Correspondence to: Jan Scholz, FMRIB Centre, John Radcliffe Hospital, Headington, Oxford OX3 9DU, UK; e-mail: jscholz@fmrib.ox.ac.uk.

1. Introduction

Over the past decades magnetic resonance imaging (MRI) and its specific applications, such as functional blood-oxygenation-level-dependent (BOLD) imaging (Ogawa et al., 1990), diffusion tensor imaging (for a review, see, Le Bihan, 2003) and the tracking of white matter pathways (for a review, see, Mori & Zijl, 2001) have become essential tools in the study of the functional and anatomical organization of the brain. Both methods – fMRI and DTI – have most often been used separately in the past. Functional MRI has been used to study functional networks isolated from the underlying anatomical connections and DTI to investigate white matter tracts without considering the specific functions of the brain areas they connect. Combining fMRI and DTI-based tractography, however, promises to reveal the structural basis of the functional connectivity *in vivo*. Instead of just adding up the information obtained from both modalities an integrative DTI-fMRI approach uses the functional information to constrain the tractography. Functional data lend themselves to define start and end points of the fibre-tracking process. This method has the advantage that one specifically investigates those fibres that connect regions activated due to a particular task or stimulus. Thus, it seems only natural to combine the independent and complementary information provided by both modalities – the functional activation and the anatomical connectivity – to form a much more comprehensive model of human brain functioning.

In the past, a combined DTI-fMRI approach has most often been applied to a clinical context, such as pre-surgical planning (Parmar et al., 2004; Schonberg 2006) and the investigation of diseases that alter the morphology of white matter tracts (Munakata et al., 2006). A survey of the literature revealed only one combined DTI-fMRI-fibretracking study that included healthy subjects as controls (Guye et al., 2003). The focus on clinical and small case studies is particularly interesting considering the potential wealth of information that such a multimodal approach can provide for neuroscientific research of normal brain functioning. In the present study we assess the utility of a combined DTI-fMRI approach in the context of the healthy adult brain. More precisely, we aim to reveal the functional and structural features of the human oculomotor system. The oculomotor system especially lends itself for this

approach, because it is well defined and has been shown to be similar between macaque and human species (Koyama et al., 2004). This correspondence will allow us to draw conclusions about the human oculomotor system on basis of macaque data acquired with methods unavailable for the human (e.g. anatomical tracers).

The primate oculomotor system involves, aside from subcortical components such as basal ganglia, thalamus, midbrain and cerebellum, a limited number of well defined cortical areas that are distributed over frontal and parietal cortices (Munoz, 2002). In the macaque the most important frontal components consist of the frontal eye fields (FEF) in the lateral prefrontal cortex and the supplementary eye fields (SEF) in the medial prefrontal cortex. The parietal cortex contains another major oculomotor area in the lateral bank of the intraparietal sulcus (IPS), the so-called lateral intraparietal area (LIP). In post mortem tracer studies, all of these areas have been shown to be anatomically connected in the monkey (Lewis & van Essen, 2000; Schall et al., 2004; Stanton et al., 1995). The putative human homologues of these areas have been suggested in the fMRI literature (Astafiev et al., 2003; Koyama et al., 2004, Sereno et al., 2001). The network of cortical oculomotor areas has been demonstrated to be similar between humans and non-human primates using fMRI (Astafiev et al., 2003; Koyama et al., 2004). The parietal cortex might constitute an exception to this rule. Schluppeck et al. suggested that several saccade-related areas can be found along the human IPS (Fig. 1), whereas only one oculomotor area has been found in the monkey.

Recently, various reports demonstrated that at least two of the cortical oculomotor regions are topographically organized in the human (Hagler & Sereno, 2006; Schluppeck et al., 2005; Sereno et al., 2001). Hagler & Sereno et al. (2006) showed that remembered saccade target location in contralateral visual space is systematically arrayed over a well defined region in the lateral prefrontal cortex. Sereno et al. found at least one region with similar topographic properties in the IPS. The connectivity of the human oculomotor system has not been determined so far.

In the present study we employ two experimental paradigms to reveal the cortical components of the human oculomotor system. A standard block design experiment in which blocks of saccades are contrasted with blocks of fixation will allow us to define the human homologues if monkey

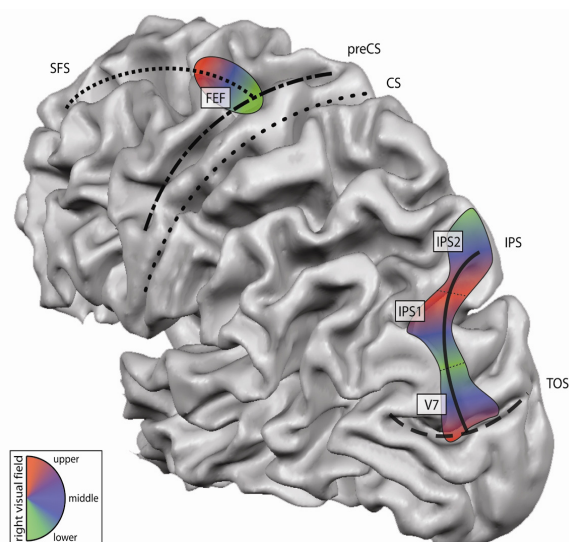


Figure 1. Topographic areas of the human oculomotor system in frontal and parietal lobes. The human oculomotor system comprises at least two major areas that include maps of remembered saccade target locations of the contralateral visual field: the frontal eye field (FEF) and areas along the IPS, such as IPS1 and IPS2. The colour map represents the phase angle of the remembered saccade targets (red, upper right visual field; blue, right horizontal; green, lower right). Retinotopic visual areas are usually coactivated during saccade tasks. Except for V7 they are not shown here for clarity. (CS = central sulcus; IPS = intraparietal sulcus; preCS = precentral sulcus; SFS = superior frontal sulcus; TOS = transoccipital sulcus)

FEF and SEF with high statistical power. A second phase-encoded paradigm will allow us to map the topographic organization of the fronto-parietal regions. In a phase-encoded paradigm spatially-specific stimuli are presented in a systematic and periodic fashion in order to successively activate the entire visual field representation. If multiple joined regions exist along the IPS, the phase-encoded paradigm will have the additional benefit of distinguishing different areas according to the orientation of the visual field representation (Fig. 1). Successfully identified oculomotor regions are then used as seed and target regions for fibre-tracking of the cortical pathways of the visuomotor system

We hypothesize that, similar to the monkey, connections between oculomotor regions in the frontal cortex and oculomotor regions in the parietal cortex exist in humans (e.g. between FEF and IPS), which can be revealed with a combined fMRI-DTI approach. To achieve this objective we will first map the human saccade-related areas using a delayed saccade task in a block design

and a phase-encoded experiment. Second, we will use the functional data to constrain the fibre-tracking, in order to reveal the connectivity of the human oculomotor system. Several different fibre-tracking procedures, such as standard streamline tracking and probabilistic tracking will be used and evaluated. Third, we will investigate whether the fibres connect regions which represent the same part of the visual field. This will give us a more fine grained view at the connectivity and reveal whether the topography of visuomotor regions is sustained by the topography of the connecting fibre tracts while simultaneously being a benchmark for the accuracy of the combined fMRI-DTI approach.

The remainder of this introduction will explain the background of the methods employed. This includes an in-depth explanation of diffusion image acquisition, diffusion models, and fibre-tracking. We will close the introduction with a comment on the limitations associated with DTI-based fibre-tracking.

2. Diffusion tensor magnetic resonance imaging (DT-MRI)

2.1 Introduction to DT-MRI

Diffusion tensor magnetic resonance imaging, abbreviated as DT-MRI or just DTI, allows us to study white matter connections between different parts of the brain noninvasively (for a review, see, Bammer et al., 2003). More precisely, DTI refers to the production of MRI-based quantitative maps of microscopic, natural displacements of water molecules that occur in brain tissues as part of the physical diffusion process. The natural displacement of water molecules is systematically affected by tissue structures. The resulting anisotropic diffusion is hypothesized to reflect the organization and orientation of white matter fibre bundles (Beaulieu, 2002). This local information can be used to globally reconstruct axonal tracts (Mori & Zijl, 2002).

The following sections will briefly describe the diffusion imaging process and the relationship of the diffusion weighted images (DWI) to the underlying white matter structure and how this data can be modelled to further the fibre-tracking process. We will end this chapter with a discussion of the problems associated with data acquisition, model, and tracking.

2.2 Data acquisition and diffusion models

Diffusion weighted imaging is based on the fact that molecules perform random translational movements due to the thermal energy they carry. The random displacement of molecules in a free medium (Brownian motion) can be described by a three-dimensional Gaussian distribution and depends on the molecules' mass, the temperature and the medium's viscosity.

Formally, an unrestricted diffusion process is described by the so-called diffusion coefficient, D , which is related to the root mean square displacement (RMSD) of freely diffusing molecules over time t_{dif} by $\text{RMSD} = (6 D t_{\text{dif}})^{1/2}$. The diffusion coefficient measured by nuclear magnetic resonance is known as the apparent diffusion coefficient (ADC). It is not only dependent on the actual diffusion coefficient of the water molecule population present in the voxel, but also on flow and transfer phenomena as well as on experimental parameters, such as the voxel size.

During typical diffusion times of about 50 to 100 ms, water molecules have a high probability of interacting with tissue components, such as the

cell membranes or the cytoskeleton. If molecular displacements are no longer uniform in space (i.e. isotropic), diffusion is called anisotropic (i.e. directionally dependent). Consequently, diffusion is no longer sufficiently characterized by a scalar ADC. Instead a symmetric second-order tensor, called the apparent diffusion tensor \mathbf{D} , is used to approximate the distance and the direction of the diffusing water molecule population. The diffusion tensor can be represented by an ellipsoid (Fig. 2, I). Main, medium, and minor axes of the ellipsoid correspond to the tensor's eigenvectors e_1 , e_2 , e_3 and the respective eigenvalues λ_1 , λ_2 , λ_3 . The eigensystem is conventionally ordered according to the size of the eigenvalues ($\lambda_1 \geq \lambda_2 \geq \lambda_3$).

Evidence suggests that the tightly packed parallel arrangement of multiple axon membranes and to a lesser degree their myelin sheaths cause the observed anisotropy in white matter by hindering water diffusion perpendicular to the long axis of the fibres relative to the preferential parallel direction (Beaulieu, 2002). If this assumption holds true, it would in principle be possible to infer local fibre direction by measuring water diffusion along different directions. Because magnetic

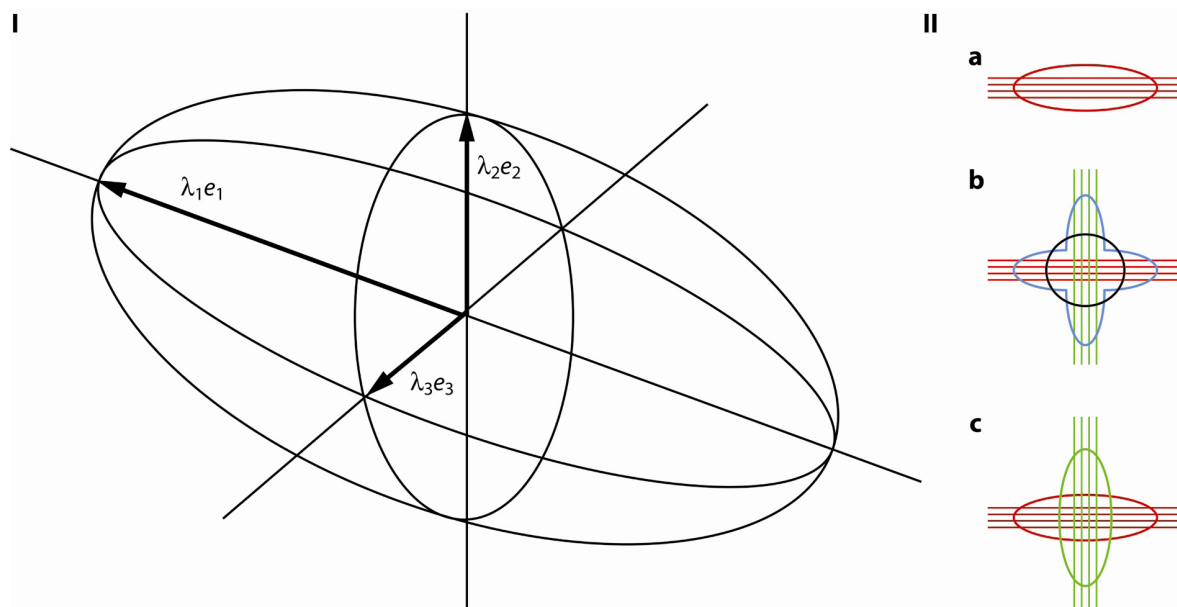


Figure 2. (I) Three-dimensional probability function of anisotropic diffusion depicted as an ellipsoid. The arrows point along the eigenvectors (e_1 , e_2 , e_3) and are scaled proportionally by their corresponding eigenvalues (λ_1 , λ_2 , λ_3). The eigensystem is conventionally ordered so that $\lambda_1 > \lambda_2 > \lambda_3$ holds true. Anisotropic diffusion is characterized by $\lambda_1 > \lambda_2 > \lambda_3$ and isotropic diffusion by $\lambda_1 \sim \lambda_2 \sim \lambda_3$. (II) Single and two-tensor models in the case of one or two crossing fibre populations. (IIa) illustrates that a single-tensor is a good local approximation of uniformly oriented fibres (i.e. the overall diffusion process occurring in intra- and extracellular compartments at this location). (IIb) shows that the single-tensor model fails if multiple fibre directions are present within one voxel. The model represents neither of the fibre populations correctly (black circle). The actual diffusion process more closely resembles the blue shape. In (IIc) two well-distinguishable fibre populations are quite accurately modelled by two tensors.

resonance measurements of diffusion are sensitive to molecular displacements along the axis of the diffusion-sensitizing gradients, diffusion along different directions can be evaluated by varying the orientation of the diffusion-sensitizing gradients. At least six different directions are required to characterize the diffusion tensor. Measuring a large number of directions (30-90) reduces signal-to-noise dependence on directions and increases the angular resolution needed to separate crossing fibres.

2.3 DTI-based fibre-tracking

The aim of the fibre-tracking process is to link the local tensor information in such a way that the resulting “virtual” fibres match the underlying neuroanatomy and/or connection probability between different regions can be inferred. There are in principle two different classes of tracking algorithms: deterministic tracking and probabilistic tracking. Both work with but are not exclusive to

the tensor model. Deterministic tracking is a subset of probabilistic tracking. It is deterministic in the sense that repeated tracking, starting from the same location, will always follow the same path (Fig. 3, Ia,b). In contrast, probabilistic tracking tracks also less likely directions, determining from each voxel's diffusion profile the likelihood of a certain fibre direction in that voxel (Fig. 3, Ic). In the following, both types of fibre-tracking approaches and their limitations are described in more detail.

One of the most common classes of deterministic tracking methods is the so-called line-propagation technique, such as the streamline algorithm known from flow computations (see, e.g., Basser et al., 2000; Mori & Zijl, 2002). It consists of three parts: seed point selection, fibre propagation and termination. Seed points are specified by a region of interest (ROI) which can be generated on the basis of anatomical or functional data. Usually more than one streamline is seeded per voxel. The fibre is then propagated through the tensor field assuming that the normalized first eigenvector (e_1),

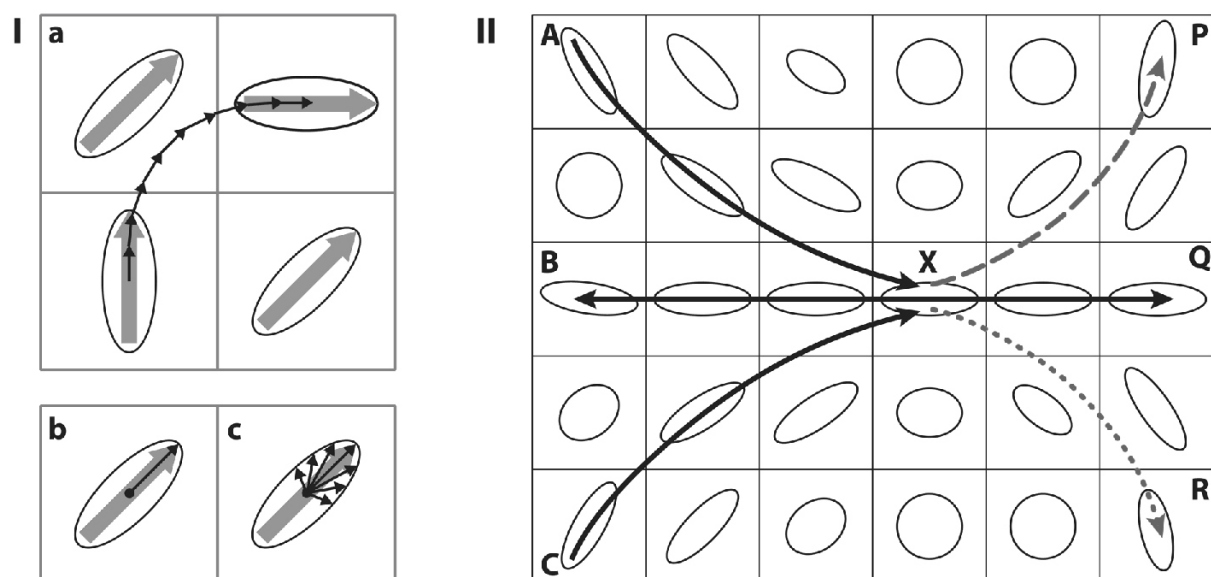


Figure 3. Schematic diagram of the fibre-tracking process and its limitations drawn in two dimensions. In (Ia) fibre-tracking is initiated in the lower left voxel. Ellipses represent a set of sampled diffusion tensors. Large arrows represent the orientation of the major eigenvectors. A fibre is propagated in a stepwise fashion through the interpolated tensor field (small black arrows). Often step sizes smaller than the voxel size are used to achieve higher accuracy. Below, the difference between deterministic (Ib) and probabilistic tracking (Ic) is illustrated. For multiple transitions of the same voxel identical directional information is used during deterministic tracking. For probabilistic tracking the directional information can vary between multiple transitions of the same voxel. (II) shows principle limitations of deterministic fibre tracking algorithms. First, the tracking is non-commutative (Dougherty et al., 2005). Fibres starting in A, B, and C will all converge onto a common point Q. But seeding Q will result in one fibre connecting only Q with B. Second, tracking is problematic in regions of crossing and kissing fibres. As soon as fibres seeded in A, B, and C have reached point X they will be propagated further up to point Q. The underlying neuroanatomy might, however, be different. The fibre starting in A might just kiss fibre BQ in X and continue to P or it might cross BQ at X and continue to R.

which is associated with the largest eigenvalue (λ_1) of the diffusion tensor, lies in parallel to the local fibre tract direction (Bammer et al., 2003).

Higher-order integration schemes, such as the fourth-order Runge-Kutta method, are used to determine the direction of the streamline propagation. These integration schemes require repeated tensor interpolation to derive a tensor at an arbitrary position. This allows for sub-voxel step sizes which increase the overall accuracy of the tracking (Fig. 3, Ia). The propagation continues until a stopping criterion is reached. This can either be a threshold based on fractional anisotropy (FA) or curvature. The former case represents the situation where no clear directionality is defined anymore and the latter the situation where the fibre follows a sharp bend that is assumed to be anatomically implausible.

Most probabilistic tracking approaches are very similar to deterministic line-propagation approaches. They include seed points, line-propagation, and stopping criteria, but differ in three important ways. First, multiple, often thousands of lines are propagated from each point and, second, the directional information used for the line-propagation is varied non-deterministically from pass to pass. Third, the output consists of a map that represents the probability of connection between seed and target points (Fig. 8, G, H). A deterministic line-propagation algorithm will only reveal whether there is a connection or not¹.

Probabilistic tracking is achieved by utilising the Monte Carlo method. Starting from the same point fibres are propagated multiple times through the tensor field while varying the estimated fibre orientation in the traversed voxels in a stochastic way. The estimated fibre orientation is not completely random but determined by the voxel's probability density function (PDF). The PDF describes the local uncertainty in fibre orientation. There are several ways to define these PDFs. The most straightforward is to interpret the tensor shape as a probability distribution (Koch et al., 2002) (Fig. 3, Ic). The process is equivalent to letting a particle diffuse through the tensor field with the probability of a jump in a particular direction from a given voxel being based on the voxel's PDF. This approach has the advantage that if the local tensor is indeterminate (i.e. disc- or sphere-like) several

possibilities will be explored, instead of just heading into a “random” direction. In other words, while deterministic tracking tries to eliminate the inherent noise in the data and find the one “true” fibre direction, probabilistic tracking takes into account the inherent ambiguity of the underlying diffusion imaging data, in the sense that it tries to interpret the data in terms of the likely underlying fibre structure.

In summary, probabilistic tracking can be seen as a superset of deterministic tracking. It combines the basic ingredients of deterministic line-propagation algorithms with the Monte Carlo method. While deterministic streamline tracking yields “virtual” fibres similar in appearance to real fibre tracts, probabilistic tracking makes explicit use of the ambiguous diffusion data to track also in less probable directions. However, the probability maps, produced by the probabilistic approach, are often diffuse and require further interpretation.

2.4 Limitations of DTI-based fibre-tracking

There are basically three possibilities for fibre tracking to fail: data, model, and the tracking itself. The data might prevent the tracking of certain fibre pathways because its resolution is too low or due to noise and distortions. Standard diffusion protocols have a resolution of 1.5 to 3.0 mm³. This is far removed from the dimensions of myelinated axons in the central nervous system, which have a diameter of roughly 2.5 μ m (Alexander, 2006), so that any cubic millimetre of white matter is traversed by about 10⁵ axonal fibres. Aside from the averaging of fibres with different orientations within a voxel, one can expect partial volume effects between different tissue types (e.g. grey/white matter, cerebrospinal fluid). Ultimately, this means that the sampled diffusion profile will no longer accurately represent the underlying fibre structure. Distortions can also hinder fibre tracking. Especially in deeper brain areas and near aerial cavities, magnetic susceptibility artefacts produce large distortions. Eddy current distortions can be partially corrected for (Jezzard and Balaban, 1995). Noise in the data affects the reliability with which multiple fibre directions within a voxel may be resolved, especially at small angular separations. Regularization or averaging of multiple sets of diffusion weighted data can help to reduce the noise in the data.

The modelling process takes centre stage in DTI-based fibre-tracking. On the one hand the

¹ It is possible to define a quasi-probability of connection for a deterministic fibre-tracking approach by calculating the ratio between all fibres leaving a certain area and the number of those hitting the target area.

model is limited by the quality of the data, on the other hand the model limits the fibre-tracking process. The single-tensor model assumes that water diffusion is Gaussian. While this holds in cases where all fibres in a voxel are oriented in parallel, it is a poor approximation where fibres cross, diverge, or have high curvature. Therefore, the single-tensor model can resolve only a single fibre orientation within each voxel. Tracking through regions of crossing fibres can be improved by fitting different models, such as the q-ball model (Tuch, 2004) or increasing the number of tensors fitted per voxel (Fig. 2, IIc). It should however first be determined if the quality of the data allows advanced diffusion models. If the angular resolution is too low (i.e. the number of imaged directions is small), fitting more than one tensor will hardly improve the tracking. On the contrary, tracking results might even deteriorate, because the multi-tensor models are more susceptible to noise. In practice, q-ball and multi-tensor models can represent more than one fibre population per voxel, but the quality of the data often limits them to represent no more than two fibre populations per voxel.

The tracking itself can encounter multiple problems, because it basically tries to follow a continuous tract through noisy, discrete DT-MRI data. Interpolation and propagation are prone to errors at discontinuities and singularities in the tensor field. The well known “crossing and kissing fibres”-problem can lead to erroneous tracts (false-positive) or might miss tracts (false-negative). Fibre tracking is especially challenging near the cortical surface where the previously large and consistently organized white matter tracts tend to be more dispersed and anisotropy values lower (Mori & Zijl, 2002).

A general problem of today’s fibre tracing methods is their validation. Well-defined probabilistic tracts usually indicate low uncertainty in fibre orientation, while diffuse or dispersing tracts reveal noise or problems with the diffusion model. But this is a highly subjective assessment. It has been suggested to cross-reference the results with known anatomy or animal models. However, these might be incomplete or false. To date, it is therefore not possible to classify tracts as likely true positive or false positive *per se*. Particularly, finding no connection does not necessarily indicate that the tract is absent in the anatomy.

In summary, DTI-based tractography is limited compared to tracer injection techniques that can be used in nonhuman animals or post mortem

in humans (Bürgel et al., 2006). It can reveal the global course of white matter fibres only indirectly and it cannot determine the cortical layer in which they terminate. Fibre tracking is especially difficult through regions where the distribution of fibre direction is nonuniform (i.e. where fibres branch, cross or kiss). Probabilistic fibre tracking can often provide a quantitative estimate of connection probability between some of the regions which show no connection in standard streamline tracking. However, interpretation of probabilistic tracking is often difficult, especially when the resulting probability maps are diffuse and widespread. Scanning at higher spatial resolution, imaging more directions, and using advanced imaging and modelling techniques can help to avoid some of the problems, but might still fail in regions with crossing and branching fibres and near the cortical surface. Despite these difficulties DTI-based tractography has enabled us to reveal major white matter tracts of the human brain in vivo (Wakana et al., 2003) and classifying brain structures according to their connectivity (Behrens et al., 2003a; Crosson et al., 2005).

3. Methods

3.1 Subjects

Six healthy subjects (two female; four male; age range, 22-36) participated in the experiments. All had normal or corrected-to-normal vision and gave written informed consent. All subjects completed one scanning session.

3.2 Stimuli and Task

Stimuli were presented using an LCD projector (EIKI LC-X986; 60 Hz; resolution, 1024×768) onto a back-projection screen at the rear-end of the scanner. Subjects viewed the screen indirectly via a 45°-tilted half-silvered mirror above the eyes. Presentation software (Neurobehavioral Systems, Albany, CA, USA) was used for stimulus presentation. An eyetracker (MEyeTrack, SMI, Berlin, Germany) which was situated at the foot end of the patient table recorded eye movements via a second 45°-tilted mirror, which was mounted above the first. Eye movements were recorded to confirm behaviour. Subjects were supine and could comfortably see the whole range of projected stimuli (maximum eccentricity, 11.5°).

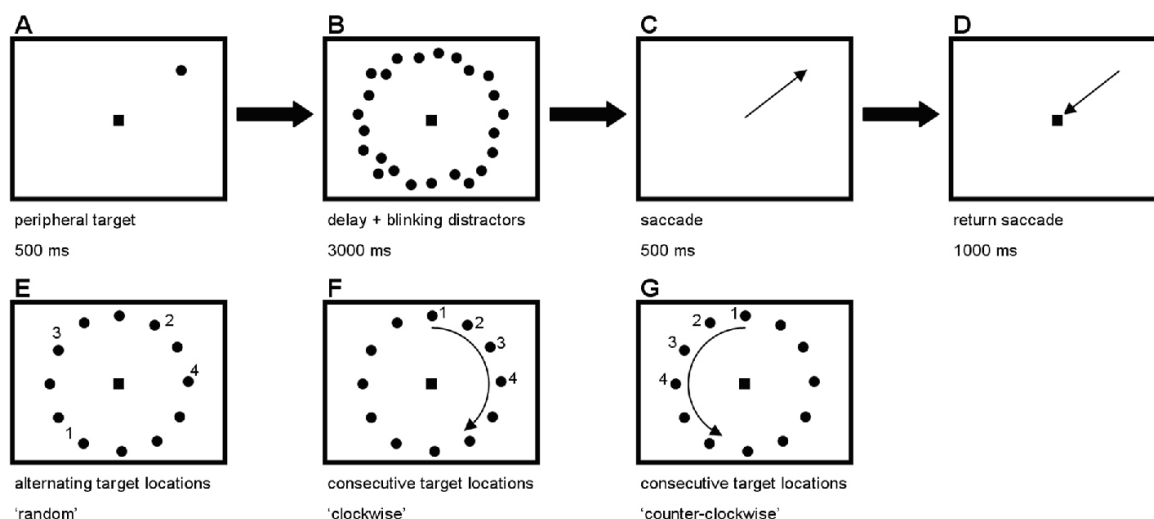


Figure 4. Visual stimuli. The first row (A-D) illustrates the visual stimuli shown to the subject during one trial of 5 s. The second row shows how target position varies between successive trials. During the random saccade task targets appear randomly at one out of 12 possible positions on the target circle (E). During the phase-encoded task targets occur at consecutive positions. More precisely, if during the first trial the target was presented at position one, then the target would be presented at position two in the second trial and so on (F, G). Target always advance in clockwise (or counter-clockwise) direction for five whole circles before the direction is changed to counter-clockwise (or clockwise).

Subjects had to perform a delayed saccade task which was incorporated in two different test paradigms. In each paradigm a target appeared on a circle with 10° eccentricity (eccentricity jitter, $\pm 1.5^\circ$) at one out of 12 possible locations which were separated by 30° , similar to the position of full hours on a clock-face (Fig. 4, E). Target angle was jittered by $\pm 5^\circ$ to make the target location less predictable. Each trial started with the presentation of the peripheral target for 500 ms, while subjects fixated a central point (A). Then a ring of 200 random, target-sized distractors (eccentricity jitter, $\pm 1.5^\circ$) flashed (at 5 Hz) for 3000 ms, while the subject maintained fixation (B). After the disappearance of the distractors and the fixation spot, subjects made a quick saccade to the remembered target location on a black screen (C), followed by an immediate return saccade to the reappearing fixation spot, which subjects continued fixating in preparation of the next trial for 1000 ms (D). Each trial lasted 5 s.

The delayed-saccade task was incorporated in two test paradigms. During the first paradigm, the random saccade paradigm, target position was varied randomly (G) from trial to trial. Blocks in which six saccades had to be executed alternated with blocks of central fixation. The length of both blocks was 30 s. Altogether there were 20 blocks. After 10 blocks there was a break of 45 s during which subjects could freely move their eyes and

blink. This paradigm lasted 10 min and 45 s.

In the second paradigm, the phase-encoded paradigm, target position was varied consecutively between trials. In the clockwise condition, the target would appear at 12 o'clock during the first trial and then at 1 and 2 o'clock during the second and third and so on (F). In the counter-clockwise condition, target positions were 12, 11, and 10 o'clock during the first three trials (G). Five cycles of clockwise target progression alternated with five cycles of counter-clockwise target progression. Each cycle required 12 saccades. Blocks of five cycles were separated by breaks of 45 s. The whole second paradigm lasted 45 min and 25 s.

3.3 MRI scanning procedure

All experiments were performed using a 3T Trio whole body scanner (Siemens, Erlangen, Germany). An eight-channel headcoil was used for signal reception. Subjects were stabilized with foam padding.

For each subject we acquired 36 axial slices using a standard gradient-echo EPI sequence (repetition time (TR), 2500 ms; echo time (TE), 35 ms; inversion time (TI), 1100ms; matrix size, 64×64 ; field of view (FoV), 192 mm; isotropic voxels, 3.0 mm; distance factor, 10%)

For each subject we acquired an additional 65 diffusion weighted images using a twice-refocused

spin echo diffusion sequence (Reese et al., 2003) (50 axial slices; TR = 6100 ms; TE = 87 ms; matrix size = 64×64 ; FoV = 192 mm; isotropic voxels, 3.0 mm, scan time: 6:43 min). These included five images with no diffusion weighting (b -value = 0 s mm²) and 60 diffusion-weighted images (b -value = 1000 s mm²) along 60 non-collinear directions (Jones et al. 1999). The signal-to-noise ratio in the diffusion weighted images was approximately 20. Resolution and position of the diffusion weighted images was chosen to match the functional protocol in order to minimize differences in distortions between the two protocols.

Finally, a high resolution structural image was collected using a standard T1 MPRAGE sequence (176 sagittal slices, TR = 2300 ms, TE = 3.93 ms, matrix size = 256×256 , FoV = 256 mm, voxel size = 1.0 mm³, scan time: 9:50 min). This image served as an anatomical reference for the functional data.

3.4 Data analysis

3.4.1 Pre-processing of functional and diffusion data

Functional MRI data were processed using BrainVoyager QX 1.4 software (BrainVoyager QX, Brain Innovation, Maastricht, Netherlands). Data from the first 10 s of each fMRI scan were discarded. Pre-processing of the remaining data included 3D motion correction, slice scan time correction, linear trend removal, and high-pass filtering.

DTI data were processed using SPM (Wellcome Department of Cognitive Neurology, Institute of Neurology, London, UK) and the Stanford VISTA software (<http://white.stanford.edu/software/>) executed in Matlab (Mathworks, Natick, MA). Basic pre-processing included coregistering all images to the first b_0 -weighted image and skull stripping with BET (part of the FSL package; Smith, 2002). Advanced processing included the calculation of tensors maps and fractional anisotropy maps. Finally, deterministic streamline fibre-tracking was performed with VISTA. For comparative purposes, probabilistic tracking was done using the method proposed by Koch et al. (2002). In addition, we performed the advanced processing part with the Camino software package (Cook et al., 2006), to visualize tensor maps and perform two-tensor deterministic streamline tracking.

Anatomical images were transformed into Talairach space, segmented at the gray-white matter

boundary and inflated for visualization purposes. Finally, pre-processed functional and diffusion data were coregistered to the high resolution anatomical image to establish a common coordinate space.

3.4.2 Statistics: fMRI

Statistical analysis of the functional data was performed using BrainVoyager QX 1.4 software. The data of the random saccade paradigm were analysed with a single study general linear model (GLM) for each subject separately. Two regressors were defined, one for saccade blocks and one for fixation blocks. The box-car-shaped regressors were convolved with a two-gamma haemodynamic response function (HRF) with a time to response peak of 5 s (time to undershoot peak, 15 s; response undershoot ratio, 6). We contrasted the saccade condition with the fixation condition and plotted the t -values on the inflated brain surface.

The data of the phase-encoded paradigm were analysed per subject using a box-car function convolved with a one-gamma HRF (delta, 2.5; tau, 1.25; n , 3) (Boynton et al., 1996). The HRF was shifted by TR (2.5 s) so that 12 shifts would cover exactly one visual hemifield (30 s). Significantly activated voxels for each lag were colour-coded for lag time (i.e. visual angle of target location). The resulting linear correlation maps for clockwise and counter-clockwise stimuli were subsequently averaged by inverting the lag time association of one map and averaging them over correlation values. The minimal cross correlation threshold was adjusted between 0.1 and 0.08 for each individual subject in order to remove as much noise as possible without degrading the maps.

We used prior knowledge about the anatomical location and topographic organization of higher visual areas (Orban et al., 2004) and visuomotor areas (Schluppeck et al., 2005) to define areas V3A, V7, IPS1, and IPS2 on the inflated cortical surface. An additional tentative area IPS3 was defined if another phase reversal (i.e. reversal of the visual field representation) occurred on the anterior border of IPS2. Further more, we also defined areas that included the adjacent upper (or lower) visual field representation of neighbouring areas (i.e. V3A/V7 upper, V7/IPS1 lower, IPS1/IPS2 upper).

3.4.3 Statistics: Fibre tracking

The regions of interest (ROIs) that were defined on the basis of the functional data (see above) were

used as seed regions for streamline and probabilistic fibre tracking. Seed regions extended orthogonal to the cortical surface three millimetres into white matter and one millimetre into grey matter.

For streamline fibre-tracking we used a maximum threshold angle of 50° that would minimize spurious connections. A conservative FA threshold of 0.15 was chosen to minimize improbable fibres connections across sulcal gaps, while at the same time allowing for enough streamline propagations to start. For each voxel four streamlines at four different positions equidistant from the voxel centre were seeded (step size, 0.5 mm; fourth-order Runge-Kutta interpolation).

Due to the highly convoluted cortical surface, it is, in general, difficult to define which fibres “hit” another ROI. We counted a hit each time a fibre terminated in a target area (i.e. in any other ROI). We excluded fibres that were only passing through

a target area, since this situation might arise when a target area picks up deeper long-range association fibres.

We looked at the connections between topographic areas V3A, V7, IPS1, IPS2, IPS3, and FEF within and between hemispheres. We did the same for the upper and lower visual hemifield representations FEF lower, FEF upper, V3d/V3A lower, V3AV7 upper, V7/IPS1 lower, IPS1/IPS2 upper, IPS2/IPS3 lower.

For probabilistic fibre-tracking we traced 2000 fibres per seed voxel with a maximum of 200 jumps (step size: 0.5 mm, angle threshold: 70°). Free parameters were adjusted so that the convergence of the tracts was heightened and the occurrence of spurious connections was minimized. Probability maps were superimposed on b_0 -images with MRICro (www.mricro.com).



Figure 5. Results of the random saccade experiment for subject S6 rendered on an inflated representation of the cortical surface of the left hemisphere. Regions showing higher activation for saccades than for fixation ($p < 0.001$) are displayed in shades from red to yellow. Map thresholds were chosen so that the activation pattern would match those of the phase-encoded task. The left side shows the medial surface of the hemisphere. Early dorsal and ventral visual areas and the SEF were activated by the random saccade task. On the right the left hemisphere is displayed from a postero-lateral point of view. A large swath of activation covers the entire IPS and its medial wall and extends up to the postcentral gyrus. A small patch of activation is located near the inferior end of the postcentral gyrus. The FEF is activated at the junction of SFS and PCS along with a second patch of activation located more lateral at the precentral gyrus. (CF = calcarine fissure; CS = central sulcus; FEF = frontal eye fields; IPS = intraparietal sulcus; PCS = precentral sulcus; POS = parieto-occipital sulcus; SEF = supplementary eye fields; SFS = superior frontal sulcus; TOS = trans-occipital sulcus)

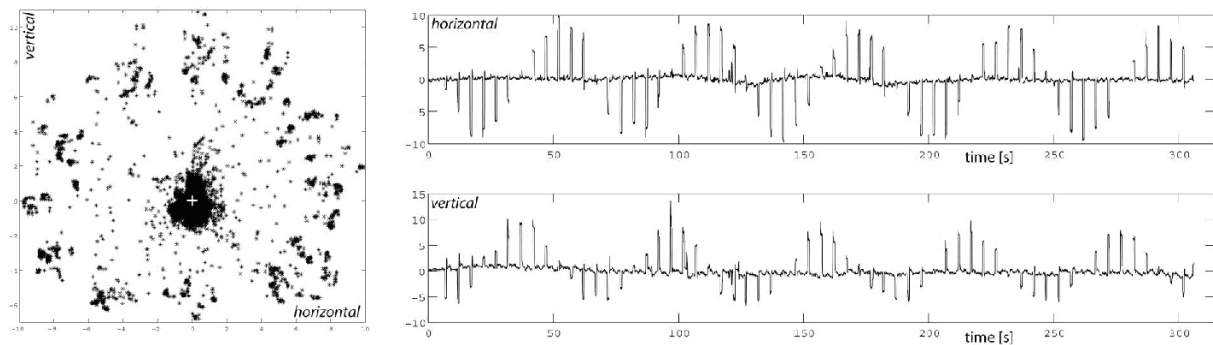


Figure 6. Behavioural data. (A) The scatter plot on the left shows eye positions for a period of 300 s (sample rate, 50 Hz) during the phase-encoded task for subject S5. Saccades were made to all 12 possible locations on the target circle. Saccade amplitudes are slightly deformed in the vertical direction due to shifts in calibration. (B) The right column shows the same data as horizontal and vertical eye position versus time. (horizontal and vertical axis are arbitrary units; artefacts were removed before plotting).

4. Results

4.1 Random saccade paradigm

The random saccade paradigm served to identify the cortical components of the oculomotor system. As expected, saccade-related activations were found throughout the frontoparietal network as well as in the occipital lobe. Figure 5 exemplifies the results with subject S6. All six subjects showed significant activation ($p < 0.001$) in early and mid-level visual areas (V1, V2, V3, V3a, V7) during the random saccade task. Some subjects also showed activation in lateral occipital areas (LO), in superior (ST) and medial temporal areas (MT). Further, all subjects showed activation along the IPS and its medial wall, often extending beyond the anterior end of the sulcus just before the postcentral gyrus. In some subjects this patch of activation extended laterally and included the inferior parts of the postcentral gyrus.

In the frontal lobe, we found significant activation in all subjects near the junction of the superior temporal sulcus (STS) and the precentral sulcus (PCS), where the putative human FEF is located (Corbetta et al., 1998). Often activation extended further lateral along the PCS. All subjects showed activation of the medial wall of the superior frontal gyrus where the putative human SEF is situated (Grosbras et al., 1999). All saccade-related activity was in general bilaterally symmetric, although SEF activation was relatively more pronounced in the left hemisphere in most subjects.

4.2 Phase-encoded paradigm

Continuously varying the angle of the

remembered target location allowed us to compute linear correlation maps similar to methodologies used to analyse retinotopy in early visual areas. Eyetracker data confirmed that subjects were able to execute saccades at the right time to the proper locations (Fig. 6). Subject S2 showed unusually noisy linear correlation maps and was therefore excluded from further phase-encoded analysis.

We found several regions in each hemisphere that contained topographic maps of contra-lateral remembered saccade targets. Figure 7 displays the phase-encoded data of all 5 subjects. Upper visual field representations are coloured in red and lower visual field representations are depicted in green. A whole sequence of topographic areas covers the IPS and adjacent regions. Each single topographic area represents the whole contralateral visual hemifield and has an opposite visual field orientation than its neighbours (white arrows). Topographic maps in the frontal cortex were often less clearly defined. Three subjects had a retinotopic FEF in both hemispheres. Subjects S3 and S6 showed phase-encoded activity only in the right hemisphere. Subject S5 showed a second topographic map in the left lateral precentral gyrus (dotted white line). No evidence was found for topography in the SEF.

In the IPS the transition from one area to the next was defined by a reversal in visual field orientation (Schluppeck et al., 2005). To identify the areas we used knowledge about their anatomical location and the visual field orientation. The most clearly discernable area along or near the IPS was area V3A. Located posterior of the caudal tip of the IPS it was largest in extent and clearly visible. Areas anterior of V3A were smaller and often affected by signal dropouts (i.e. the signal was below the statistical threshold). Borders between successive topographic areas were usually

Mean Talairach coordinates of topographic regions

Brain Region	N	coordinates (left)			N	coordinates (right)		
		x	y	z		x	y	z
V3A	5	-22.4 ± 5.2	-87.2 ± 4.0	10.0 ± 4.5	5	21.0 ± 3.6	-82.0 ± 3.7	15.2 ± 5.5
V7	5	-25.4 ± 0.9	-76.8 ± 5.9	23.0 ± 8.0	5	24.4 ± 4.7	-71.6 ± 6.6	26.2 ± 4.9
IPS1	5	-19.0 ± 4.6	-72.4 ± 3.0	35.2 ± 10.7	5	18.8 ± 5.8	-69.8 ± 1.9	37.4 ± 4.7
IPS2	5	-18.6 ± 3.4	-65.8 ± 4.5	44.0 ± 11.6	5	17.2 ± 4.4	-67.0 ± 3.8	48.0 ± 5.7
IPS3	2	-19.0 ± 1.4	-68.0 ± 12.7	44.0 ± 12.7	2	19.0 ± 4.2	-65.5 ± 9.2	49.5 ± 6.4
FEF	3	-24.7 ± 7.0	-9.8 ± 4.4	49.2 ± 2.9	5	24.7 ± 4.2	-11.5 ± 4.1	48.8 ± 5.4

Table 1. Average positions of topographic regions (mm ± SD). The number of hemispheres showing a particular topographic map is indicated (N). x (lateral/medial), y (anterior/posterior), and z (superior/inferior) according to Talairach and Tournoux (1988).

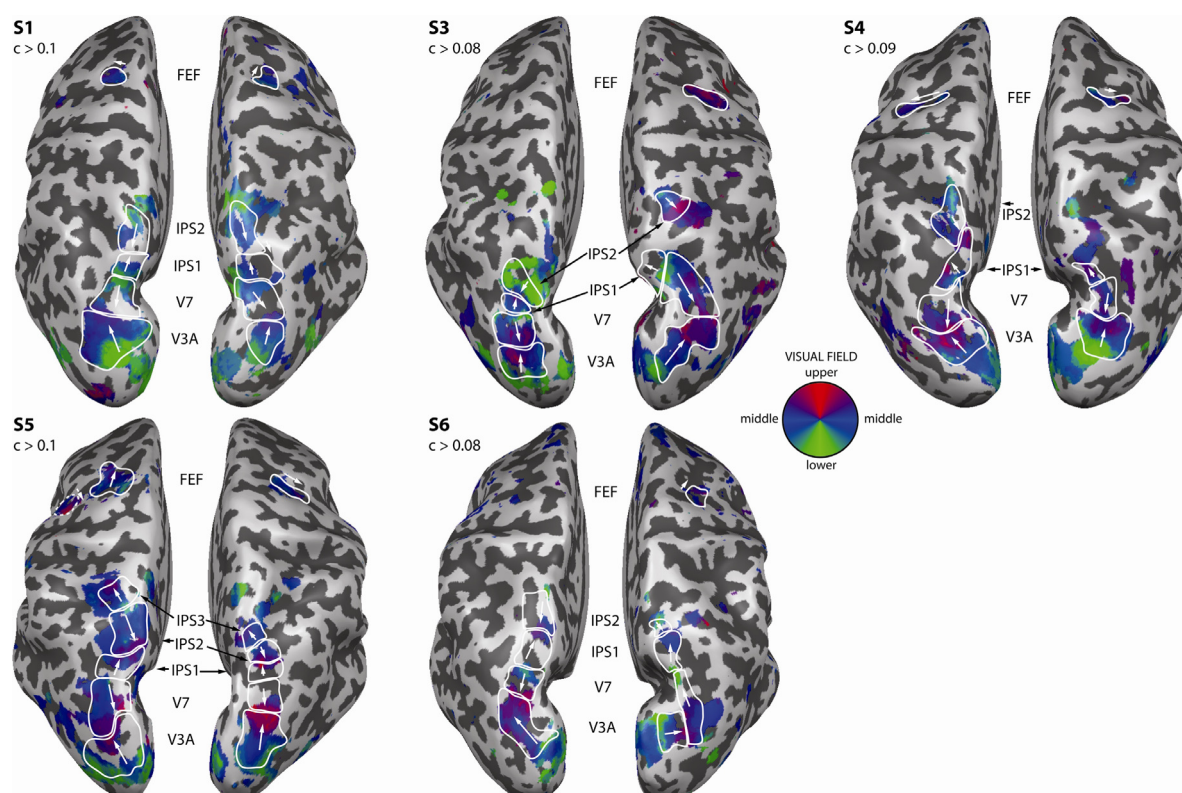


Figure 7. Topography for delayed saccades. Linear correlation maps of the contralateral visual field have been rendered on inflated cortical surface representations. Shown are the dorsal surfaces of each hemisphere for five subjects from a posterior point of view. The hue indicates the response phase. Correlation thresholds were chosen separately for each subject and are indicated. Topographic areas are encircled by a white continuous line. The dashed white line indicates a second frontal topographic area found only in subject S5. White arrows point into the direction of the steepest phase gradient of each individual area. They point from lower to upper vertical meridian. Black arrows help to identify the areas.

orthogonal to the orientation of the IPS (i.e. the direction of fastest phase change was tangential to the orientation of the IPS). The whole sequence of bordering topographic maps usually covered more of the medial bank of the IPS than the lateral bank. Relative to anatomical landmarks, there was little variance between the individual subjects regarding the location of periodically activated regions.

We defined the posterior border of area V7 as

the anterior border of V3A. The border between V7 and IPS1 was consequently at the next phase gradient reversal, and so on. The posterior parts of areas V7 and IPS2 represent the upper visual field and their anterior parts the lower visual field. The posterior parts of areas V3A, IPS1 and tentative IPS3 represent the lower visual field and their anterior parts the upper visual field (Fig. 7). The

posterior border of V7 was situated at or posterior to the junction of transoccipital sulcus (TOS) and the IPS. In some subjects the sequence of areas V3A, V7, and IPS1 covered the whole extent of the IPS, so that IPS2 was rostral to the anterior tip of the IPS, bordering the postcentral gyrus (S3, S4, S5). Despite the individual differences we report the Talairach coordinates of areas V7, IPS1, and IPS2 for comparison (Table 1). Locations of these areas were symmetric across hemispheres and similar to Schluppeck et al.' findings. Schluppeck et al. found the following coordinates, averaged over eight hemispheres: V7, $<\pm 25, -80, 27>$; IPS1, $<\pm 21, -76, 42>$; IPS2, $<\pm 18, -71, 52>$. The tentative region IPS3 was found in only one subject (S5). It

was visible in both hemispheres, had a visual field orientation opposite to IPS2, and its size and significance was comparable to other visuomotor regions in the same subject. The single topographic map found by Sereno et al. was located at $<24, -65, 53>$. Its location was closer to IPS3 (8.4) found in this study than to IPS2 (9.8) (Euclidian distances).

4.3 Fibre-tracking results

Streamline-tracking starting in the FEF often revealed a large tract running from the cortex lateral to the ventricles and then curving medially to the

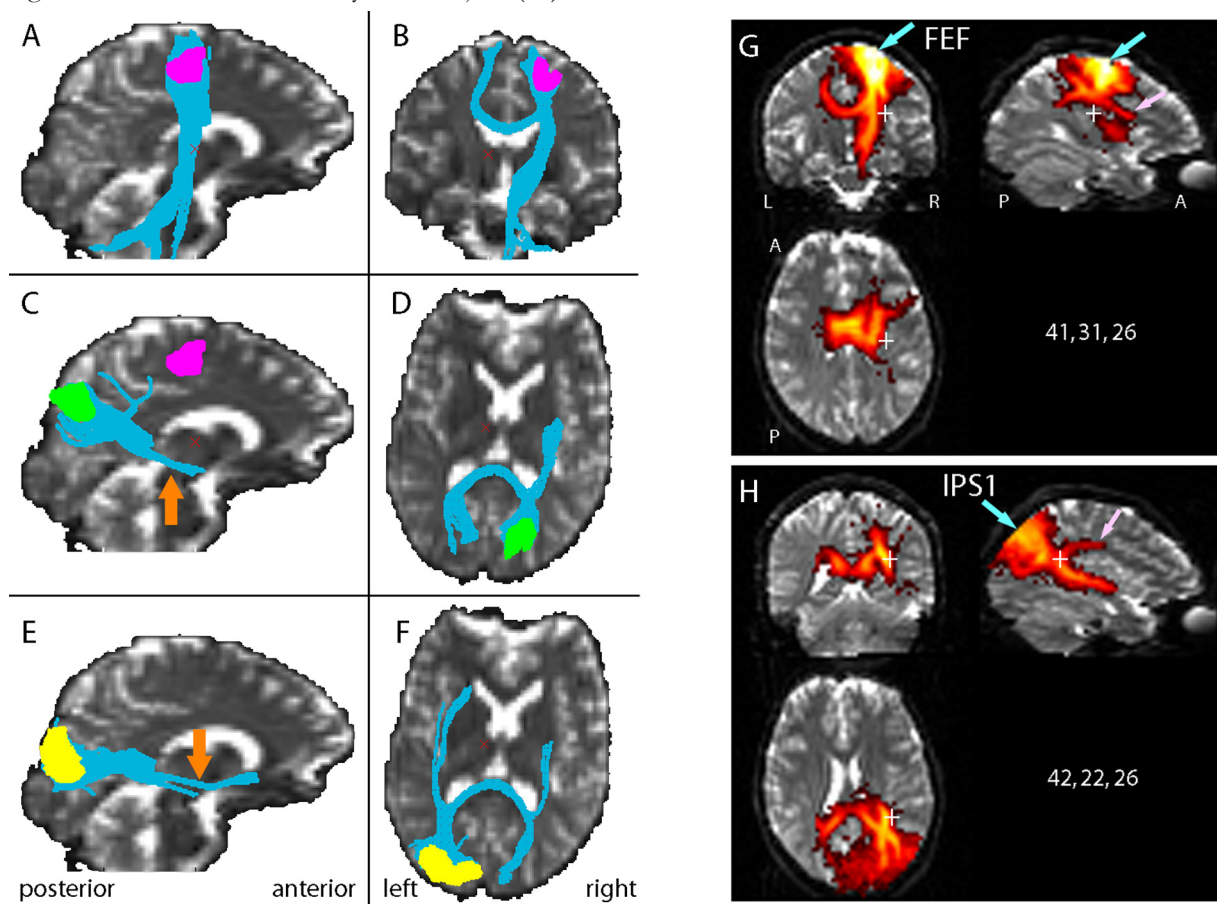


Figure 8. Representative fibre-tracking results for deterministic streamline tracking (left columns) and probabilistic tracking (right column). (A-F) Projection of streamline fibres seeded in respective ROIs of subject S1 onto central b0-slices. (A, B) show fibres originating in the right FEF (pink). (C, D) show fibres originating in the right IPS1 (green). (E, F) show fibres originating in the left V3A (yellow). The left column shows sagittal views and the right column axial views except for (B) which shows a coronal view. For reference we indicated FEF also in (C). Orange arrows point to the inferior longitudinal fasciculus. (G, H) Probabilistic tracking results for subject S5. The probability of a connection between the respective seed region and any other voxel in the respective slice is indicated by the hue. Cyan arrows point to the seed region and pink arrows to the superior longitudinal fasciculus (SLF). In (G) the right FEF was seeded. On the coronal slice one can clearly see cross-callosal connections and a tract running from the cortical surface towards the brainstem. The major body of the SLF is revealed by the probabilistic tracking as depicted on the sagittal slice. In (H) the right IPS1 was seeded. Posterior parts of the superior and inferior longitudinal fasciculi are tracked. Slice numbers are indicated by a small cross (voxels = 643; voxelsize = 3 mm³; x (sagittal slices), y (coronal slices), and z (axial slices)).

brainstem (Fig. 8, A, B). In addition, fibres crossing to the contralateral side were revealed. These fibres most often connected regions located medially of the FEF (B). These fibres did not start in the ROI but were picked up the FEF-ROI, which was in general deeply embedded into a sulcal fundus, when they had already travelled some millimetres through white matter. The probabilistic tracking confirmed these results and in addition revealed a large part of the superior longitudinal fasciculus (SLF) (pink arrow, Fig. 8, G).

Higher visual and visuomotor regions V7, IPS1, IPS2, and IPS3 were connected by the inferior longitudinal fasciculus (ILF) to fronto-temporal regions (orange arrow, Fig. 8, C, D). The posterior part of the fibre bundle between the cortical surface and the posterior end of the ILF was inclined depending on how superior respectively anterior the seed region was situated. Cross-callosal connections, again, terminated in medial regions of the contralateral hemisphere (D). Streamline tracking did not reveal larger parts of the SLF or any other possible connection between IPS and FEF. Figure C, shows one of few rare cases where streamline tracking revealed the most posterior part of the SLF. It does, however, not quite reach the FEF. On the other hand, probabilistic tracking consistently revealed the most posterior part of the SLF (pink arrow, Fig. 8, H). We found no branches that left the central part of the SLF and reached the cortical surface for frontal regions such as the FEF.

Area V3A was connected to fronto-temporal regions by a large fibre bundle, the ILF, running lateral to the posterior horns of the lateral ventricles and lateral to the Putamen (Fig. 8, E, F). The tract often terminated in a hook-like structure in the frontal lobe. Cross-callosal connections were found between regions located medially of left and right V3A.

Connections between adjacent regions (%)

Regions	left hemisphere	right hemisphere
V3A → V7	11.7	7.5
V7 → V3A	6.2	5.3
V7 → IPS1	5.4	11.5
IPS1 → V7	6.6	5.9
IPS1 → IPS2	13.5	2.0
IPS2 → IPS1	3.9	1.0
IPS2 → IPS3	1.1	5.8
IPS3 → IPS2	2.1	4.9

Table 2. Connections between adjacent areas along the IPS as found by deterministic streamline tracking. The percentage indicated is the ratio between the sum of all fibres that connect two region A with region B and the sum of all fibres leaving the first region A, across all subjects.

The group statistics based on streamline tracking show consistent connections between neighbouring areas in the same hemisphere (Table 2). Excluding IPS3, on average there were 1967 fibres (SD = 899) tracked from each ROI. The great majority of these fibres connected neighbouring regions within the same hemisphere. Three subjects (S2, S5, S6) showed a small number of fibres (1-5) that connected non-neighbouring areas. However, these connections existed only in one direction (A → B) and were not found in the opposite direction (B → A).

The great variability between hemispheres, for example, there are more than six time more connections between IPS1 and IPS2 in the left hemisphere than in the right, can be attributed to the different number of fibres that were seeded in the respective areas (left IPS1, 907; right IPS1, 2058). This might be due to accumulating errors in the chain of image registrations. Functional images were first registered to anatomical images which were then registered to the DTI images. Imprecisely located ROIs might not have penetrated white matter deep enough to initiate fibre propagation. A further source of variance is the highly variable fibre tracking process itself.

Because these results basically contradicted our hypothesis that the anatomical connections between fronto-posterior oculomotor regions can be revealed by DTI, we investigated the tensor maps at specific places in detail. Figure 9 shows an enlarged section of the tensor map of subject S4 on the left and directionally colour-coded FA maps on the right. We hypothesised that the preference of deterministic streamline tracking based on a single-tensor model for following the most dominant fibre direction was the reason for the lacking IPS-FEF connections. This limitation can potentially be overcome by either allowing the tracking algorithm to follow directions distinct from the orientation of the major eigenvector, or by adjusting the model to represent more than one fibre orientation per voxel. The former was done by means of probabilistic tracking, the latter by modelling two tensors per voxel. A combination of both was not available for this study.

As described above, probabilistic tracking revealed parts of the SLF but did not find connections between the IPS and the FEF. On the other hand, two-tensor streamline tracking, as implemented in the Camino software package, turned out to be highly susceptible to noise and generated many spurious connections even after

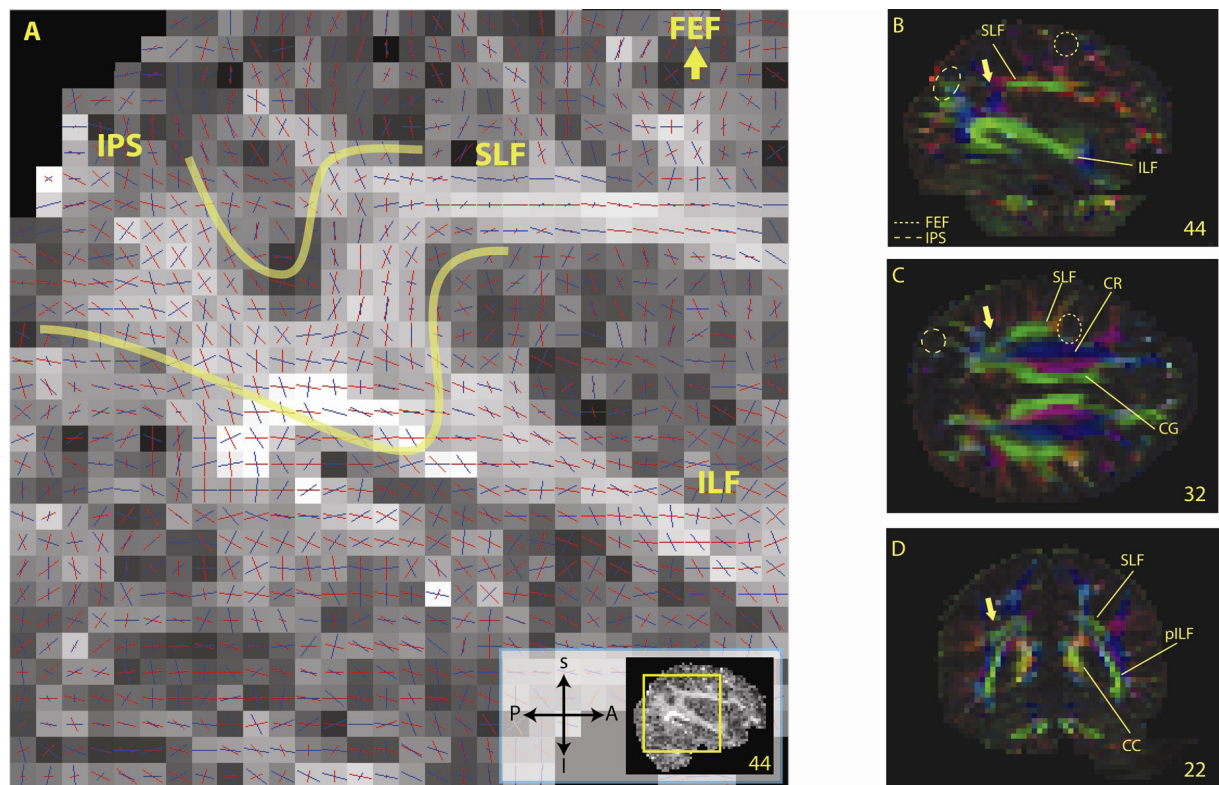


Figure 9. (A) Two-Tensor orientation map overlaid on a fractional anisotropy map of subject S4 (lateral sagittal slice). Red and blue lines represent projections of the major eigenvectors of the first and second tensor on the image plane. Brighter shades represent larger FA values and darker shades smaller FA values. The inset shows position of the enlarged section. A possible connection between parietal and frontal areas might be located between the two yellow lines. (B-D) FA maps of single-tensor model, coloured according to the anatomic direction of the major eigenvector of the diffusion tensor (red: left-right, green: anterior-posterior, blue: inferior-superior). (B) shows the same sagittal slice as the enlarged section on the right. The ILF and to a lesser extent the SLF contain high FA values and tensors oriented in anterior-posterior direction (bright green). (C) shows a horizontal slice at the height of the SLF. Three different fibre bundles can be identified. Going from medial to lateral one first encounters the fibres of the limbic system running along the medial surface of the hemisphere in anterior-posterior direction (CG, green). The violet and blue coloured regions contain callosal fibres curving upward from the body of the corpus callosum towards the medial surface and ascending cortico-spinal fibres (superior corona radiate, CR). More lateral and posterior the SLF is shown in green. (D) shows a coronal slice at the position indicated by the arrows on the other slices. Posterior-laterally oriented fibres of the corpus callosum (CC) are shown as two yellow compact dots. Lateral are the fibres of the posterior region of ILF. The posterior end of the SLF is located more superior (grey/green).

adjusting the FA and angle thresholds. A detailed analysis of the tensor orientations of a two-tensor model (Fig. 9, A) revealed that a potential connection between IPS and SLF would have to follow the direction of the primary tensors (red) from the IPS until the posterior end of the ILF, then follow the secondary tensors (blue) for three or four voxels, and finally switch back to the primary tensor. In essence, this procedure amounts to a single-tensor model, by setting the orientation of the single tensor to either the orientation of the primary tensor or the orientation of the secondary tensor. Classification of voxels as Gaussian or non-Gaussian, reveals voxels which potentially contain

several fibres of different orientations. To avoid tracking in the most dominant direction we set the orientation of the single tensor in all non-Gaussian voxels to the orientation of the secondary tensor of the two-tensor model. In summary, this approach was about tracking into non-dominant directions in all voxels that were assumed to contain more than one fibre orientation, and following the dominant fibre direction in all voxels that were assumed to contain only one fibre orientation. This procedure, however, did not improve on the conventional streamline tracking. We attributed this to the secondary tensor's high susceptibility to noise and the incoherent results of the voxel classification.

Voxel classification depended on arbitrary thresholds and yielded non-Gaussian voxels, which were almost randomly distributed throughout the white matter. Noise-related problems can be potentially overcome by imaging more directions and thereby improving the signal-to-noise ratio and the angular resolution of the two-tensor model.

To sum up, although the quality of the functional results allowed us to define proper seed regions for the fibre-tracking, multiple approaches to reveal fronto-parietal connections between cortical oculomotor regions failed. In the discussion we will try to give reasons for the failure of the methods.

5. Discussion

In this study we combined functional MRI data with DTI-based tractographic data to investigate the anatomical connectivity between cortical oculomotor areas in the healthy human. We successfully located the most important cortical oculomotor areas, such as FEF, SEF, and several areas in the IPS. On the basis of previous findings, we predicted that the FEF and several intraparietal visuomotor areas were retinotopically organized (Hagler and Sereno, 2005; Sereno et al., 2001; Schluppeck et al., 2005). We were able to show significant retinotopy using considerably less saccades (480) than Schluppeck et al. (720-1440). Based on functional results in the human and extrapolating from macaque tracer studies we expected that these areas would be anatomically connected in humans. We hypothesised that a combined DTI-fMRI approach would reveal these connections, especially a fronto-parietal pathway connecting the human homologue of monkey LIP with the FEF. Overall, our tractographic results were negative. Below we will discuss the functional results followed by an in-depth look at the tracking results and an attempt to explain the fact that the hypothesised connections were not found.

5.1 Retinotopic maps

The functional results were in general agreement with previous findings (Schluppeck et al., 2005) with the exception of the unusual layout of retinotopic areas found in subject S5 (Fig. 7). Not only did the subject show a third topographic region anterior of IPS2, but also a second frontal region lateral of the left FEF. Further retinotopic prefrontal regions are

left FEF. Further retinotopic prefrontal regions are usually not activated by a simple delayed-saccade task. Hagler and Sereno (2006) found multiple topographically organized frontal and prefrontal areas using a phase-encoded two-back identity task with faces. The co-activation of regions involved in working memory and processing of more complex stimuli might indicate that the subject used a different processing technique. After all, saccade target locations in a delayed-saccade task could be memorized in a number of ways: visually, as a covert motor program, as a more abstract description of the target position, such as the number on the clock face in the same position (possibly even including verbalization), or as any combination of the above. The design of the present study can, however, not discern between different processing strategies and different functional anatomy.

Position and visual field orientation of the tentative IPS3 region that we found in subject S5 approximately match those of the single topographic region found by Sereno et al. (2001). The visual field orientation of IPS3 is opposite to IPS2 and its location is well anterior to the superior terminus of the parieto-occipital sulcus and slightly closer to the central sulcus than to the occipital pole. It is, however, not clear why a retinotopic area in this region consistently showed up only in Sereno et al.'s study, because the task they used is basically identical to the task used in Schluppeck et al. and the present study. Further, it is puzzling that the latter two studies were able to show IPS1 and IPS2, which were not reported by Sereno et al. Incidentally, although its position has not been reported, IPS3 also seems to show up during Hagler and Sereno's phase-encoded two-back identity task. At this point we can only speculate whether the reasons for this discrepancy are of methodological nature, such as different field strengths and acquisition times, or due to other uncontrolled experimental parameters, such as individual differences between subjects and the way they processed the stimuli.

In conclusion, although the functional data confirmed previous findings, inter-subject variability is large. Further experiments are needed to differentiate the multifaceted characteristics of the IPS.

5.2 Limitations of the combined DTI-fMRI approach

Despite its principal limitations, DTI-based

fibre-tracking has successfully identified a larger number of white matter tracts in the healthy human brain (see, e.g., Wakana et al., 2003). Why did the tracking of an IPS-FEF connection through the SLF fail? In general, tracking can fail for a large number of reasons. Some of them are of rather fundamental nature, like the ones described in the introduction, some depend on the specific nature of the tracts that one attempts to reveal, and others depend on the particular combination of MR methods that were used in the present study. In the following we will work out what these limitations are and how they influenced our results.

One should note that there is an important difference between this study and studies that try to reveal major fibre bundles. There is no doubt that DTI-based fibre-tracking has proved to accurately and consistently reveal the fibres of the corpus callosum and the cortico-spinal tract, which have made for numerous cover pictures and illustrations. However, there are essential differences between the present approach and most other tractographic studies. The goal of this study was not to reveal entire anatomical tracts, but to find connections between distinct cortical regions. Studies that aim to create a fibre tract-based atlas (Wakana et al., 2003) track from all pixels inside the brain (“brute force” approach) and then use multiple manually defined ROIs to select the tracts of interest. These so-called multi-ROI approaches use very large, box-shaped seed regions. These ROIs are used in conjunction with logical operators AND, OR, and NOT to select the desired tracts and remove fibres belonging to anatomically different pathways (Mori and Zijl, 2002). To eliminate the subjectivity inherent in this multi-ROI approach we decided against an operator-defined tractography and only use the functionally defined seed regions.

Studies that are interested in tracing connections between specific regions most often define the seed areas in subcortical white matter (Behrens et al., 2003a; Croxson et al., 2005; Johansen-Berg et al., 2005). In general, tracing connections between cortical areas is more difficult and less robust, because the relative low white matter penetration of cortical areas and the high complexity or spreading, as fibres reach grey matter, can mean that the diffusion anisotropy is too low to initiate reliable probabilistic tractography from the cortex (Croxson et al., 2005). Most studies circumvent this problem by either defining subcortical seed regions or using seed regions in white matter fascicles associated with particular cortical regions. We anticipated this

difficulty and let the seed regions penetrate into white matter for at least one voxel. Of 49 seed regions only two (4%) did not initiate any fibre tracking. This shows that connections between seed regions could in principle have been found, because seed and target regions contained white matter voxels with FA values high enough to trace fibres.

Figure 9 is an attempt to identify the exact location of the problem and ways to solve it. Fibres seeded in the IPS descend along a vertically oriented tract of reasonably high FA (green/blue, B) until they meet the posterior part of the ILF. Here they should travel in a horizontal direction for the length of two or three voxels before starting to ascend again as illustrated by the enlarged section on the left (A). Indeed, there is a vertical tract where the arrow points at (B). However, instead of ascending, almost all fibres continue following the ILF to the frontal and lateral lobes. This behaviour can be explained by looking at the tensor orientations in detail. A tracking algorithm based on the single tensor model will prefer tracing the ILF over the SLF for two reasons. First, diffusion anisotropy is much higher in the ILF than in its surrounding. Second, the stream-line algorithm used in this study prefers the most collinear tensor orientation. That means that changes in direction with an angle larger than 90° are impossible. A sharper turning angle might be required at the current resolution. In fact, many of the primary tensors that descend from the IPS and from the SLF align almost parallel or in a V-like angle at the posterior tip of the ILF. Because of the collinearity criterion increasing the threshold angle does not help in deterministic streamline tracking.

The situation is quite similar for the FEF, only that here the superior part of the corona radiata (SCR) acts as a sink (blue, Fig. 9, C). Most of the fibres seeded in the FEF initially drift medially and then follow through the internal capsule towards the brain stem. The SCR is by far the most dominant fibre bundle in the dorsal part of the frontal lobe, having coherently oriented tensors and high FA (blue-violet, Fig. 9, C). The FEF is located rostral of the anterior end of the SLF. Although the SLF is known to have projections into the temporal lobe (Mori et al., 2002) these are hardly visible on the FA map and are not picked up by conventional streamline tracking.

The problem can be summarized by an affinity of the deterministic streamline tracking for following the most dominant fibre direction. We hypothesised that it would be possible to improve

the tracking by switching either to a two-tensor model or to probabilistic tracking.

The two-tensor approach, however, failed to locally model two fibre directions. Two-tensor models are usually difficult to estimate, because the fitting process of the tensors is prone to local minima. As a rule, higher b -values and a larger number of directions are needed for higher-order models (Frank, 2001). The present study's b -value of 1000 s mm^{-2} and 60 directions were sufficient for a single-tensor model, but probably inadequate for higher-order models.

The disappointing performance of the probabilistic tracking can also be attributed to an inadequate local model. If the angular resolution is not sufficient to dissociate several fibre orientations, as depicted in Figure 2 (IIc), or if the model allows only a single tensor, the fitting might yield an indiscriminate disc or sphere-shaped tensor. Although the tensor includes the orientations of secondary fibres *inter alia*, these directions will only be traced on the expense of tracing all other directions represented by the tensor. Thus, probabilistic tracking will trace the correct fibre directions but also give a large number of false-positives. In practice, this yields very diffuse probability maps, in which the seed voxel is connected to a large number of brain areas. Probabilistic fibre-tracking algorithms usually have a number of free parameters which allow adjusting the probability by which less likely fibre directions will be traced, thereby controlling the “sharpness” of the tracts between deterministic and random. However, if the local model is too indiscriminate, adjusting this threshold will be a very delicate procedure and often reveal only the major tracts or diffuse and uninterpretable connections. In addition, it is hard to scientifically justify a certain arbitrary threshold. Unless the model accurately represents the local fibre structure, probabilistic tracking of crossing or branching fibre structures will not lead to robust and reproducible results.

Another explanation for the negative findings is the possible absence of the hypothesised tracts in humans. However this explanation seems unlikely given the abundant evidence in the qualitatively very similar macaque brain (Schall et al., 1995; Stanton et al., 1995; Vincent et al. (unpublished)). In addition, Behrens et al. (2006) could reveal medial portion of the SLF with a probabilistic tractography approach that supports multiple fibres per voxel (Behrens et al. 2003b).

They explicitly show that the SLF is invisible to the single fibre approach, because it is obscured by the medial motor projections.

In summary, in the case of single-tensor streamlining, the high FA values and the coherent organization of the tensors contained in the ILF have acted as a sink for the line-propagation. Streamlines that entered the ILF were “caught” in the tract and could not branch off in other directions. This is a deficiency of the deterministic single-tensor streamline tracking, which in general does not allow the tracking of any other than the most dominant fibre direction. In other words, non-dominant fibre directions are obscured by the dominant fibre direction. Probabilistic tracking approaches are based on the very idea of tracking in non-dominant directions. These approaches are doomed to fail if the local model is indiscriminate. The successful tracking of the SLF in Behrens et al. (2006) suggests that a higher resolution ($2 \times 2 \times 2 \text{ mm}^3$) and averaging over three sets of diffusion-weighted data provides a sufficient basis for subsequent probabilistic tracking of multiple fibres per voxel.

6. Conclusion

Limitations of a combined DTI-fMRI approach can be mainly attributed to limitations of DTI rather than fMRI. DTI suffers, over and above several fundamental methodological limitations (e.g. poor resolution of DTI compared to the size of fibre tracts), from the additional requirements imposed by the cortical seed regions. Fibre tracking in its current state is much more suited to study the properties of white matter tracts isolated from their cortical targets rather than the connections between specific cortical regions. That is why most of the applied DTI-based fibre-tracking studies have focused on tracking significant white matter fascicles to either classify them (Wakana et al., 2003) or to analyse their properties during development and in presence of lesions (Guye et al., 2003; Munakata et al., 2006; Schonberg et al. 2006).

The fundamental lesson to be learnt from this study is that DTI-based fibre-tracking is in need of further methodological development to overcome the limitations inherent in the method and to be up to the additional requirements of specific cortico-cortical tracking. Major improvements are needed regarding the three limitations presented in the introduction: data, model, and tracking. The

resolution and SNR of the diffusion weighted images has to improve to be able to dissociate complex fibre structures near the cortical surface and in regions of crossing fibres. The diffusion model has to represent the underlying fibre structure as close as possible and optimally improve the tracking by removing redundant information. The tracking should support tracing fibres through regions of crossing and branching fibres, yield a connection probability map, and represent fibres in a way that matches their natural appearance.

Substantial improvements are already expected by switching from a single-tensor model to a model that represents multiple fibre orientation per voxel and by switching from deterministic to probabilistic tracking. Of course, the quality of the data (i.e. number of directions, *b*-value, SNR) has to support this. Single-tensor deterministic tracking is certainly not adequate for the tracking of long-range cortico-cortical connections through regions of crossing or branching fibres.

Nevertheless, once these problems have been overcome, a combination of fMRI and DTI-based tractography seems to be a most promising area of application. The mapping of both, functional active areas and their anatomical connections, in vivo, will help us to better understand functional and anatomical connectivity and thus enable much more comprehensive models of the brain.

Acknowledgements

I would like to thank both my supervisors – Pieter Medendorp and David Norris – for their outstanding support during the course of this challenging project. Furthermore, I would like to acknowledge Hubert Fonteijn's help with the technical aspects of the analysis and Paul Gaalman's help with the scanning. I am more than thankful for the support and suggestions of the F. C. Donders' MR group. Last but not least I would like to thank Ian Fitzpatrick for his comments on the first draft of this thesis.

References

Alexander, D. C., Barker, G. J., & Arridge, S. R. (2002). Detection and modeling of non-Gaussian apparent diffusion coefficient profiles in human brain data. *Magn Reson Med*, 48(2), 331-340.

Alexander, D. C. (2006). An introduction to

computational diffusion MRI: the diffusion tensor and beyond. In "Visualization and image processing of tensor fields" edited by J. Weickert and H. Hagen, Springer 2006.

Astafiev, S. V., Shulman, G. L., Stanley, C. M., Snyder, A. Z., Van Essen, D. C., & Corbetta, M. (2003). Functional organization of human intraparietal and frontal cortex for attending, looking, and pointing. *J Neurosci*, 23(11), 4689-4699.

Baker, J. T., Patel, G. H., Corbetta, M., & Snyder, L. H. (2006). Distribution of activity across the monkey cerebral cortical surface, thalamus and midbrain during rapid, visually guided saccades. *Cereb Cortex*, 16(4), 447-459.

Bammer, R., Acar, B., & Moseley, M. E. (2003). In vivo MR tractography using diffusion imaging. *Eur J Radiol*, 45(3), 223-234.

Basser, P. J., Pajevic, S., Pierpaoli, C., Duda, J., & Aldroubi, A. (2000). In vivo fiber tractography using DT-MRI data. *Magn Reson Med*, 44(4), 625-632.

Beaulieu, C. (2002). The basis of anisotropic water diffusion in the nervous system - a technical review. *NMR Biomed*, 15(7-8), 435-455.

Behrens, T. E., Johansen-Berg, H., Woolrich, M. W., Smith, S. M., Wheeler-Kingshott, C. A., Boulby, P. A., et al. (2003a). Non-invasive mapping of connections between human thalamus and cortex using diffusion imaging. *Nat Neurosci*, 6(7), 750-757.

Behrens et al., 2003b T.E.J. Behrens, M.W. Woolrich, M. Jenkinson, H. Johansen-Berg, R.G. Nunes, S. Clare, P.M. Matthews, J.M. Brady and S.M. Smith, Characterization and propagation of uncertainty in diffusion-weighted MR imaging, *Magn. Reson. Med.* 50 (2003), pp. 1077-1088

Behrens, T. E., Johansen-Berg, H., Jbabdi, S., Rushworth, M. F. S., Woolrich, M. W. (2006). Probabilistic diffusion tractography with multiple fibre orientations: What can we gain? *NeuroImage*, 34(1), 144-155.

Boynton, G. M., Engel, S. A., Glover, G. H., & Heeger, D. J. (1996). Linear systems analysis of functional magnetic resonance imaging in human V1. *J Neurosci*, 16(13), 4207-4221.

Burgel, U., Amunts, K., Hoemke, L., Mohlberg, H., Gilsbach, J. M., & Zilles, K. (2006). White matter fiber tracts of the human brain: three-dimensional mapping at microscopic resolution, topography and intersubject variability. *Neuroimage*, 29(4), 1092-1105.

Cook, P. A., Bai, Y., Nedjati-Gilani, S., Seunarine, P. A., Hall, M. G., Parker, G. J., Alexander, D. C. (2006). Camino: Open-Source Diffusion-MRI Reconstruction and Processing, 14th Scientific Meeting of the International Society for Magnetic Resonance in Medicine, Seattle, WA, USA, 2759.

Croxson, P. L., Johansen-Berg, H., Behrens, T. E., Robson, M. D., Pinski, M. A., Gross, C. G., et al. (2005). Quantitative investigation of connections of the prefrontal cortex in the human and macaque

- using probabilistic diffusion tractography. *J Neurosci*, 25(39), 8854-8866.
- Dougherty, R. F., Ben-Shachar, M., Bammer, R., Brewer, A. A., & Wandell, B. A. (2005). Functional organization of human occipital-callosal fiber tracts. *Proc Natl Acad Sci U S A*, 102(20), 7350-7355.
- Frank, L. R. (2001). Anisotropy in high angular resolution diffusion-weighted MRI. *Magn Reson Med*, 45(6), 935-939.
- Guye, M., Parker, G. J., Symms, M., Boulby, P., Wheeler-Kingshott, C. A., Salek-Haddadi, A., et al. (2003). Combined functional MRI and tractography to demonstrate the connectivity of the human primary motor cortex in vivo. *Neuroimage*, 19(4), 1349-1360.
- Hagler, D. J., Jr., & Sereno, M. I. (2006). Spatial maps in frontal and prefrontal cortex. *Neuroimage*, 29(2), 567-577.
- Jezzard, P., & Balaban, R. S. (1995). Correction for geometric distortion in echo planar images from B0 field variations. *Magn Reson Med*, 34(1), 65-73.
- Johansen-Berg, H., Behrens, T. E., Robson, M. D., Drobniak, I., Rushworth, M. F., Brady, J. M., et al. (2004). Changes in connectivity profiles define functionally distinct regions in human medial frontal cortex. *Proc Natl Acad Sci U S A*, 101(36), 13335-13340.
- Jones, D. K., Horsfield, M. A., & Simmons, A. (1999). Optimal strategies for measuring diffusion in anisotropic systems by magnetic resonance imaging. *Magn Reson Med*, 42(3), 515-525.
- Koch, M. A., Norris, D. G., & Hund-Georgiadis, M. (2002). An investigation of functional and anatomical connectivity using magnetic resonance imaging. *Neuroimage*, 16(1), 241-250.
- Koyama, M., Hasegawa, I., Osada, T., Adachi, Y., Nakahara, K., & Miyashita, Y. (2004). Functional magnetic resonance imaging of macaque monkeys performing visually guided saccade tasks: comparison of cortical eye fields with humans. *Neuron*, 41(5), 795-807.
- Le Bihan, D. (2003). Looking into the functional architecture of the brain with diffusion MRI. *Nat Rev Neurosci*, 4(6), 469-480.
- Lewis, J. W., & Van Essen, D. C. (2000a). Mapping of architectonic subdivisions in the macaque monkey, with emphasis on parieto-occipital cortex. *J Comp Neurol*, 428(1), 79-111.
- Lewis, J. W., & Van Essen, D. C. (2000b). Corticocortical connections of visual, sensorimotor, and multimodal processing areas in the parietal lobe of the macaque monkey. *J Comp Neurol*, 428(1), 112-137.
- Mori, S., Kaufmann, W. E., Davatzikos, C., Stieltjes, B., Amodè, L., Fredericksen, K., et al. (2002). Imaging cortical association tracts in the human brain using diffusion-tensor-based axonal tracking. *Magn Reson Med*, 47(2), 215-223.
- Mori, S., & van Zijl, P. C. (2002). Fiber tracking: principles and strategies - a technical review. *NMR Biomed*, 15(7-8), 468-480.
- Munakata, M., Onuma, A., Takeo, K., Oishi, T., Haginoya, K., & Iinuma, K. (2006). Morphofunctional organization in three patients with unilateral polymicrogyria: combined use of diffusion tensor imaging and functional magnetic resonance imaging. *Brain Dev*, 28(6), 405-409.
- Munoz, D. P. (2002). Commentary: saccadic eye movements: overview of neural circuitry. *Prog Brain Res*, 140, 89-96.
- Ogawa, S., Lee, T. M., Kay, A. R., & Tank, D. W. (1990). Brain magnetic resonance imaging with contrast dependent on blood oxygenation. *Proc Natl Acad Sci U S A*, 87(24), 9868-9872.
- Orban, G. A., Van Essen, D., & Vanduffel, W. (2004). Comparative mapping of higher visual areas in monkeys and humans. *Trends Cogn Sci*, 8(7), 315-324.
- Parmar, H., Sitoh, Y. Y., & Yeo, T. T. (2004). Combined magnetic resonance tractography and functional magnetic resonance imaging in evaluation of brain tumors involving the motor system. *J Comput Assist Tomogr*, 28(4), 551-556.
- Reese, T. G., Heid, O., Weisskoff, R. M., & Wedeen, V. J. (2003). Reduction of eddy-current-induced distortion in diffusion MRI using a twice-refocused spin echo. *Magn Reson Med*, 49(1), 177-182.
- Schall, J. D. (2004). On the role of frontal eye field in guiding attention and saccades. *Vision Res*, 44(12), 1453-1467.
- Schall, J. D., Morel, A., King, D. J., & Bullier, J. (1995). Topography of visual cortex connections with frontal eye field in macaque: convergence and segregation of processing streams. *J Neurosci*, 15(6), 4464-4487.
- Schluppeck, D., Glimcher, P., & Heeger, D. J. (2005). Topographic organization for delayed saccades in human posterior parietal cortex. *J Neurophysiol*, 94(2), 1372-1384.
- Schonberg, T., Pianka, P., Hendler, T., Pasternak, O., & Assaf, Y. (2006). Characterization of displaced white matter by brain tumors using combined DTI and fMRI. *Neuroimage*, 30(4), 1100-1111.
- Sereno, M. I., Pitzalis, S., & Martinez, A. (2001). Mapping of contralateral space in retinotopic coordinates by a parietal cortical area in humans. *Science*, 294(5545), 1350-1354.
- Sereno, M. I., & Tootell, R. B. (2005). From monkeys to humans: what do we now know about brain homologies? *Curr Opin Neurobiol*, 15(2), 135-144.
- Silver, M. A., Ress, D., & Heeger, D. J. (2005). Topographic maps of visual spatial attention in human parietal cortex. *J Neurophysiol*, 94(2), 1358-1371.
- Smith, S. M. (2002). Fast robust automated brain extraction. *Hum Brain Mapp*, 17(3), 143-155.
- Stanton, G. B., Bruce, C. J., & Goldberg, M. E. (1995). Topography of projections to posterior cortical areas from the macaque frontal eye fields. *J Comp Neurol*, 353(2), 291-305.
- Talairach, J., & Tournoux, P. (1988). Co-planar

- stereotaxic atlas of the human brain : 3-dimensional proportional system : an approach to medical cerebral imaging. Stuttgart
- Tuch, D. S. (2004). Q-ball imaging. *Magn Reson Med*, 52(6), 1358-1372.
- Vincent, J. L., Patel, P. H., Fox, M. D., Snyder, Baker, Snyder, Corbetta, Raichle (submitted) The Intrinsic Functional Architecture of the Primate Oculomotor Network.
- Wakana, S., Jiang, H., Nagae-Poetscher, L. M., van Zijl, P. C., & Mori, S. (2004). Fiber tract-based atlas of human white matter anatomy. *Radiology*, 230(1), 77-87.
- Weickert, J., & Hagen, H. (2006). Visualization and processing of tensor fields. Berlin: Springer.

Functional connectivity in healthy subjects with auditory verbal hallucinations

Kelly Diederer³

Supervisors: Iris Sommer³, Indira Tendolkar^{1,2}

¹*F.C. Donders Centre for Cognitive Neuroimaging, Nijmegen, The Netherlands*

²*University Medical Centre, Nijmegen, The Netherlands*

³*University Medical Centre, Utrecht, The Netherlands*

Auditory verbal hallucinations (AVH) are a core feature of schizophrenia. Previous studies have provided evidence for dysfunctional integration of language regions to underlie AVH. However, schizophrenia is a complex syndrome consisting of psychotic, cognitive and negative symptoms. In order to learn whether this mechanism plays a causal role in the pathophysiology of AVH, the “pure” form of AVH should be investigated, which can be found in healthy subjects with AVH. Functional integration was assessed with psychophysiological interactions (PPI's) in 10 healthy subjects with AVH, 10 schizophrenia patients and 10 healthy controls matched for age, handedness and education. Subjects were scanned while covertly performing a paced letter fluency task. Schizophrenia patients and healthy subjects with AVH displayed dysfunctional connectivity between the left anterior cingulate cortex (ACC) and the left dorsolateral prefrontal cortex (DLPFC) and between the left inferior frontal gyrus (IFG) and the left superior temporal gyrus (STG). Additionally, dysfunctional connectivity between the left ACC and the left STG was found in the schizophrenia patients. These findings suggest a dysfunction between the production and the perception of speech in healthy subjects with AVH and schizophrenia patients. Furthermore, the difference between healthy subjects with AVH and schizophrenia patients provides an explanation why healthy subjects with AVH can execute some control over their hallucinations, in contrast to schizophrenia patients.

Keywords: Auditory verbal hallucinations, language, functional connectivity, fMRI

1. Introduction

Auditory verbal hallucinations (AVH) are a common symptom in several psychiatric disorders and a core feature of schizophrenia in which they occur with a prevalence of 60% (Nayani & David, 1996). Clarity on the basis of the underlying pathology has not been provided yet. Previous studies have provided testable models, relating AVH to a language dysfunction (Hoffman, 1986; Frith & Done, 1988). Since elementary language functions, the production and perception of speech, are intact in subjects with AVH, disruption of functional language areas is not likely. However, the dysfunctions could well be derived from the integration of regions implicated in the production and perception of speech. One major theory looking at dysfunctional integration as the underlying basis of AVH has been proposed by Frith (1992). According to Frith (1992), hallucinations can be considered as a mis-attribution of internally generated speech to an outside agency. Evidence that speech is formed during AVH stems from studies that show that AVH are accompanied by increased electro-myographic activity of the speech muscles (Grossberg, 2000) and increased activity of speech production regions (McGuire et al., 1993; Dierks et al., 1999). The mis-attribution is thought to arise from a dysfunction of the corollary discharge. The corollary discharge functions as an efferent copy of the formed speech which is sent to the auditory cortex preparing it for perceiving speech as self-generated (Creutzfeldt et al., 1989). Corollary discharges are thought to be sent from the frontal speech producing regions (the left inferior frontal gyrus, IFG), via the left anterior cingulate cortex (ACC) to the speech perception regions (left superior temporal gyrus, STG) through the so-called Fronto-cingulo-Temporal (FCT) circuit. In this circuit the left ACC is presumed to serve as a relay station between frontal areas sending information about produced speech and the left STG, enabling the disentanglement of external and internal speech.

The problem in this approach, however, stems from the fact that in this model the corollary discharge via the FCT circuit is necessary for speech perception and hence the AVH. If this process is dysfunctional inner speech would not arrive at the speech perception region and therefore would not be able to lead to AVH. In order to compensate for this shortcoming a second circuit is needed: the Cortico Cortical (CC) circuit. The CC circuit forms

the connection crucial for the perception of self-formed speech. The CC circuit relates the left IFG to the left STG, establishing a direct connection between the speech production and perception regions. According to this hypothesis, the dual-route-self-monitoring-hypothesis, inner speech via the CC circuit generates the AVH related activity in the speech perception regions (Aleman et al., 2001). The CC circuit is then responsible for the perception of inner speech and the FCT circuit for inhibiting the perception of inner speech. The dual-route-self-monitoring-hypothesis predicts dysfunctions in both processes arising from hypo-activity of both circuits.

Functional neuroimaging studies in healthy subjects have revealed a distributed network during execution of a verbal fluency task grossly similar to the circuit mentioned in the dual-route-self-monitoring-hypothesis (Indefrey & Levelt, 2000). Verbal fluency involves the generation of words from verbal cues. The task can be presented in a variety of forms: auditory or visual; paced or unpaced; overt or covert and with random or constraint output (Curtis et al., 1998).

An additional circuit which has been implicated in prior studies exists of the connection between the left ACC and the left DLPFC (Fu et al., 2005, 2006). Previous studies on language in schizophrenia patients with AVH have provided support for the dual-route-self-monitoring hypothesis. Neurons in the STG, one of the regions implicated in the hypothesis, showed reduced responsiveness to self-produced speech in healthy subjects. (Creutzfeldt et al. 1989b; Muller-Preuss and Ploog, 1981; Frith et al., 1991b; Schlösser et al., 1998; Friedman et al., 1998; Hutchinson et al., 1999; Friston et al., 1991). This decreased responsiveness was not present in schizophrenia patients with AVH (Liddle, 1997; Frith et al., 1995; Yurgelun-Todd et al., 1996). Considering the integration of regions within this language network, several differences have been pointed out between healthy subjects and schizophrenia patients. Schizophrenia patients failed to show the pattern of connectivity present in controls between the left ACC and the left DLPFC (Spence et al., 2000; Fletcher et al., 1999). Additionally the left ACC didn't show the normal interaction with the left temporal region in schizophrenia patients. It displayed a quite different pattern characterized by widespread activation throughout prefrontal and parietal regions, with no significant activations in the primary or medial language regions in the left hemisphere (Boksman

et al., 2005). The latter was replicated by Whalley et al. (2005) in subjects at high genetic risk for schizophrenia.

Additional findings on connectivity in schizophrenia originate from Diffusion Tensor Imaging studies (DTI). DTI is a technique to measure structural connectivity by assessing the osmotic movements of water within the white matter tracts. Recent studies found reduced fractional anisotropy (water diffusion) in the white matter tracts in the left Uncinate Fasciculus and reduced as well as increased fractional anisotropy in the left Arcuate Fasciculus (Burns et al., 2003; Hubl et al. 2004). The Uncinate Fasciculus is the largest of the three fiber tracts connecting the frontal and temporal lobes, and dissection studies have demonstrated that the bulk of these fibers connect the Orbital and Medial Prefrontal cortex (including ACC) to the Amygdala, Entorhinal Cortex and rostral STG (Petrides & Pandya, 1988; Morris et al., 1999). The Arcuate Fasciculus is a major association tract connecting large parts of the frontal association cortices with parietal and temporal association areas (Dejerine, 1895). It also forms the main connection between the left STG and the left IFG (Burns et al., 2003).

Summarizing the results described above, combined with the dual-route-self-monitoring-hypothesis, it can be concluded that in schizophrenia patients with AVH reductions in functional connectivity are present between the left ACC and the left DLPFC, the left ACC and the left STG and the left STG and the left IFG. These deviations may be predisposing factors for AVH. However one can not be certain that these anomalies can be derived from the AVH itself since most studies have been conducted in schizophrenia which is a complex syndrome consisting of psychotic, cognitive and negative symptoms. So far, healthy subjects with AVH as an isolated symptom have not been studied. Thus, abnormalities in schizophrenia may not be specifically related to hallucinations. In order to learn whether these mechanisms play a causal role in the pathophysiology of auditory hallucinations, the “pure” form of AVH should be investigated. This can be achieved by studying healthy subjects who experience AVH, without other psychotic or cognitive symptoms and who have no history of hospitalisation or chronic medication use. Recent studies demonstrated that 10% to 15% of individuals from the normal population report AVH (Van Os, 2000; Aleman et al., 2001). Based on these findings, it can be concluded that hallucinatory

experiences form a continuum in the healthy population.

We hypothesize that the anomalies summarized above for the schizophrenia patients with AVH will also be evident in healthy controls with isolated AVH. Healthy subjects with AVH will therefore be compared to a group of schizophrenia patients with severe AVH, serving as a reference condition for our findings, and a group of control subjects. The connections expected to be dysfunctional are displayed in Figure 1. The task will consist of a verbal fluency task for comparison with previous studies (Boksman et al., 2005; Spence et al., 2000; Lawrie et al., 2002; Fu, 2005).

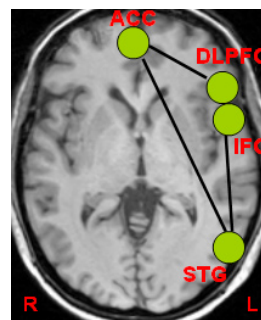


Figure 1. Graphic representation of the circuits expected to be dysfunctional in healthy subjects with AVH and schizophrenia patients.

2. Methods

2.1 Participants

Ten healthy controls without any psychotic experiences, ten healthy subjects with frequent AVH and ten schizophrenia patients were included. Participants from the first and the second group were informed about the study through a website built for this purpose. Attention to the website was drawn by means of flyers, internet links and media attention. On the website, subjects were asked to fill out an electronic questionnaire. The website contained only sparse information about the study since it could influence the answers to the questionnaire. The questionnaire consisted of 6 items relating to auditory hallucinations. Based on their scores on these items subjects were contacted and screened by telephone. When subjects fulfilled the criteria concerning age and the absence of substance abuse, they were asked to come to the UMC Utrecht where the final screening took place.

The following inclusion criteria were used for both groups. All subjects had to be aged 18-65, have no history of drugs or alcohol abuse and no diagnosis of a psychiatric disorder. These criteria were addressed in detail during the screening at the

UMC Utrecht. Screening for psychiatric disease was performed on the basis of DSM-IV as determined by an independent psychiatrist and one of the researchers using the Comprehensive Assessment of Symptoms and History (CASH) (Andreasen et al., 1992). The presence of AVH was further assessed with the Launay Slade Hallucination Scale (LSHS) (Laroi et al. 2004; Aleman et al. 2001).

Schizophrenia Patients were asked to participate by an independent psychiatrist. All were diagnosed on the basis of DSM-IV as determined by an independent psychiatrist using the CASH (Andreasen et al., 1992). All patients were using antipsychotic drugs at adequate levels, but continued to experience AVH at a frequent (daily) base.

All groups were matched for age and handedness. Healthy subjects with and without AVH were also matched for their years of education. The latter was not measured for the schizophrenia patients, since the onset of their disease interfered with their education. For safety reasons the following exclusion criteria were used: metal objects in or around the body that could not be removed (i.e. cochlear implant, surgical clips, piercings, cardiac pacemaker), history of eye trauma with a metal object, professional metal workers, alcohol abuse and possibility of pregnancy. Participants had to fill out an informed consent for participation in the study. They received an honorarium and a compensation for their traveling expenses. This study has been approved by the local hospital Medical Ethics Committee.

2.2 Experimental task

All participants were scanned using the same design and set-up. The verbal fluency task chosen in this study consisted of a letter fluency task. Letter fluency is a classical neuropsychological task of language production, which involves the generation of words beginning with a specified letter. In this paradigm the subjects were asked to covertly generate a word starting with a letter displayed on the screen in front of the subject. Since it is harder

to use these letters to form words, the letters X, Q and C were excluded. Stimuli were presented in 8 activation blocks, each block lasting 30 seconds. In each activation block 10 letters were displayed at a rate of one letter every 3 seconds. As a reference condition for functional MRI image analysis, a baseline condition was presented in which a cross was projected on the screen in order to correct for visual input. Activation blocks were alternated with the reference condition. Presentation of letters was randomized in each block.

Apart from the covert word generation of the experimental trial, a short trial consisting of only two blocks, in which subjects had to generate words overtly, was used in order to measure behavioral performance of the subjects while subjects were still in the scanner. Subjects thought these blocks were part of the actual study in order to keep their performance steady. All participants performed the task correctly. However, the change from covert articulation to overt articulation was confusing for the schizophrenia patients. Therefore these behavioral blocks were not used during patient scans. Patients were trained extensively before the actual scanning started. Only patients capable of performing the task correctly were included.

2.3 Data acquisition

Activation maps were obtained using a Philips Achieva 3 Tesla Clinical MRI scanner at the University Medical Centre (UMC) in Utrecht. 400 weighted echo-planar images, depicting BOLD contrast, were acquired with the following parameter settings: 20 (axial) slices EPI, TE/TR 1200/35 ms, flip angle 35°, FOV 256x80x208, matrix 64x64x20, voxelsize 4 mm isotropic. After completion of the functional scans, a high resolution anatomical scan, with the following parameters TR/TE: 25/1.68 ms, 1x1x1 voxels, flip angle 30°, was acquired to improve localisation of the functional data. A mirror allowed the participant to view a screen, which facilitated the presentation of the letter fluency paradigm via a LCD projector outside the RF cabin. Head movement was minimized by a

Group	N	Age	Sex		Handedness		Years of Education
		Mean/(SD)	M	F	L	R	
Controls	10	45/(13)	4	6	1	9	6.5/ (.5)
AVH	10	44(11)	1	9	1	9	5.3/ (.2)
Schizophrenia	10	39(11)	10	0	1	9	

Table 1. Demographic variables of the participant groups.

forehead strap and subjects wore noise insulated ear protectors.

2.4 Data analysis

FMRI data were analyzed using statistical parametric mapping (SPM2; Wellcome Department of Cognitive Neurology, London, UK). Preprocessing included reorientation and within subject image realignment with rigid-body transformations using the first image as reference. This procedure corrected images for any three-dimensional head movement that occurred between scans, and hence improved the sensitivity of analyses by reducing the amount of artefactual signal intensity changes present in the image series due to movement. Afterwards, coregistration of the functional and anatomical image took place, followed by spatial normalization to a standard template. Finally, images were smoothed using an 8-mm full width at half maximum (FWHM) Gaussian kernel to increase signal-to-noise ratio, accommodate normal variability in functional and gyral anatomy, and facilitate intersubject averaging of measured BOLD signal changes.

2.5 Statistics

2.5.1 Main effects

Functional images were analyzed on a voxel by voxel basis using multiple regression analysis (Worsley and Friston 1995) with one factor coding for activation (task versus rest), and 6 for movement related activation extracted from the realignment parameters. The threshold corresponded to a p-value of 0.001. The 6 movement related regressors were used as covariates in the analysis. Following first level analysis, second level random-effects analyses were conducted for within group effects (t-tests) with a p-value of $p < 0.01$. All p-values were uncorrected for multiple comparisons.

2.5.2 Psychophysiological interactions

The basic idea behind psychophysiological interactions (PPI's) is that the activity of one area is regressed on the activity of a second region. The slope of this regression reflects the correlation between the first and the second region. The way in which this slope changes under influence of the psychological condition baseline versus language

is called the psychophysiological interaction. It is a measure of how the slope is modulated by the experimental factor. Using PPI's we can determine which regions are functionally connected during language as compared to during baseline (Friston et al., 1997). In order to perform PPI analysis three vectors have to be established. The first vector consists of the first eigenvariate time series from the seed region. From each seed region a voxel is chosen to represent the activity in this region. The standard procedure, used in this study, is to select the highest activated voxel in a ROI across all subjects. A second vector consists of the psychological variable representing the experimental paradigm (language versus baseline). Finally a third vector has to be constructed representing the interaction between the first and the second vector. This third vector represents the interaction between the activity in the seed region and every other region in the brain modulated by the psychological factor. These vectors, extracted from each subjects individual dataset, are then entered into a second analysis for each subject with the first two vectors as covariates of interest and the third vector as the vector of interest with a contrast of $0\ 0\ 1$. Afterwards, second level random effect analyses are conducted for within group effects separately for every seed region yielding the PPI maps for each group. A significant effect means that the covariance between the source and other regions during language is significantly different from that during the baseline condition. Important in this routine is deconvolving the BOLD signal since the interactions are expressed at the neuronal level. This deconvolving is already present in the PPI routine in spm2.

3. Results

3.1 Phenomenology of AVH

A comparison made between the AVH reported by the schizophrenia patients and the AVH reported by the healthy subjects revealed both differences and similarities. Statements are based upon the CASH interview (Andreasen et al., 1992). Therefore they are mostly qualitatively instead of quantitatively. Both groups reported that the voices they experienced sounded very real, as coming from a person standing next to them. In addition both the schizophrenia patients and the healthy subjects with AVH localized the voices as

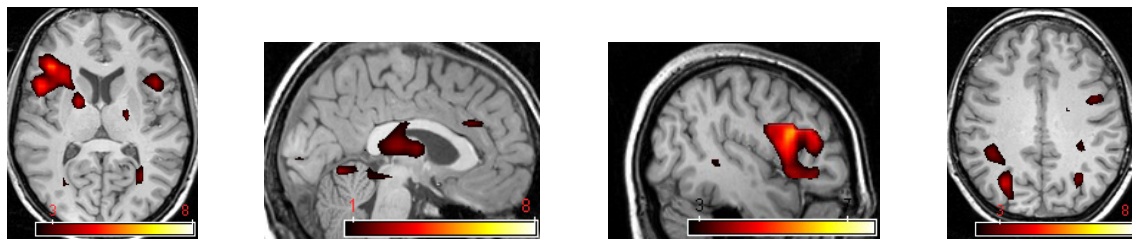


Figure 2A. SPM(T)'s for the healthy controls.

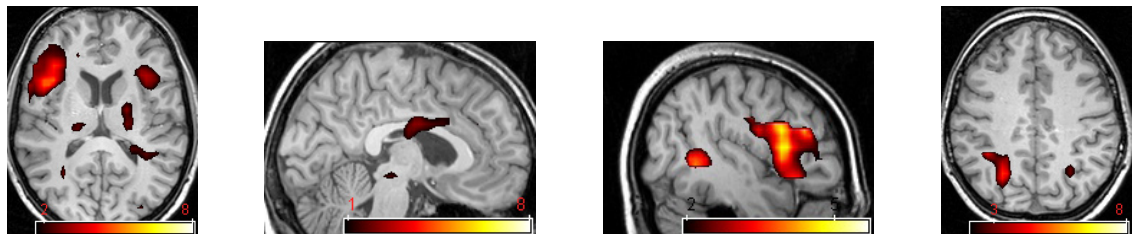


Figure 2B. SPM(T)'s for the healthy subjects with AVH.

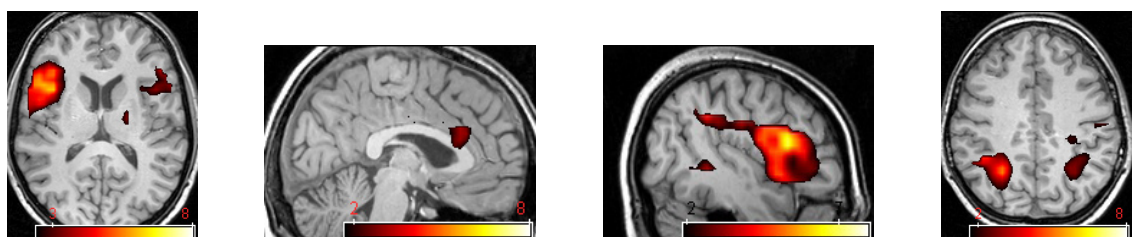


Figure 2C. SPM(T)'s for the schizophrenia patients.

coming from ‘the outside world’. Also all subjects experienced up to 6 different voices, mostly the voices of relatives, friends or other acquaintances. Differences were apparent in the frequency of the experienced hallucinations, the amount of positive versus negative content and the control the subjects could execute over their hallucinations. While the frequency of the hallucinations varied from multiple times per hour till once every three months in the healthy subjects with AVH, the schizophrenia patients experienced hallucinations almost constantly. Furthermore, all of the schizophrenia patients reported that the hallucinations made them either anxious or uncomfortable. Only one of the healthy subjects reported the hallucinations to be fearful occasionally. The same person reported the content of the voices to be negative sporadically. For the schizophrenia patients the content of the voices was negative, regularly. Moreover, the healthy subjects with AVH claimed to be able to execute come control over their hallucinations, meaning they could stop the hallucinations whenever they interfered with their daily activities. This was not the case for the schizophrenia patients. The only control they could execute was by focusing their attention on something different in which they succeeded occasionally.

During the verbal fluency task both groups

reported the absence of hallucinations.

3.2 ROI Main-effects Analysis

Figures display activation in the ROI's only. Images are in neurological orientation. Figure 2 shows the SPM(T)'s of the group averages of the control subjects (Figure. 2A), the healthy subjects with AVH (Figure. 2B) and the schizophrenia patients (Figure. 2C) after applying a threshold of $p < 0.01$. These results demonstrate that greater activity was observed in the left ACC, left IFG, left STG and left DLPFC during language relative to rest in all groups ($p < 0.01$).

3.3 Psychophysiological interaction analysis

3.3.1 Left ACC

Significant functional connectivity between the left ACC and the left temporal lobe, mainly the STG was found for both the controls subjects and the healthy subjects with AVH. This pattern was not found for the schizophrenia patients. The latter only showed one localized region of significant functional connectivity with the left ACC consisting of the right cingulate gyrus. This

Group	Coordinates			Z score	P value
	X	Y	Z		
Control subjects					
R DLPFC	12	51	16	2.63	0.004
L Middle Temporal Gyrus	-51	-64	20	2.18	0.015
R Cingulate Gyrus	8	-45	35	1.97	0.025
L DLPFC	-8	48	20	1.81	0.035
R Middle Temporal Gyrus	51	-65	20	1.81	0.035
Corpus Callosum	4	27	2	1.77	0.038
R Medial Frontal Gyrus	8	59	11	1.68	0.047
L Superior Temporal Gyrus	-51	-61	21	2.18	0.015
R Superior Temporal Gyrus	51	-61	21	1.68	0.046
AVH					
R Thalamus	12	-34	13	3.07	0.001
R Postcentral Gyrus	44	-26	34	2.76	0.003
L Lateral Ventricle	-20	-34	16	2.71	0.003
R Middle Temporal Gyrus	51	-66	7	2.71	0.003
R Precentral Gyrus	40	-2	33	2.69	0.004
L Claustrum	-28	12	7	2.63	0.004
L Middle Temporal Gyrus	-36	-65	18	2.43	0.008
R Caudate	20	-2	30	2.22	0.013
Interhemispheric	0	12	7	2.05	0.020
L Superior Frontal Gyrus	-20	48	4	2.19	0.014
R Superior Temporal Gyrus	40	-38	17	2.56	0.005
L Superior Temporal Gyrus	-48	-20	-2	1.96	0.025
Schizophrenia Patients					
R Cingulate Gyrus	8	-26	31	2.19	0.014

Table 2. Summary of psychophysiological interaction analyses for the left ACC.

connection was not present in the other groups.

For the control subjects significantly greater activity for the interaction between the left ACC and the left DLPFC was observed during letter fluency relative to the baseline condition. This finding was not replicated for the subjects with AVH and the schizophrenia patients. Furthermore the subjects with AVH displayed multiple widespread nonlocalized covarying activity with the left ACC. The SPM(T)'s from this analysis are shown in Figure 4 and table 4 the locations of the maximally activated voxels are shown. Images are in neurological orientation. Results for the schizophrenia patients are displayed in sagittal instead of transverse view in order to show the localized interaction with the cingulate gyrus. Using a transverse view this cannot be visualized very well.

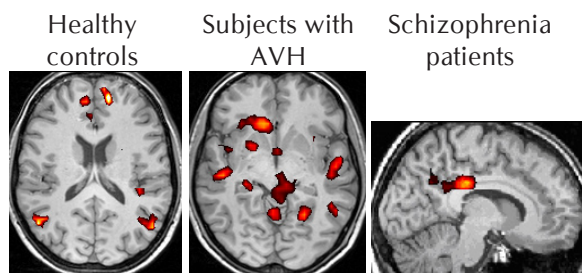


Figure 3. SPM(T)'s for the PPI analyses for the left ACC.

3.3.2 Left STG

The hypothesized interaction between the left STG and the left IFG was found in the control subjects. The healthy subjects with AVH and the schizophrenia patients failed to show this Interaction. The SPM(T)'s of this analysis are shown in Figure 5 and in table 4 the locations of the maximally activated voxels are shown. Images are in neurological orientation.

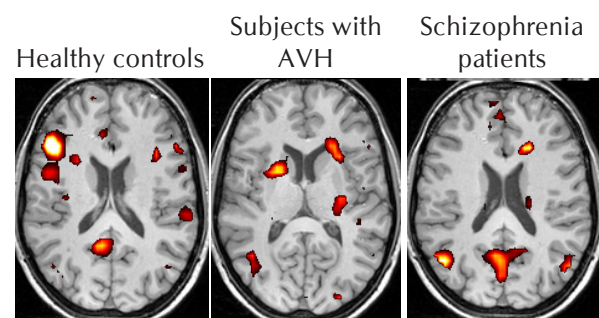


Figure 4. SPM(T)'s for the PPI analyses for the left STG.

4. Discussion

To date, language connectivity has not been examined in healthy subjects experiencing AVH. We examined this group in order to be able to study this symptom in isolation. Hallucinating healthy subjects were compared to non-hallucinating

healthy subjects as well as to hallucinating schizophrenia patients.

The functional connectivity analysis that tested for the interaction between activity in the left ACC and word fluency task performance in the healthy controls revealed a clear interaction with the left STG. Healthy subjects with AVH showed the same interaction with the left STG, however, they showed a more widespread pattern throughout the brain which is in agreement with Boksman et al. (2005). In their study, the schizophrenia patients didn't show any interaction with the temporal cortex. In the current study, the only interaction the schizophrenia patients displayed with the left ACC as the seed region consisted of the right cingulate gyrus. This is in accordance with Boksman et al. (2005) in which never treated schizophrenia also displayed an interaction with the right cingulate gyrus. In the current study an interaction between the left ACC and the right cingulate gyrus was observed in the control subjects as well, but not in the healthy subjects with AVH. The cingulate gyrus has been reported to be involved in attention, executive processes, word generation, and memory (Petersen et al., 1988). Verbal fluency tasks are besides a measure of language, a measure of executive function and working memory. According to the dual-route-self-monitoring-hypothesis, the ACC functions as a control center, interacting with regions crucial in adequate execution of the experimental task. The isolated interaction with the right cingulate gyrus in the schizophrenia patients could be implying the high demands placed on these subjects in order to carry out the task correctly. The widespread pattern of activation covarying with ACC activation in the healthy subjects with AVH could be indicative of the inability of the ACC to monitor recruitment and activation of other areas, effectively, leading to recruitment of regions of less interest in execution of the task.

The healthy people with AVH differ from the schizophrenia patients not solely on the basis of the multitude of symptoms but also on the way they regulate the hallucinations. The first group claims that they are generally able to stop the hallucinations or call on them. The ACC plays a major role in executive cognitive, attention and motor functioning as well as mediating emotions (Devinsky et al., 1995; Paus, 2001; Yucel et al., 2003). Since our subjects with AVH have the ability to regulate their hallucinations, connectivity with the left temporal region is perhaps not disrupted in this subgroup. In order to determine this relationship

further research should focus on comparing people with AVH on the basis of the criterion control versus no control over the hallucinations. A different explanation is that differences in connectivity between the schizophrenia patients and the healthy subjects are related to the frequency of the hallucinations or to the general cognitive decline present in the schizophrenia patients. Secondly, the healthy controls showed a focal localized interaction between the left ACC and the left DLPFC. This pattern was not found in the other groups. Fletcher et al. (2001) established dysfunctional connectivity between the left prefrontal cortex and the left ACC and the left STG in schizophrenia patients during the performance of a language task. Their interpretation was dysfunctional cingulate modulation of prefrontal influence of the left STG. Since we did not find prefrontal-STG dysconnectivity their findings could also be interpreted as a dysfunction of both ACC-prefrontal dysconnectivity and ACC-STG dysconnectivity. This interpretation is in agreement with Spence et al. (2000) who demonstrated reduced functional connectivity between the left DLPFC and the left ACC in schizophrenia patients, but not between the left DLPFC and the left STG.

For the PPI analysis with the left STG as the seed region a localized interaction was found with the left IFG for the healthy controls. For the healthy subjects with AVH and the schizophrenia patients this connection was absent as was also found by Burns et al., (2003) using structural connectivity analysis (e.g. DTI). Our findings point to a disruptive or dysfunctional connection between language areas for execution and perception of speech. These disruptions could be the basis for the liability to AVH, since they are possibly responsible for differentiating between self formed speech and external speech.

From the results described above it can be concluded that the dysfunctional connections present in the schizophrenia patients replicate the results of previous studies. Considering the healthy subjects with AVH the same dysconnections are present apart from the connection between the left ACC and the left STG. These findings are partly in agreement with the dual-route-self-monitoring-hypothesis. The interaction between the left IFG and the left ACC as predicted in the dual-route-self-monitoring-hypothesis was not present in either of the groups. However, there was a clear interaction between the left DLPFC and the left ACC.

The anatomical boundaries of the DLPFC have

not been precisely defined. The term DLPFC is commonly used to refer to part of the frontal lobe and comprises of the inferior frontal gyrus the middle frontal gyrus and the lateral aspect of the superior frontal gyrus (John et al., 2006). Brodmann area 46 which is generally accepted to be part of the DLPFC, as was the case in our study, is often referred to be part of the IFG. With this in mind one could argue in favor of the dual-route-self-monitoring-hypothesis. Nevertheless, in future research, one should focus on the relation between the DLPFC and the IFG.

4.1 Limitations and suggestions for future research

The results of this study should be interpreted with caution for multiple reasons. Firstly we only studied a small sample of participants in each group due to the fact that recruiting healthy subjects with AVH is quite challenging.

Secondly the participant groups were not matched for sex. The group of schizophrenia patients existed of 9 male and only one female participant, while the group of healthy people with AVH was comprised of only one male participant. This was due to the fact that most schizophrenia patients volunteering were males and almost all healthy participants that responded to our website were females. Furthermore, of the schizophrenia patients volunteering for this study, all but one woman had to be excluded because of scanner anxiety. Considering the healthy subjects experiencing AVH, the researchers are not aware whether the higher amount of women volunteering was due to a response bias or whether the percentage of women experiencing AVH without meeting the criteria for a psychiatric diagnose, is actually higher. A future study should attempt to seek out which is the case. Therefore, we focused on exact matching of our subgroups on other characteristics. However, a study by Weiss et al. (2003) showed that men and women, that did not differ significantly in verbal fluency task performance, showed a very similar pattern of brain activation. Also differences in language lateralization between men and women are absent (Sommer et al., 2004).

Thirdly since our scanning protocol consisted of a 20 slice EPI our analysis was limited to our regions of interest. Additional regions with the possibility of differential activations could not be mentioned in this study. Using a larger scanning

protocol would enable us to have a look at additional regions such as the cerebellum.

Also the measures of behavioral performance used are qualitative in origin. Therefore a direct relationship between the performance level and the measured activation cannot be determined. A quantitative measure could solve this.

Finally there are some limitations to the method used. In the PPI routine it is assumed that the task represented by an experimental condition is mediated by a network of interacting brain regions and those different tasks correspond to different functional networks. The problem however lies in the fact that large covariances in interregional activity can come about by both direct and indirect effects. Two regions' activities may have a large correlation if they are anatomically linked, and if that link is functional in a specific task. However, they also could have a large correlation if they receive inputs from a common region. Most likely, a combination of both direct and indirect effects occurs at the same time, presenting a major interpretation problem for the covariance paradigm (Horwitz et al., 1999). Furthermore, it is not possible to determine the weight of the correlation coefficients between interacting regions. Different methods like structural equation modeling should be used in addition to determine direct and indirect effects and the path coefficients between interconnected regions.

Also, even though the contrast used as the psychological factor differs in a meaningful way, language versus baseline, it is only informative about language in a broad sense. Interpretations about how the differences are related to AVH are rather loose. Therefore it would be meaningful to study execution versus perception of language a contrast which is believed to be important in the origin of AVH.

In summary, schizophrenia patients and healthy subjects with AVH display dysfunctional connectivity between the regions important in the perception and production of speech. Furthermore, the presence of a functional connection between the left ACC, important in executing cognitive control, presumes that healthy subjects with AVH can execute some control over their hallucinations. Future research should focus on more sophisticated methods to study the integration between brain regions important in the perception and production of speech in subjects with AVH.

References

- Aleman, A., Bocker, KB., De Haan, EH. (2001). Hallucinatory predisposition and vividness of auditory imagery: self-report and behavioral indices. *Perceptual Motor Skills* 93 (1), 268-74.
- Andreasen, NC., Flaum, M., Arndt, S (1992). The comprehensive assessment of symptoms and history (CASH): An instrument for assessing psychopathology and diagnosis, *Arch. Gen. Psychiatry* 49, 615-623.
- Boksman, K., Theberge, J., Williamson, P., Drost, DJ., Malla, A., Densmore, M., Takhar, J., Pavlosky, W., Menon, RS., Neufeld, RW. (2005). A 4.0-T fMRI study of brain connectivity during word fluency in first-episode schizophrenia. *Schizophrenia Research* 15;75 (2-3), 247-63.
- Burns, J., Job, D., Bastin, ME., Whalley, H., Macgillivray, T., Johnstone EC., Lawrie, SM. (2003). Structural disconnectivity in schizophrenia: a diffusion tensor magnetic resonance imaging study. *British Journal of Psychiatry* 5 (182), 439
- Curtis, VA., Bullmore, ET., Brammer, MJ., Wright, IC., Williams, SCR., Morris, RG., Sharma, TS., Murray, RM., McGuire, PK. (1998). Attenuated frontal activation during a verbal fluency task in patients with schizophrenia. *American Journal of Psychiatry* 155 (8), 1056-1063
- Creutzfeldt, O., Ojemann, G., Lettich, E (1989a). Neuronal activity in the human lateral temporal lobe: Responses to speech. *Experimental Brain Research* 77 (3), 451-75
- Creutzfeldt, O., Ojemann, G., Lettich, E (1989b). Neuronal activity in the human lateral temporal lobe: Responses to the subjects own voice. *Experimental Brain Research* 77 (3), 476-89.
- Dejerine, J. (1895). *Anatomie des Centres Nerveux. Paris: Rueff et Cie*
- Devinsky, O., Morrell, MJ., Vogt, BA. (1995). Contributions of anterior cingulate cortex to behaviour. *Brain* 118(1), 279-306.
- Dierks, T., Linden, DE., Jandl, M., Formisano, E., Goebel, R., Lanfermann, H., Singer, W. (1999). Activation of Heschl's gyrus during auditory hallucinations. *Neuron* 22, 615-621
- Fletcher, P., McKenna, PJ., Friston, KJ., Frith, CD., Dolan, RJ (1999). Abnormal cingulate modulation of fronto-temporal connectivity in schizophrenia. *Neuroimage* 9(3), 337-42
- Friedman, L., Kenny, JT., Wise, AL., Wu, D., Stuve, TA., Miller, DA., Jesberger, JA., Lewin, JS. (1998). Brain activation during silent word generation evaluated with functional MRI. *Brain and language* 64, 231-256.
- Friston, KJ., Frith, CD., Liddle, PF., Frackowiak, RSJ. (1991). *Biological Sciences* 244 (1310), 101-106
- Friston, KJ., Buechel, C., Fink, GR., Morris, J., Rolls, E., Dolan, RJ. (1997). Psychophysiological and modulatory interactions in neuroimaging. *Neuroimage* 6 (3), 218-29.
- Frith, CD., Done, DJ. (1988). Towards a neuropsychology of schizophrenia. *British Journal of Psychiatry* 153, 437-43.
- Frith, CD., Friston, KJ., Liddle, PF., Frackowiak, RSJ. (1991b). Willed action and the prefrontal cortex in man: A study with PET. *Proceedings of the Royal Society of London* 244, 241-246.
- Frith, CD. (1992). *The Cognitive Neuropsychology of Schizophrenia. Lawrence Erlbaum, Sussex, UK.*
- Frith, CD., Friston, KJ., Herold, S., Silbersweig, D., Fletcher, P., Cahill, C., Dolan, RJ., Frackowiak, RSJ., Liddle, PF. (1995). Regional brain activity in chronic schizophrenic patients during the performance of a verbal fluency task. *British Journal of Psychiatry* 167, 343-349
- Fu, CH., Suckling, J., Williams, SC., Andrew, CM., Vythelingum, GN., McGuire, PK. (2005). Effects of psychotic state and task demand on prefrontal function in schizophrenia: an fMRI study of overt verbal fluency. *American Journal of Psychiatry* 162 (3), 485-494.
- Fu, CHY., McIntosh, AR., Kim, J., Chau, W., Bullmore, ET., Williams, SCR., Honey, GD., McGuire, PK. (2006). Modulation of effective connectivity by cognitive demand in phonological verbal fluency. *Neuroimage* 30(1), 266-71.
- Grossberg, S. (2000). How hallucinations may arise from brain mechanisms of learning, attention and volition. *J.Int. Neuropsychol. Soc.* 6, 583-592.
- Hoffman, RE. (1986). Verbal hallucinations and language production processes in schizophrenia. *Behavioral and Brain Sciences* 9, 503-548.
- Horwitz, b., Tagamets, MA., McIntosh, AR. (1999). Neural modeling, functional brain imaging and cognition. *Trends Cogn. Sci.* 3 (3), 91-98
- Hubl, D., Koenig, T., Strik, W., Federspiel, A., Kreis, R., Boesch, C., Maier, SE., Schroth, G., Lovblad, K., Dierks, T. (2004). Pathways that make voices: white matter changes in auditory hallucinations. *Archives of Genetic Psychiatry* 61(7), 658-68.
- Hutchinson, M., Schiffer, W., Joseffer, S., Liu, A., Schlosser, R., Dikshit, S., Goldberg, E., Brodie, JD. (1999). Task-specific deactivation patterns in functional magnetic resonance imaging. *Magnetic Resonance Imaging* 17(10), 1427-36.
- Indefrey, P., Levelt, WJM. (2000). The neural correlates of language production. *Gazzaniga, MS., The New Cognitive Neurosciences, second edition The MIT Press, Cambridge, MA*, 845-865.
- John, PJ., Wang, L., Amanda, J., Moffitt, Harmeeta, Singh, K., Mokhtar, Gado, H., Csernansky, JG. (2006) Inter-rater reliability of manual segmentation of the superior, inferior and middle frontal gyri. *Psychiatry Res.* 1;148(2-3), 151-63
- Laroi, F., Marczewski, P., Van der Linden, M. (2004). Further evidence of the multi dimensionality of hallucinatory predisposition: factor structure of a modified version of the Launay-Slade Hallucinations

- Scale in a normal sample. *Eur Psychiatry* 19(1), 15-20
- Liddle, PF. (1997). Dynamic neuroimaging with PET, SPET, or fMRI, *International Review of Psychiatry* 9(4), 331-337.
- McGuire, PK., Shah, GM., Murray, RM. (1993). Increased blood flow in Broca's area during auditory hallucinations in schizophrenia. *Lancet* 342 (8873): 703-706
- Morris, R., Pandya, DN., Petrides, M. (1999). Fiber system linking the mid-dorsolateral frontal cortex with the retrosplinal/presubicular region in the rhesus monkey. *Journal of Comparative Neurology*, 407, 183-192
- Müller-Preuss, P., Ploog, D. (1981). Inhibition of auditory cortical neurons during phonation. *Brain Res* 215, 61-76
- Nayani, TH., David, AS. (1996). The auditory hallucination: a phenomenological survey. *Psychological Medicine* 26 (1), 177-89.
- Paus, T (2001). Primate anterior cingulate cortex: where motor control, drive and cognition interface. *NatRev Neurosci* 2 (6), 417-24.
- Petrides, M, Pandya, DN. (1988). Association fiber pathways to the frontal cortex from the superior temporal region in the rhesus monkey. *Journal of Comparative Neurology* 273, 52-66
- Petersen, SE., Fox, PT., Posner, MI. (1988). Positron emission tomographic studies of the cortical anatomy of single-word-processing. *Nature* 331, 585-589
- Schaufelberger, M., Senhorini, MC., Barreiros, MA., Amaro, E., Menezes, PR., Scazufca, M., Castro, CC., Ayres, AM., Murray, RM., McGuire, PK., Busatto, GF. (2005). Frontal and anterior cingulate activation during overt verbal fluency in patients with first episode psychosis. *Rev Bras Psiquiatr* 27(3), 228-32
- Schlösser, R., Hutchinson, M., Joseffer, S., Rusinek, H., Saarimaki, A., Stevenson, J., Dewey, SL, Brodie, JD. (1998). Functional magnetic resonance imaging of human brain activity in a verbal fluency task. *Journal of Neurology, Neurosurgery and Psychiatry* 64, 492-498
- Spence, A., Liddle, PF., Stefan, MD., Hellewell, JSE., Sharma, T., Friston, KJ., Hirsch, SR., Frith, CD., Murray, RM., Deakin, JFW., Grasby, PM. (2000). Functional anatomy of verbal fluency in people with schizophrenia and those at genetic risk. *British Journal of Psychiatry* 176, 52-60.
- Van Os, J., Hanssen, M., Bijl, RV., Ravelli, A. (2000). Strauss (1969) revisited: a psychosis continuum in the general population? *Schizophrenia Research* 29 (1-2), 11-20.
- Whalley, HC., Simonotto, E., Marshall, I., Owens, DG., Goddard, NH., Johnstone, EC., Lawrie, SM. (2005). Functional disconnectivity in subjects at high genetic risk of schizophrenia. *Brain* 12 (9), 2097-108.
- Worsley, KJ., Friston, KJ. (1995). Analysis of fMRI time-series revisited again. *Neuroimage* 2 (3), 173-81
- Yucel M, Pantelis C, Stuart GW, Wood SJ, Maruff P, Velakoulis D, et al. (2002). Anterior cingulate activation during Stroop task performance: a PET to MRI coregistration study of individual patients with schizophrenia. *Am J Psychiatry* 159(2), 251-4.
- Yurgelun-Todd, DA., Wateriaux, CM., Cohen, BM., Gruber, SA., English, CA., Renshaw, PF. (1996). Functional magnetic resonance imaging of schizophrenic patients and comparison subjects during word production, *American Journal of Psychiatry* 153, 200-205.

Effects of sentence context in L2 natural speech comprehension

Ian FitzPatrick^{1,2}
Supervisors: Peter Indefrey^{1,2}

¹*F.C. Donders Centre for Cognitive Neuroimaging, Nijmegen, The Netherlands*

²*Max Planck Institute for Psycholinguistics, Nijmegen, The Netherlands*

Electrophysiological studies consistently find N400 effects of semantic incongruity in non-native written language comprehension. Typically these N400 effects are later than N400 effects in native comprehension, suggesting that semantic processing in one's second language (L2) may be delayed compared to one's first language (L1). In this study we were firstly interested in replicating the semantic incongruity effect using natural auditory speech, which poses strong demands on the speed of processing. Secondly, we wished to investigate whether a possible delay in semantic processing might be due to bilinguals accessing lexical items from both their L1 and L2 (a more extensive lexical search). We recorded EEG from 30 Dutch-English bilinguals who listened to English sentences in which the sentence-final word was: (1) semantically fitting, (2) semantically incongruent, (3) initially congruent: semantically incongruent, but sharing initial phonemes with the most probable sentence completion within the L2, (4) semantically incongruent, but sharing initial phonemes with the L1 translation equivalent of the most probable sentence completion. We found an N400 effect in each of the semantically incongruent conditions. This N400 effect was significantly delayed to L2 words that were initially congruent with the sentence context. We found no effect of initial overlap with L1 translation equivalents. Taken together these findings firstly demonstrate that non-native listeners are sensitive to semantic incongruity in natural speech, secondly indicate that semantic integration in non-native listening can start on the basis of word initial phonemes, and finally suggest that during L2 sentence processing listeners do not access the L1 lexicon.

Keywords: Language, Bilingualism, Speech Comprehension, Lexicon, Semantics, Phonology, Event-Related Potentials

Correspondence to: Ian FitzPatrick, F.C. Donders Centre for Cognitive Neuroimaging, P.O. Box 9101, NL-6500 HB, Nijmegen, The Netherlands; e-mail: Ian.FitzPatrick@fcdonders.ru.nl.

1. Introduction

Language comprehension in a language other than one's native language can be a challenging feat. Interestingly, electrophysiological studies of written language comprehension in bilinguals have consistently revealed a delay in bilingual semantic processing relative to monolinguals (Ardal, Donald, Meuter, Muldrew, & Luce, 1990; Hahne, 2001; Weber-Fox, Davis, & Cuadrado, 2003).

Bilinguals have also been shown to perform slower than monolinguals in lexical decision tasks (e.g., Scarborough, Gerard, & Cortese, 1984; Soares & Grosjean, 1984). This observation has been related to bilinguals having to perform a more extensive lexical search than monolinguals (Soares & Grosjean, 1984).

Later studies, also employing lexical decision paradigms, revealed that bilinguals are slower at recognising interlingual homophones (Dijkstra, Grainger, & Van Heuven, 1999) and pseudohomophones (Nas, 1983) than control items. This indicates that lexical items, from both the bilinguals L1 and L2, compete for selection during word recognition.

To date, only a handful of studies have been published that directly investigate non-native auditory sentence comprehension. As far as we know, only one such study has employed natural connected speech (Sanders & Neville, 2003). Therefore, in the present study, we are firstly interested whether we can replicate the finding of delayed semantic processing in bilinguals using natural speech, and secondly, whether this delayed semantic processing, at the sentence level, is due to bilinguals non-selectively accessing lexical candidates from both L1 and L2, thus performing an extensive lexical search.

1.1 Non-selective lexical access

There is converging evidence that word recognition in bilinguals occurs in a language non-selective manner (for an overview see: Dijkstra, 2005). In the domain of auditory word recognition, findings indicate that even though bilinguals have been shown to be able to accurately judge language membership on the basis of very little acoustic information (Grosjean, 1988; Li, 1996), interlingual competition is still very much apparent. In a cross-modal priming, lexical decision paradigm Schulpen, Dijkstra, Schriefers and Hasper (2003) found evidence for priming in Dutch-English bilinguals

from both English and Dutch pronunciations of an interlingual homophone (/li:f/ (Dutch)-LEAF; /li:f/ (English)-LEAF) as compared to unrelated control words. This suggests that interlingual homophones activate lexical candidates from both languages, which then compete for selection. More compelling evidence was obtained by Spivey and Marian (1999), who showed that Russian-English bilinguals fixated on interlingual and intralingual competitors more often than on unrelated competitors in an eye-tracking paradigm while listening to spoken Russian; thus indicating the existence of competition both within and between languages in bilingual speech comprehension (Marian & Spivey, 2003a, 2003b; Marian, Spivey, & Hirsch, 2003; Spivey & Marian, 1999). This observation was replicated by Weber and Cutler (2004) in Dutch-native speakers of English listening to spoken English.

Thus it seems that, for bilingual speakers, even in a purely monolingual situation, there is spurious activation from the non-target language.

1.2 Event-related potentials

The most studied electrophysiological effect in language comprehension is a negative deflection in the ERP, that peaks around 400 ms after stimulus onset, termed the N400 (Kutas & Hillyard, 1980). The N400 occurs in response to words which are semantically incongruous within the current language context but can also be observed after presentation of non-words (Holcomb & Neville, 1990) or words with a low cloze probability in a particular sentence (Kutas & Hillyard, 1984). The amplitude of the N400 has been shown to be sensitive to word frequency (Van Petten & Kutas, 1990), with less frequent words eliciting a larger N400. The most commonly held interpretation of the N400 is that it is related to semantic processing of the eliciting word and that its amplitude indexes the ease of semantic integration (e.g., Brown & Hagoort, 1993; Hagoort & Brown, 2000; Holcomb, 1993). Interestingly, non-native language comprehension has been associated with a delayed peak latency of the N400 effect (Ardal et al., 1990) and N400 component (Weber-Fox & Neville, 1996) and an attenuated N400 effect (Hahne, 2001) in response to semantic incongruity versus congruity, and a larger N400 in response to non-words (Sanders & Neville, 2003). Furthermore, Hahne (2001) observed a more negative N400 component for semantically congruous words in L2 speakers as compared to native speakers.

Other electrophysiological evidence of an influence of sentence context on word recognition relates to an early negative effect preceding the N400. This early negative effect has, in some cases, been interpreted as a discernible ERP component referred to as the N200 or *phonological mismatch negativity* (PMN).¹ In an auditory word recognition task using high cloze probability sentence contexts (Connolly, Stewart, & Phillips, 1990) found an early negative effect in the 270-300 ms range, which they initially termed the N200 and later refer to as the PMN (Connolly & Phillips, 1994; Connolly, Phillips, Stewart, & Brake, 1992). A PMN was elicited when the initial phonemes of the critical word in a sentence did not match those of the highest cloze probability word.

Van Petten, Coulson, Rubin, Plante and Parks (1999) found an early negative effect to semantically incongruent target words (e.g., “It was a pleasant surprise to find that the car repair bill was only seventeen *scholars*”) compared to semantically congruent target words (e.g., “It was a pleasant surprise to find that the car repair bill was only seventeen *dollars*”). This early negative effect preceded the isolation point of the target words and was absent in cases where the target word shared initial phonemes with the semantically congruent sentence completion (e.g., “It was a pleasant surprise to find that the car repair bill was only seventeen *dolphins*”). The authors took this as evidence that semantic integration can start even on incomplete acoustic information.

In a similar study, Van den Brink, Brown and Hagoort (2001) found evidence of an effect of sentence context, possibly even as early as 140 ms after word onset. They contrasted three conditions in an experimental setting in which participants listened to high cloze sentences. In the fully congruent (FC) condition, the critical word, in the sentence final position, was a high cloze probability word. In the fully incongruent (FI) condition, the critical word was semantically incongruent in relation to the sentence. Finally, in the initially congruent (IC) condition, the critical word shared a phonemic onset with the highest cloze probability sentence continuation. Event Related Potentials time-locked to the onset of the critical word revealed an N400 component that was significantly more negative in the FI and IC conditions. This was taken to reflect the difficulty of integrating a semantically incongruent word with the sentence context. More interestingly they also found an early negative effect (N200) in the 150-250 ms time

window in each condition, which was significantly more negative in the FI condition. Thus, in the situation where the incoming initial phonemes of the sentence final word matched those of the most probable continuation of the sentence (i.e., in the FC and IC conditions) the early negative effect was attenuated. Additionally, in the aforementioned studies, the N400 in the initially congruent conditions was delayed with respect to its onset (Van den Brink et al., 2001) and peak latency (Connolly & Phillips, 1994; Van Petten et al., 1999).

In a recent study, Diaz and Swaab (in press), investigated the early negative effect in response to violations of expectancy in auditorily presented alliterative word lists (e.g., “chat, champ, chaff, chant, challis, chad, chap, *address/chapter*”), categorical word lists (e.g., “giraffe, sheep, bear, wolf, rabbit, lamb, elephant, *desk/dog*”), and sentence contexts that were either (1) semantically congruent, (2) initially semantically congruent, (3) semantically congruent but of a lower cloze probability, or (4) semantically incongruent. The authors found a dissociation between the early negative effect, which was evident in alliterative word list contexts in response to phonologically incongruent words, and the N400 effect, which arose in the comparison between congruent and incongruent words in categorical lists. In sentence contexts the authors replicated the finding of an early negative effect that was greater for semantically incongruent words than for semantically congruent words, but did not differ between initially congruent words and congruent words. The early negative effect in response to phonological violations in list contexts had a different scalp topography compared to the early negative effect in response to semantic violations in sentence contexts, the latter having a distribution consistent with that of the N400.

The mechanisms underlying the early negative effect are subject to debate. Connolly and Phillips (1994) argue that the PMN reflects the matching of the incoming initial phonemes to an acoustic template, which is generated based on the expectation of the upcoming word. Newman (2003) made an intriguing case for this interpretation. They presented participants with a visual prime word (CLAP) and instructed them to internally delete the initial phoneme (LAP). They then aurally presented the correct deletion (LAP), an incorrect deletion (CAP), a deletion of the initial cluster (AP) or an unrelated word (NOSE). The PMN was comparable across all incorrect conditions, but was found to be attenuated in the correct condition suggesting that

the PMN indeed reflects an acoustic comparison process.

In contrast to this phonological account, Van den Brink et al. propose a semantic account for the N200, namely that the N200 cannot be interpreted as a mismatch negativity as the early negative effect is present in all experimental conditions including conditions that are initially or fully congruent (when there is no mismatch). Van den Brink, et al. (2001) suggest that the N200 could reflect a process whereby candidates in the auditory cohort are individually assessed as to their goodness-of-fit within the sentence context (a lexically driven process) and would thus be part of the lexical selection process. There are also suggestions that the early negative effect could be an early onset of the N400 (Diaz & Swaab, in press; Van Petten et al., 1999), based on the fact that a number of studies do not find a differential scalp topography between the early negative effect and the N400 (Connolly & Phillips, 1994; Diaz & Swaab, in press; Van den Brink & Hagoort, 2004) or indeed any evidence pointing to two discernible components in either single subject averages or grand averages (Van Petten et al., 1999).

Clearly, while interpreting sentences in one's native language, sentence context can influence the recognition of high cloze probability words even on the basis of only their initial phonemes. Given the complexities of non-native language comprehension, it is an open question whether contextual constraints can exert a similar early influence on word recognition in non-native language comprehension as is evident in native language comprehension.

1.3 Objectives

Thus our main question is whether we can obtain electrophysiological evidence for an early influence of sentence context in non-native language comprehension at all.

Secondly, given the converging evidence for language non-selective access to the bilingual lexicon, we are interested whether we could find evidence for activation of L1 lexical items in L2 natural speech comprehension.

Additionally we hope to find evidence that will elucidate the functional nature of the early negative effect and would enable us to further the debate surrounding its interpretation.

To investigate this we presented participants with auditory sentences in their L2, in an ERP paradigm similar to the one employed by Van den Brink et al. (2001). The study incorporated the Fully Congruent (FC) and Fully Incongruent (FI) conditions from the original design. It additionally included a within language overlap condition in which the initial overlap was with the highest cloze probability word (ICL2), and a between language overlap condition in which the initial overlap was with the translation of the highest cloze probability word into the participants' L1 (ICL1) (see Table 1 for examples of stimulus materials).

We hypothesise that if non-native listeners are capable of utilising contextual information at an early stage of the word recognition process we will notice an attenuated early negative effect and/or a delayed N400 component in the ICL2 condition as compared to the FI condition.

Secondly, if the early negative effect and N400 component are similarly attenuated and/or delayed in the ICL1 condition in comparison to the FI condition, we will have compelling evidence that lexical candidates from the participants' L1 are active even in a monolingual L2 sentence context.

This finding would be appealing, in terms of our third research question, as it has the potential of distinguishing between the conflicting interpretations of the early negative effect. Given that the highest cloze probability item and its direct translation equivalent greatly if not completely overlap in terms of their semantic features, the absence of an early negative effect in the ICL1

Condition	Sentence	Target
FC	To get water from a well, you need a <i>bucket</i> .	bucket
FI	The window cleaner carried a sponge, a ladder and a <i>pie</i> .	bucket
ICL1	The cleaning lady used soapy water from a large iron <u>embassy</u> .	bucket (Dutch: <u>emmer</u>)
ICL2	You need to put something under that leaky roof; do you have a <u>bubble</u> ?	<u>bucket</u>

Table 1. Examples of stimulus materials. Underlining illustrates phonemic overlap.

condition compared to the FC condition would clearly suggest that the initial overlap activates lexical candidates from the participants' L1. As it is highly unlikely that participants would explicitly expect an L1 word in an L2 sentence context, it would indicate that the early negative effect could not simply reflect the acoustic matching of incoming phonemes to a template, but must rather be interpreted as an effect of semantic processing.

2. Methods

2.1 Participants

Thirty right-handed Dutch-English bilinguals participated in the experiment, 26 of which were included in the final analysis (7 men; mean age 23.7 years). The participants' English proficiency was assessed using the average z-scores on 50 grammaticality judgement items of the Oxford Placement Test (Allan, 1992) (mean score: 43.65, SD = 2.68; maximum score: 50) and a non-speeded lexical decision test (60 items), created by Meara (1996) and later adapted by Lemhöfer, Dijkstra and Michel (2004) (mean score: 44.42, SD = 5.78; maximum score: 60). Participants were either paid a small fee or they received study credits. None of the participants had any neurological impairment. All participants gave their written informed consent.

Dutch	English
a:	ɑ:
α	Λ
ɛ, ɵ	ɛ, æ²
ɪ	ɪ
î	î:
ɔ	ɒ
o:	ɔ:, əʊ
u, ʏ	u:
@	@
ɔ̥	aʊ

Table 2. Phoneme correspondences between Dutch and English, displayed using the International Phonetic Alphabet (IPA) (International Phonetic Association, 1999), used to define phonemic overlap.

2.2 Materials

Participants listened to English sentences that belonged to one of four conditions. In the

FC condition sentences ended in a high cloze probability word, e.g., “When you buy duty free goods, you don’t have to pay *tax*”. In the FI condition sentences ended in a semantically incongruent word, e.g., “When you buy duty free goods, you don’t have to pay *contact*”. In the ICL2 condition the sentence final word shared initial phonemic overlap with the highest cloze probability word, e.g., “When you buy duty free goods, you don’t have to pay *tadpole*” (initial overlap with *tax*). In the ICL1 condition the sentence final word shared initial phonemic overlap with the direct translation of the highest cloze probability word in the participant’s L1, e.g., “When you buy duty free goods, you don’t have to pay *baboon*” (initial overlap with “*belasting*” where *belasting* is Dutch for *tax*). We defined a number of correspondences between Dutch and English vowels and diphthongs (see Table 2) which we considered to be sufficiently similar to constitute an overlap. In each case the extent of the overlap was the vowel and initial consonant or consonant cluster.

We created 152 sentence frames in 38 quadruplets. The target words for each quadruplet consisted of one high cloze probability word (FC condition) and three semantically incongruent words (FI, ICL1 and ICL2 conditions). We created two stimulus lists, each with a different pairing of target word and sentence frame. Each sentence frame occurred only once per stimulus list. Seventy-six semantically congruent filler sentences were created and added to both lists to balance the number of sentences that were incongruent and congruent. Half of the participants were presented with stimuli from the first list, and half were presented with stimuli from the second list.

To give us a clear marker of critical word onset for time-locking the EEG, all critical words were chosen from English nouns that had either a plosive onset or vowel onset with a glottal stop. The distribution of critical words with a voiced plosive, unvoiced plosive, and vowel onset was kept constant over conditions. Critical words were controlled across conditions with respect to the number of phonemes and word frequency (see Table 3). Word frequencies were taken from the CELEX English lemma database (Baayen, Piepenbrock, & van Rijn, 1993). None of the critical words were cognates or homophones between English and Dutch.

The experimental sentences, fillers, and practice items were spoken by a female English native speaker with normal intonation and at a normal speaking rate. The materials were digitally recorded

Condition	Frequency (SD)	Phonemes (SD)
FC	3.34 (0.95)	5.29 (2.30)
FI	3.061 (1.03)	5.17 (1.90)
ICL1	2.94 (1.19)	4.90 (1.55)
ICL2	2.89 (1.29)	5.60 (1.90)

Table 3. Mean log frequency per million and mean number of phonemes for the: FC, FI, ICL1 and ICL2 conditions. Standard deviations are given in parentheses.

in a sound attenuating booth and digitised at a rate of 14.4 kHz. Sound files were later equalised to eliminate any differences in sound level.

2.3 Procedure

Participants were exclusively addressed in English by an English native speaker, both preceding and during the experiment, in order to make certain they were in a monolingual L2 language mode (Grosjean, 1982). Participants were placed in a sound attenuating booth and were instructed to listen attentively to the sentences, which were played over two loudspeakers at a distance of roughly 1.5 m, and to try to understand

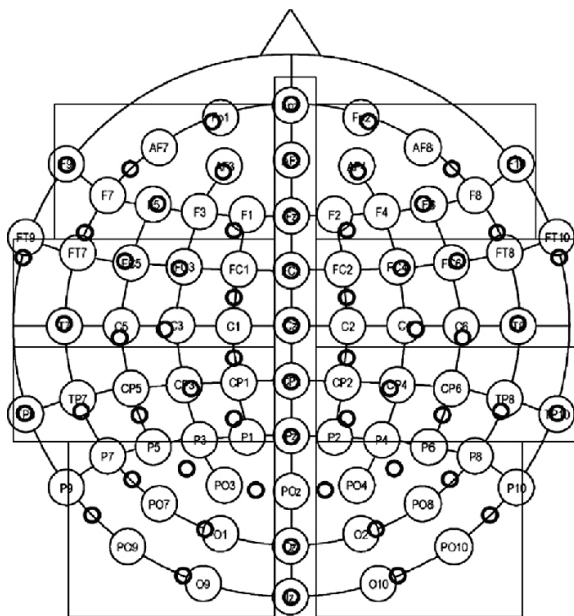


Figure 1. Electrode setup. Radial projection of electrode positions of the 10%-system (black circles) relative to the 10-20 system. Boxes denote regions for statistical analyses. Apostrophes denote not standard electrode locations.

them. The sound level was kept constant over participants. To ensure that participants remained focussed on the task, they were prompted to make an animacy decision regarding the previous sentence, at random intervals during the experiment. They could respond by means of a button box. These data were not analysed. Each trial began with a 300 ms warning tone, followed by 1200 ms of silence, then a spoken sentence. The next trial began 4100 ms after the sentence offset. To ensure that participants did not blink during and shortly after presentation of the sentence, 1000 ms prior to the beginning of the sentence a fixation point was displayed. Participants were instructed not to blink while the fixation point was on the screen. The fixation point remained until 1600 ms after the offset of the spoken sentence. Participants had a practice session with five sentences to familiarize themselves with the experimental setting.

After the EEG recording the participants completed a word translation test on the critical items to verify that they were known and a cloze test on all the experimental sentence frames to check whether participants expected the sentence continuation that we had envisaged.

2.4 EEG Recording

The EEG was recorded continuously from 64 sintered Ag/AgCl electrodes, each referred to an electrode on the nose of the participant. The electrodes were mounted in an equidistant elastic cap (<http://www.easycap.de>) and placed according to the extended 10% system (see Figure 1. for the electrode distribution). The EEG and EOG recordings were amplified with a BrainAmp DC amplifier (Brain Products, München, Germany) using a high-cutoff of 200 Hz, a time constant of 10s (0.016 Hz), and a sampling rate of 500 Hz. Impedances were kept below 5 k Ω . Trials with eye blinks or deflections exceeding 100 μ V were rejected.

3. Results

3.1 ERP analysis

Using the results from the post tests, EEG analysis was restricted to those trials for which participants chose the same continuation as we had envisaged (ICL1, ICL2 and FI conditions) or for which they had correctly translated the critical word

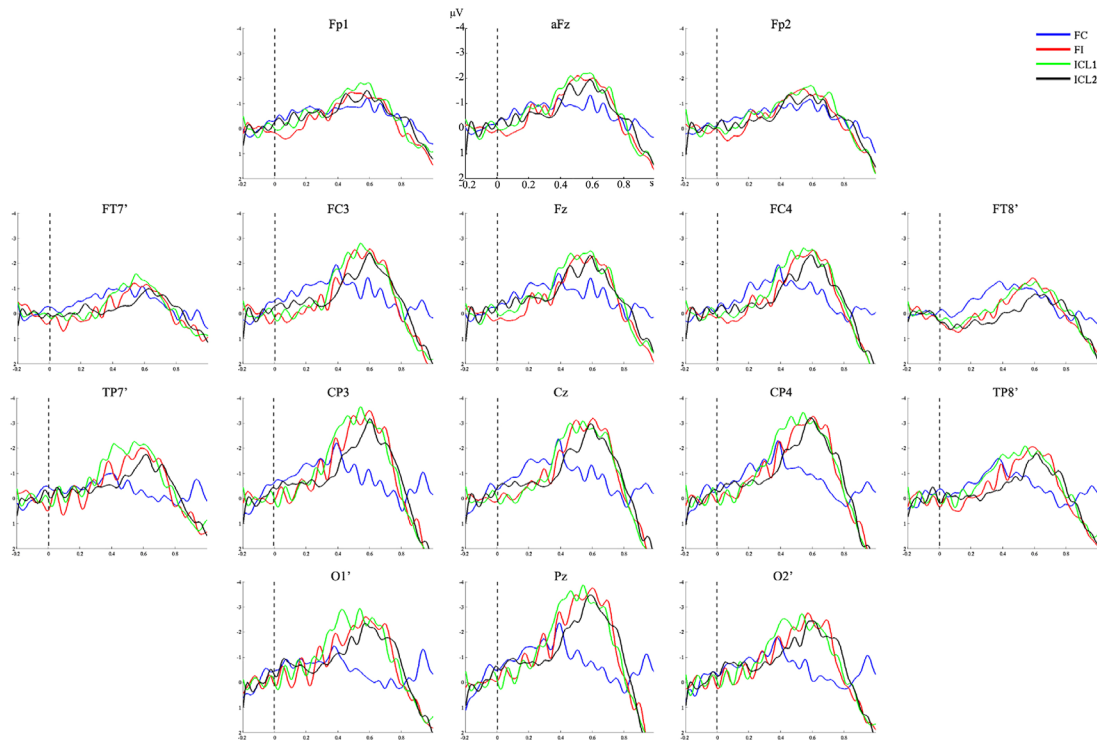


Figure 2. Grand average waveforms. FC (blue), FI (red), ICL1 (green), and ICL2 (black) on 16 scalp electrodes.

(FC condition).

Data from four participants were not analysed. Two participants were excluded due to excessive alpha. Data from one participant were incomplete due to a technical malfunction. One other participant was left out due to failure to complete the post-tests.

The data were analysed using the FieldTrip (<http://www.ru.nl/fcdonders/fieldtrip>) toolbox for Matlab (<http://www.mathworks.com>). EEG data were time-locked to critical word onset. Average waveforms were calculated for each participant using a 200 ms pre-stimulus baseline. Grand average waveforms were calculated by averaging the individual average waveforms. Statistical analysis was performed on the grand averaged data, in the latency ranges 150-300 ms and 300-800 ms, using an omnibus analysis of variance (ANOVA) with condition (4 levels) and site (9 levels; see Figure 1) as within subject factors. The latency ranges were chosen based on the previous literature and visual inspection of the grand average waveforms. All p values are reported after Greenhouse-Geisser correction (Greenhouse & Geisser, 1959). Contrasts between pairs of conditions were tested using a randomization approach that corrects for multiple comparisons (Maris, 2004). We now include a brief overview of this method.

The cluster randomization approach investigates

the hypothesis that the observed ERP data is independent of the condition in which it is observed.

In a first step dependent samples t -statistics are computed for each sensor \times time pair over a specified latency range (here between 300 and 800 ms after critical word onset for the N400). Those t -statistics that exceed a pre-defined threshold, that is based on the parametric t -distribution ($\alpha=0.05$, one tailed for: condition X < fully congruent), are passed to a cluster finding algorithm that creates clusters of sensor \times time pairs which show the same effect that are adjacent either in time or with respect to their location on the scalp. For each cluster the combined t -statistic over the cluster is computed. This is called the cluster-level statistic.

Secondly, the distribution of the cluster-level statistic under the null hypothesis is computed by randomly permuting the order of the conditions over all subjects. A Monte Carlo approximation of the distribution is calculated from 500 randomizations. To correct for multiple comparisons the maximum cluster-statistic is used in the reference distribution.

The p -value for a given cluster is the proportion of random draws with a cluster-level statistic that exceeds the observed maximum cluster-level statistic. This p -value can be compared with a critical alpha level which corresponds to the

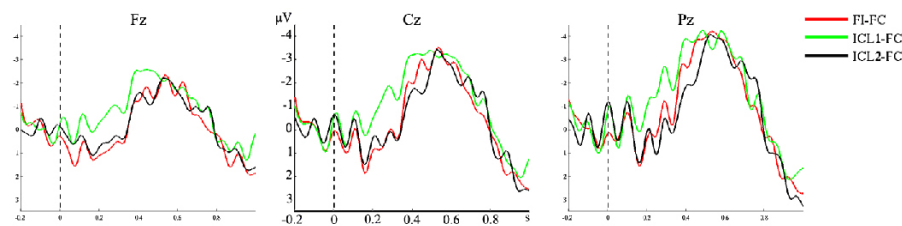


Figure 3. Difference waveforms. FI-FC (red), ICL1-FC (green), and ICL2-FC (black) on 3 midline electrodes.

probability of falsely identifying at least one cluster-level statistic as being significant.

Cluster randomization was performed on the following pairs of conditions: FI versus FC, ICL1 versus FC, ICL2 versus FC, ICL1 versus FI, and ICL2 versus FI; using the same latency ranges as the ANOVA (150-300 ms, 300-800 ms).

To determine the peak latency of the N400, for the three semantically incongruent conditions, we applied a low-pass filter at 7 Hz to the individual averages. The peak of the N400 component was defined as the minimum of the filtered individual averages, in the 300-800 ms latency range. A repeated measures ANOVA was performed on the peak latency of the N400 in the three incongruent conditions with condition (3 levels) as within subject factor. We tested two a priori pair-wise comparisons: ICL1 versus FI, and ICL2 versus FI (see Table 4).

Visual quantification of onset latencies was complicated due to variability of individual averages. We therefore estimated the onset of the N400 effect by performing a repeated measures ANOVA on successive 100-ms latency bins (c.f., Van Petten et al., 1999) with the following a priori pair-wise comparisons: FI versus FC, ICL1 versus FC, and ICL2 versus FC (see Table 5).

Finally, we performed a median split on the participants based on their pooled scores on both

proficiency tests. We performed an additional omnibus ANOVA, in the 300-800 ms latency range, with condition (4 levels) and site (9 levels) as within subject factors, and proficiency as between subject factor.

3.2 Grand averages

Figure 2 shows the grand average of each condition on 16 scalp electrodes. The waveforms for the three incongruent conditions (FI, ICL1, and ICL2) show an increased negativity in the 300-800 ms latency range relative to the fully congruent condition. This negativity is most pronounced on the centro-parietal electrodes.

Figure 3 shows the difference waveforms of the incongruent conditions minus the fully congruent condition on three midline electrodes. Figure 4 shows the topographical distribution of potentials in each condition as well as the topography of the significant differences between the incongruent and congruent conditions.

3.3 Omnibus ANOVA

In the 150-300 ms latency range, the ANOVA yielded no significant effect of condition ($F(3, 75) = 2.193$, $p_{GG} = n.s.$, $\epsilon = 0.899$) and no interaction with site ($F(24, 600) = 1.233$, $p_{GG} = n.s.$, $\epsilon = 0.241$).

In the 300-800 ms latency range, the ANOVA yielded a significant main effect of condition ($F(3,75) = 5.613$, $p_{GG} < 0.01$, $\epsilon = 0.866$) and a significant interaction with site ($F(24,600) = 5.508$, $p_{GG} < 0.001$, $\epsilon = 0.239$).

3.4 Fully Incongruent

Relative to the FC condition, there was a significant negative cluster starting at 414 ms after critical word onset ($p < 0.001$, cluster size = 5783 data points) and lasting until 708 ms. This negativity first diverged from the FC condition in the 400-500 ms latency bin (Table 5) and its peak was estimated at 461 ms.

Source	Peak latency		
	<i>df</i>	<i>F</i>	<i>p</i> <
Condition	2,50	5.455	0.01
ICL1 vs. FI	1,25	0.341	n.s.
ICL2 vs. FI	1,25	9.378	0.01

Table 4. Repeated measures ANOVA of the peak latency of the N400 in the semantically incongruent conditions.

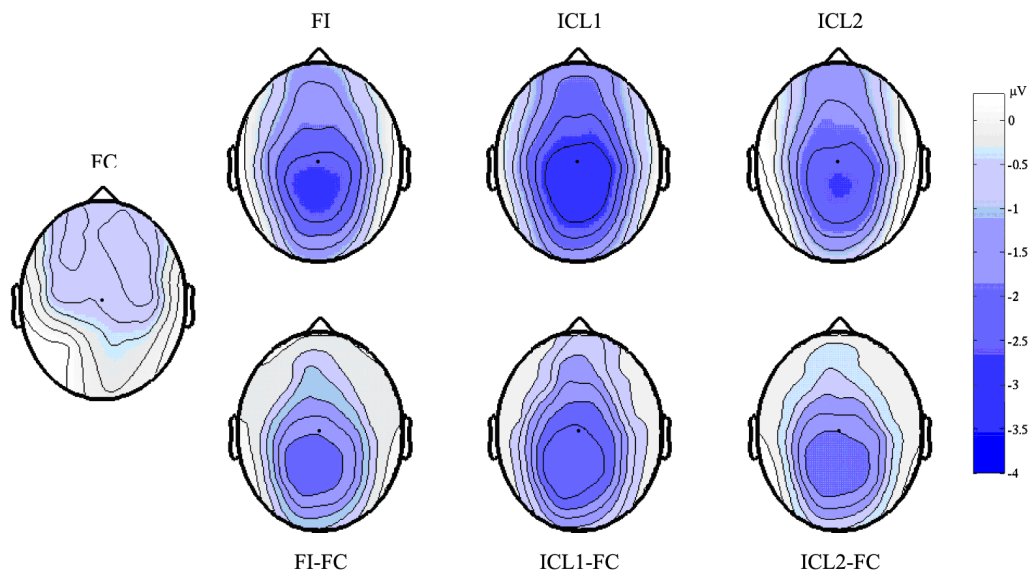


Figure 4. Topographic plots. (top) Topographic distribution of potentials between 300 and 800 ms for the FC (far left), FI (left), ICL1 (centre), and ICL2 (right) conditions. Blue denotes a negative value, white denotes a positive value. (bottom) Cluster randomization results for FI-FC(left), ICL1-FC(middle), and ICL2-FC(right) averaged between 300 and 800 ms and masked with the significant cluster.

3.5 Initially Congruent with the L1

Relative to the FC condition, there was a significant negative cluster starting at 358 ms ($p < 0.01$, cluster size = 7887 data points) and lasting until 712 ms. No significant clusters were found in the comparison of the ICL1 condition with the FI condition. The negativity first diverged from the FC condition in the 400-500 ms latency bin (Table 5) and the peak latency in the 300-800 ms time window was not significantly different from the corresponding negativity in the FI condition (see Table 4).

3.6 Initially Congruent with the L2

Relative to the FC condition, there was a negative cluster starting at 476 ms ($p < 0.001$, cluster size = 5738 data points) and lasting until 776 ms. No significant clusters were found in the comparison of the ICL2 condition with the FI condition. The negativity first diverged from the FC condition in the 500-600 ms latency bin (Table 5) and the peak latency in the 300-800 ms time window was significantly delayed compared to the corresponding negativity in the FI condition (see Table 4). The average delay was estimated at 67 ms.

3.7 Proficiency

Figure 5 shows the global field potentials for each condition for both high proficient and low

proficient participants. Although low proficient participants seemed to have attenuated negativities in the 300-800 ms latency range in comparison with high proficient participants, no significant interactions were found between proficiency and condition ($F(3,72) = 1.304$, $p_{GG} = n.s.$, $\epsilon = 0.850$) proficiency and site ($F(8,192) = 0.914$, $p_{GG} = n.s.$, $\epsilon = 0.325$), and there was no significant three-way interaction between condition, site, and proficiency ($F(24,576) = 1.288$, $p_{GG} = n.s.$, $\epsilon = 0.240$).

4. Discussion

The present study investigated the effect of sentence context and both intra- and interlingual initial phonemic overlap, on L2 natural speech comprehension. English-Dutch bilinguals listened to sentences in English that ended in a word that was: semantically congruent (FC condition), semantically incongruent (FI condition), semantically incongruent but initially overlapping with the most probable sentence completion (ICL2 condition), or semantically incongruent but initially overlapping with the L1 translation equivalent of the most probable sentence completion.

4.1 Influence of sentence context in non-native listening

We observed a significant N400 effect in each of the semantically incongruent conditions compared

latency bin (ms)	FI vs. FC		ICL1 vs. FC		ICL2 vs. FC	
	F(1,25)	p<	F(1,25)	p<	F(1,25)	p<
0-100	1.982	n.s.	0.001	n.s.	0.03	n.s.
100-200	2.416	n.s.	0.226	n.s.	1.184	n.s.
200-300	0.393	n.s.	1.844	n.s.	0.394	n.s.
300-400	0.242	n.s.	2.668	n.s.	0	n.s.
400-500	6.417	0.05	9.05	0.05	1.944	n.s.
500-600	15.104	0.01	15.054	0.01	14.582	0.01
600-700	13.864	0.01	17.155	0.001	15.556	0.01
700-800	2.609	n.s.	5.461	0.05	9.363	0.01

Table 5. Time course of the semantic incongruity effect. Latency bins are measured from critical word onset.

to the fully congruent condition. As far as we know, the only studies of natural speech processing in monolingual English speakers to report peak latency measures of the N400 to semantically incongruent sentence final words are Connolly and Phillips (1994) and Federmeier, McLennan, De Ochoa and Kutas (2002). Whereas the N400 in their semantic incongruity conditions peaked around 420 ms and 406 ms respectively, we found the average peak latency of the N400 in the Fully Incongruent condition to be approximately 460 ms. Although our study did not include a monolingual control condition, which would allow for a more direct comparison of N400 latencies in native and non-native listening, we note that this apparent delay is consistent with earlier findings of delayed N400s in non-native written language comprehension (Ardal et al., 1990; Hahne, 2001; Weber-Fox & Neville, 1996).

Also in line with earlier findings (e.g., Hahne, 2001; Weber-Fox et al., 2003; e.g., Weber-Fox & Neville, 1996), we observed a non-significant trend for the N400 to be attenuated in low proficient participants. We consider it likely that the high- and low proficient groups in our study differed insufficiently in terms of their language proficiency to observe a significant differential ERP effect. However this may also be attributable to a low signal-to-noise ratio by virtue of having too few participants per group.

In contrast to studies of monolingual auditory language comprehension, we did not observe an early negative effect in non-native listeners. This discrepancy could arise from differential processing requirements between native and non-native listening. While semantic integration in native listening may start on the basis of very little acoustic information (Van Petten et al., 1999), activation of the appropriate L2 lexical candidates might require the availability of a larger portion of the speech signal. For instance, using an auditory gating task whereby Dutch and English words were progressively revealed in increments of 40 ms, Schulpen et al. (2003) report that Dutch-English bilinguals are later and less proficient at identifying English words than they are at identifying Dutch words. For English words, they also consider multiple candidates even after the correct target can be uniquely identified on the basis of the acoustic information. Thus, in the latency range of the early negative effect, the available acoustic/phonological information may be insufficient for the non-native listener to be able to ascertain the presence of a semantic incongruity. Delayed semantic processing in non-native listening could potentially result in the absence of the early negative effect.

Alternatively, one might argue, following suggestions from Van Petten (1999) and Diaz (in press) that we can reconcile our findings with

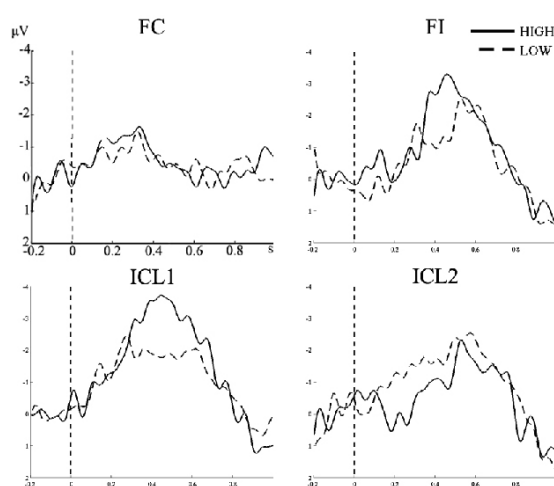


Figure 5. Proficiency. Global field potentials, for each condition, for high proficient participants (solid line) and low proficient participants (dashed line)

observations of an early negative effect by assuming that initial incongruity with a sentence context elicits an early N400. Logically, when there is no phonological and/or semantic incongruity on the basis of the initial phonemes of the target word, the onset of the N400 would be delayed (until such an incongruity arises). This delayed onset would show up as an absence of negativity in the latency range preceding the main N400 component. In our study the delayed N400 in the initially congruent with the L2 condition is evidenced by the delay in the peak latency of the N400.

4.2 Effects of initial phonological overlap with an L2 target word

We hypothesised that if non-native listeners are capable of utilising contextual information at an early stage of the word recognition process we would observe an attenuated early negative effect and/or a delayed N400 component in the initially congruent with the L2 condition as compared to the fully incongruent condition. While we did not find evidence for a negative ERP component preceding the N400 in any of our conditions (c.f., Van den Brink et al., 2001; Van den Brink, Brown, & Hagoort, 2006; Van den Brink & Hagoort, 2004) initial phonemic overlap with the most probable sentence continuation delayed the peak latency of the N400 by nearly 70 ms compared to the semantically fully incongruent condition. Furthermore, the initially congruent with the L2 condition began to diverge from the fully congruent condition in the 500-600 ms latency range, whereas the fully incongruent condition already diverged from the fully congruent condition in the 400-500 ms latency range.

In addition to the PMN, Connolly and Phillips (1994) also report a delayed peak latency of the N400 to items with initial phonological overlap with the correct target item. They propose that this observation reflects a delay in the semantic process underlying the N400. In conditions with initial phonological overlap, the incongruity is only apparent after the initial phonemes of the critical word. Thus the electrophysiological effects of the semantic mismatch would be delayed until the incongruity is detected. We interpret this finding as a confirmation of our hypothesis as non-native listeners treat the initial segment of critical words in the initially congruent with the L2 condition as if they were congruent with the sentence context.

4.3 Activation of L1 candidates

Our second hypothesis related to the question of language non-selectivity. If the early negative effect and N400 component were attenuated and/or delayed in the initially congruent with the L1 condition in comparison to the fully incongruent condition, we could interpret this as evidence for language non-selective activation of L1 lexical candidates. We found no differential effect between in the initially congruent with the L1 and fully incongruent conditions in the early latency range. Nor did we find a delay in the peak latency of the N400 in the initially congruent with the L1 condition as was the case in the initially congruent with the L2 condition. Also, the initially congruent with the L1 condition diverged from the fully congruent condition in the 400-500 ms latency range, as was the case in the fully incongruent condition. Although this is a negative finding it does suggest to us that non-native listeners do not treat initial overlap with the translation of the most likely sentence continuation as though it were initially congruent with the sentence context. This, in turn, would imply that word candidates from the participants' L1 are neither explicitly expected nor available for semantic processing, in non-native processing of natural speech.

This finding contrasts with studies that observe non-selective access to the bilingual lexicon. This may be due to the fact that many such studies employed single word paradigms (Paulmann, Elston-Guettler, Gunter, & Kotz, 2006; Schulpen et al., 2003) rather than investigating lexical access in the presence of a sentence context. A sentence context may be sufficient to restrict the lexical search process of a non-native listener to items from only the relevant language.

Eye-tracking paradigms such as those employed by Marian and Spivey (Marian & Spivey, 2003a, 2003b; Spivey & Marian, 1999) generally do embed target words in a sentence context. Notably though, these studies typically employ invariant sentence contexts, such as: "Pick up the *stamp*." (Spivey & Marian, 1999). This calls into question whether such experiments can be considered to reflect true sentence processing. Furthermore, participants in eye-tracking studies, by necessity, have a visual representation of the target objects before them, which would enable them to retrieve word-form and semantic information about the targets before they are referred to in the experimental sentences.

4.4 Semantics or phonology?

Our third research question related to the possibility of an absence of an early negative effect in the initially congruent with the L1 condition compared to the fully congruent condition. Such a finding would have allowed us to confidently state that the early negativity does not reflect a phonological mismatch but rather an effect of the initial semantic mismatch, as it is unlikely that participants would create a phonological expectation of an L1 word in an L2 context. As we did not find a negativity preceding the N400, these data do not allow us to rule out the phonological account. Nonetheless, given the indistinguishable scalp distributions between the N400 and the early negativity in monolingual speech comprehension (Connolly & Phillips, 1994; Diaz & Swaab, in press; Van den Brink & Hagoort, 2004; Van Petten et al., 1999), we do consider the semantic account to be more parsimonious.

5. Summary and Conclusions

Firstly, while a number of N400 studies have shown that non-natives are sensitive to semantic incongruity in written language processing, our study shows that non-native listeners are also sensitive to semantic incongruity in natural speech.

Secondly, consistent with previous findings, the peak latency of the N400 component seems to be longer in non-native listeners compared to latencies observed in monolingual natural speech comprehension.

Thirdly, the delayed peak latency of the N400, in the condition with initial phonological overlap with the most probable continuation, indicates that semantic integration in non-native natural speech comprehension can start on the basis of the word-initial phonemes.

Finally, we find no evidence that L1 lexical items are active during non-native natural speech comprehension.

Footnotes

1. This does not refer either to the N2 component (often referred to as the N200) observed in go/no-go paradigms (e.g., Rodriguez-Fornells et al., 2005; Schmitt, Schiltz, Zaake, Kutas, & Munte, 2001) or the N200 component in studies of orthographic processing (e.g.,

Elston-Guettler & Friederici, 2005; Kramer & Donchin, 1987; Niznikiewicz & Squires, 1996).

2. It is well established that Dutch natives are insensitive to the phonemic contrast between /ɛ/ and /æ/. Thus they would not be able to discriminate minimal pairs such as *cattle* and *kettle* (c.f., Weber & Cutler, 2004).

Acknowledgements

We thank Ton Dijkstra, Daniëlle van den Brink and Robert Oostenveld and three anonymous reviewers for their insightful comments. We also express our gratitude to Michel Bex, Vasiliki Folia, Jana Hanulova, Lilla Magyari, Stephan Miedl, Anouk Peijnenborgh, Willemijn Schot, and Kirsten Weber for assisting with the EEG electrode application.

References

- Allan, D. (1992). *Oxford Placement Test*. Oxford: Oxford University Press.
- Ardal, S., Donald, M. W., Meuter, R., Muldrew, S., & Luce, M. (1990). Brain Responses to Semantic Incongruity in Bilinguals. *Brain and Language*, 39(2), 187-205.
- Baayen, H., Piepenbrock, R., & van Rijn, H. (1993). The CELEX lexical database [CD-ROM]. Philadelphia, PA: University of Pennsylvania, Linguistic Data Consortium.
- Brown, C., & Hagoort, P. (1993). The Processing Nature of the N400 - Evidence from Masked Priming. *Journal of Cognitive Neuroscience*, 5(1), 34-44.
- Connolly, J. F., & Phillips, N. A. (1994). Event-Related Potential Components Reflect Phonological and Semantic Processing of the Terminal Word of Spoken Sentences. *Journal of Cognitive Neuroscience*, 6(3), 256-266.
- Connolly, J. F., Phillips, N. A., Stewart, S. H., & Brake, W. G. (1992). Event-Related Potential Sensitivity to Acoustic and Semantic Properties of Terminal Words in Sentences. *Brain and Language*, 43(1), 1-18.
- Connolly, J. F., Stewart, S. H., & Phillips, N. A. (1990). The Effects of Processing Requirements on Neurophysiological Responses to Spoken Sentences. *Brain and Language*, 39(2), 302-318.
- Diaz, M. T., & Swaab, T. Y. (in press). Electrophysiological differentiation of phonological and semantic integration in word and sentence contexts. *Brain Research*.
- Dijkstra, T. (2005). Bilingual Visual Word Recognition and Lexical Access. In J. F. Kroll & A. M. B. de Groot (Eds.), *Handbook of bilingualism: Psycholinguistic approaches* (pp. 179-201). New York: Oxford University Press.

- Dijkstra, T., Grainger, J., & Van Heuven, W. J. B. (1999). Recognition of cognates and interlingual homographs: The neglected role of phonology. *Journal of Memory and Language*, 41(4), 496-518.
- Elston-Guettler, K. E., & Friederici, A. D. (2005). Native and L2 processing of homonyms in sentential context. *Journal of Memory and Language*, 52(2), 256-283.
- Federmeier, K. D., McLennan, D. B., De Ochoa, E., & Kutas, M. (2002). The impact of semantic memory organization and sentence context information on spoken language processing by younger and older adults: An ERP study. *Psychophysiology*, 39(2), 133-146.
- Greenhouse, S. W., & Geisser, S. (1959). On Methods in the Analysis of Profile Data. *Psychometrika*, 24(2), 95-112.
- Grosjean, F. (1982). *Life with two languages: An introduction to bilingualism*. Cambridge, MA: Harvard University Press.
- Grosjean, F. (1988). Exploring the recognition of guest words in bilingual speech. *Language and Cognitive Processes*, 3, 233-274.
- Hagoort, P., & Brown, C. M. (2000). ERP effects of listening to speech: semantic ERP effects. *Neuropsychologia*, 38(11), 1518-1530.
- Hahne, A. (2001). What's different in second-language processing? Evidence from event-related brain potentials. *Journal of Psycholinguistic Research*, 30(3), 251-266.
- Holcomb, P. J. (1993). Semantic Priming and Stimulus Degradation - Implications for the Role of the N400 in Language Processing. *Psychophysiology*, 30(1), 47-61.
- Holcomb, P. J., & Neville, H. J. (1990). Auditory and Visual Semantic Priming in Lexical Decision - a Comparison Using Event-Related Brain Potentials. *Language and Cognitive Processes*, 5(4), 281-312.
- Kramer, A. F., & Donchin, E. (1987). Brain Potentials as Indexes of Orthographic and Phonological Interaction during Word Matching. *Journal of Experimental Psychology-Learning Memory and Cognition*, 13(1), 76-86.
- Kutas, M., & Hillyard, S. A. (1980). Reading Senseless Sentences - Brain Potentials Reflect Semantic Incongruity. *Science*, 207(4427), 203-205.
- Kutas, M., & Hillyard, S. A. (1984). Brain Potentials during Reading Reflect Word Expectancy and Semantic Association. *Nature*, 307(5947), 161-163.
- Lemhöfer, K., Dijkstra, T., & Michel, M. C. (2004). Three languages, one ECHO: Cognate effects in trilingual word recognition. *Language and Cognitive Processes*, 19(5), 585-611.
- Li, P. (1996). Spoken Word Recognition of Code-Switched Words by Chinese-English Bilinguals. *Journal of Memory and Language*, 35(6), 757-774.
- Marian, V., & Spivey, M. (2003a). Bilingual and monolingual processing of competing lexical items. *Applied Psycholinguistics*, 24(2), 173-193.
- Marian, V., & Spivey, M. (2003b). Competing activation in bilingual language processing: Within- and between-language competition. *Bilingualism: Language and Cognition*, 6(2), 97-115.
- Marian, V., Spivey, M., & Hirsch, J. (2003). Shared and separate systems in bilingual language processing: Converging evidence from eyetracking and brain imaging. *Brain and Language*, 86(1), 70-82.
- Maris, E. (2004). Randomization tests for ERP topographies and whole spatiotemporal data matrices. *Psychophysiology*, 41(1), 142-151.
- Meara, P. M. (1996). *English vocabulary tests: 10k*. Swansea, UK: Center for Applied Language Studies.
- Nas, G. (1983). Visual Word Recognition in Bilinguals - Evidence for a Cooperation between Visual and Sound Based Codes during Access to a Common Lexical Store. *Journal of Verbal Learning and Verbal Behavior*, 22(5), 526-534.
- Newman, R. L., Connolly, J. F., Service, E., & Mcivor, K. (2003). Influence of phonological expectations during a phoneme deletion task: Evidence from event-related brain potentials. *Psychophysiology*, 40(4), 640-647.
- Niznikiewicz, M., & Squires, N. K. (1996). Phonological processing and the role of strategy in silent reading: Behavioral and electrophysiological evidence. *Brain and Language*, 52(2), 342-364.
- Paulmann, S., Elston-Guettler, K. E., Gunter, T. C., & Kotz, S. A. (2006). Is bilingual lexical access influenced by language context? *Neuroreport*, 17(7), 727-731.
- Rodriguez-Fornells, A., van der Lugt, A., Rotte, M., Britti, B., Heinze, H. J., & Munte, T. F. (2005). Second language interferes with word production in fluent bilinguals: Brain potential and functional imaging evidence. *Journal of Cognitive Neuroscience*, 17(3), 422-433.
- Sanders, L. D., & Neville, H. J. (2003). An ERP study of continuous speech processing II. Segmentation, semantics, and syntax in non-native speakers. *Cognitive Brain Research*, 15(3), 214-227.
- Scarborough, D. L., Gerard, L., & Cortese, C. (1984). Independence of Lexical Access in Bilingual Word Recognition. *Journal of Verbal Learning and Verbal Behavior*, 23(1), 84-99.
- Schmitt, B. M., Schiltz, K., Zaake, W., Kutas, M., & Munte, T. F. (2001). An electrophysiological analysis of the time course of conceptual and syntactic encoding during tacit picture naming. *Journal of Cognitive Neuroscience*, 13(4), 510-522.
- Schulpen, B., Dijkstra, T., Schriefers, H. J., & Hasper, M. (2003). Recognition of interlingual homophones in bilingual auditory word recognition. *Journal of Experimental Psychology-Human Perception and Performance*, 29(6), 1155-1178.
- Soares, C., & Grosjean, F. (1984). Bilinguals in a Monolingual and a Bilingual Speech Mode - the Effect on Lexical Access. *Memory & Cognition*, 12(4), 380-386.
- Spivey, M., & Marian, V. (1999). Cross talk between native and second languages: Partial activation of an

- irrelevant lexicon. *Psychological Science*, 10(3), 281-284.
- Van den Brink, D., Brown, C. M., & Hagoort, P. (2001). Electrophysiological evidence for early contextual influences during spoken-word recognition: N200 versus N400 effects. *Journal of Cognitive Neuroscience*, 13(7), 967-985.
- Van den Brink, D., Brown, C. M., & Hagoort, P. (2006). The cascaded nature of lexical selection and integration in auditory sentence processing. *Journal Of Experimental Psychology-Learning Memory And Cognition*, 32(2), 364-372.
- Van den Brink, D., & Hagoort, P. (2004). The influence of semantic and syntactic context constraints on lexical selection and integration in spoken-word comprehension as revealed by ERPs. *Journal of Cognitive Neuroscience*, 16(6), 1068-1084.
- Van Petten, C., Coulson, S., Rubin, S., Plante, E., & Parks, M. (1999). Time course of word identification and semantic integration in spoken language. *Journal of Experimental Psychology-Learning Memory and Cognition*, 25(2), 394-417.
- Van Petten, C., & Kutas, M. (1990). Interactions between Sentence Context and Word-Frequency in Event-Related Brain Potentials. *Memory & Cognition*, 18(4), 380-393.
- Weber-Fox, C., Davis, L. J., & Cuadrado, E. (2003). Event-related brain potential markers of high-language proficiency in adults. *Brain and Language*, 85(2), 231-244.
- Weber-Fox, C. M., & Neville, H. J. (1996). Maturation constraints on functional specializations for language processing: ERP and behavioral evidence in bilingual speakers. *Journal of Cognitive Neuroscience*, 8(3), 231-256.
- Weber, A., & Cutler, A. (2004). Lexical competition in non-native spoken-word recognition. *Journal of Memory and Language*, 50(1), 1-25.

The faster one has blinkers on: The role of co-representation in response inhibition and error detection

Stephan Miedl¹

Supervisors: Ellen de Bruijn¹, and Harold Bekkering¹

¹*Nijmegen Institute for Cognition and Information, Nijmegen, The Netherlands*

Earlier experiments have shown that the formation of a co-representation of the task of others influences one's own action behaviour. The aim of the present study was to investigate how differences in co-representation, while doing a go-nogo task together with a second participant, influence one's own action-monitoring processes. The results showed a smaller NoGo P3, more errors and a reduced ERN on stimuli requiring only the response of the other participant compared to stimuli requiring the inhibition of both participants. Moreover, significant interactions with competitive response strategy revealed that the monitoring processes of fast responders were least affected by shared action representations. These results create evidence that the existence of a co-representation in a joint task leads to specific modulations of action-monitoring processes. Interestingly, these effects may also depend on the response strategies people employ in a competitive setting.

Keywords: ERN, response inhibition, error detection, co-representation

1. Introduction

Until recently, action-monitoring studies focused solely on single-actor settings while in daily life humans often work together on tasks. Consequently, action-monitoring processes like response inhibition and error detection have not been investigated thoroughly in joint action. When performing a task together, humans often divide subtasks among the actors involved. As a result, people form not only a representation of their own tasks, but also of the others' tasks. However, the possible effects of this shared action representation or so-called co-representation on action monitoring are not yet known. In addition, competitive elements in a joint task create different response strategies depending on the individual speed-accuracy trade-off. In the current study, we want to investigate (1) how differences in co-representation affect response inhibition, (2) whether differences in co-representation influence performance levels and error-detection processes, and (3) what role competitive response strategies may play in these processes.

1.1 Joint action

When approaching a green traffic light that is about to turn red, while having a car in front of you, the chance is high that the driver in the car in front of you will stop. This makes you slow down, to prevent an accident. Therefore successful driving means dealing with the appropriate behaviour of your own as well as the behaviour of other traffic participants.

The concept of joint action is related to mentally representing the task, acting together with other people, and being part of a group. One of the basic assumptions in joint-action research was proposed by Prinz (1995), who created a new framework to understand the functional relationship between perception and action. He raised two principles. First, the common-coding principle states that perception and action share a common representational domain. Second, the action-effect principle indicates that the outcome of actions influences planning and control of these actions. These two principles play a crucial role in joint action. The common-coding principle enables integrating information of the other person's behaviour in one's own representation system. The action-effect principle is responsible for using this integrated information in a goal-directed manner.

This means observing another person grasping a cup should not only activate my own motor system for grasping, but also activate part of the motor system to bring the cup to my mouth. Support for this came from Ramnani & Miall (2004), who conclude that predicting the actions of others activates brain areas engaged in mental state attribution, reflecting a formed representation of an intentional relation. Therefore, we define joint action broadly, which means not only situations where people work together physically, but also mentally, in situations where people have to achieve a common goal in mind. Action representations become shared as soon as people are aware that they are part of a group and tasks are distributed within this group (Sebanz, Knoblich, and Prinz, 2005). This means that any member of a group forms, along with one's own task representation a co-representation of the tasks of other members. There is evidence that own actions and other's actions are represented in a functionally similar way. Sebanz et al. (2003) demonstrated an action-selection conflict for stimuli requiring an action from both actors in a "Go-NoGo" task, where participants were sitting next to each other. Interestingly, each actor integrated the co-actor's action alternative in his/her action planning, even when it was not possible to observe the other's actions. Additional support comes from an experiment by van Schie et al. (2004) where subjects had to observe actions performed by another person. Importantly, motor activation of the observer continued to develop for observed correct responses and decreased for incorrect ones, suggesting that similar neural mechanisms are responsible for monitoring one's own and others' task performance. In addition Sebanz et al. (2005) showed an action-selection conflict in participants, when a response was required to a stimulus to which the partner had to respond. Furthermore, task representations are not static with respect to a moment in time, obviously people realize goals by using own and other's past experiences, own and other's consequences of actions, and own and other's desired outcomes of actions for action prediction (Sebanz, Bekkering, and Knoblich, 2006). All above mentioned studies focused on the more general effects of joint-action settings on aspects of action control, in a way that one actor's performance is influenced by the other's task. Up to now joint-action experiments always clearly discriminated between a solo condition, where participants had to act alone and a joint condition, where participants

performed the task together. There is clear evidence that forming a co-representation of the task of the second participant influences one's own behaviour. However, until now no study has investigated how differences within the formed co-representation might influence action-monitoring processes.

1.2 Action monitoring

In daily traffic situations, people have to continuously monitor their actions to prevent errors or to detect them as fast as possible. While waiting in front of a red traffic light that turns to green one may immediately start to accelerate. However the exact time when one accelerates depends on the fact whether or not there is a car in front of you waiting for a green light. Having a car in front of you implies that you must withhold your tendency to accelerate until the other car starts moving. When you do start too early, or when the car in front of you accelerates slower than expected, you will immediately have to hit the brakes to avoid an accident.

An appropriate method to measure joint-action monitoring is to record electrical activity of the brain by means of EEG while doing a joint-action task. In the current study, we will focus on two specific action-monitoring processes. First, pre-response inhibition on correct trials, as reflected in the stimulus-locked NoGo P3 potential (Pfefferbaum et al., 1984, Falkenstein et al., 1995). The NoGo P3 is maximal at frontocentral locations and a valuable electrophysiological indicator for inhibitory function, related to the frontal lobe (Bokura et al., 2005). It is assumed that frontocentral NoGo P3 is a better candidate for response inhibition than the N2 component (Donkers et al., 2004), which is recently found to be a correlate of response conflict rather than response inhibition (Nieuwenhuis and Yeung, 2003). A recent study of Sebanz et al. (2006) showed a higher NoGo P3 in joint-action conditions compared to single conditions. The authors concluded that increased response inhibition was necessary to withhold subjects from responding on NoGo trials in the group condition.

Second, the process of error detection can be measured electrophysiologically by the response-locked error negativity (Falkenstein et al., 1991) or error-related negativity (ERN; Gehring et al., 1993) with maximal amplitude within 100 ms after an error has been made. The ERN has a common neural source within the medial frontal cortex

and is seen as the product of action monitoring, used to enhance future performance. Humans' anterior cingulate cortex (ACC) is thought to be the generator of the ERN; it has connections to the limbic system, the motor system, and to prefrontal regions (Ridderinkhof et al., 2004). Originally, the ERN was taken to be a result of a mismatch of the comparison between the representation of the correct response and the representation of the actual response (Falkenstein et al. 1991; Gehring et al., 1993; Coles, Scheffers, and Holroyd, 2001). More recently, the ERN has also been linked to the emotional response to an error or to the affective evaluation of actions (Gehring and Willoughby, 2002). So far no experiments have investigated error monitoring while two participants performing a task together at the same time. **Consequently, relatively** little is known about how a co-representation of another person's action modulates the process of error monitoring. A study by Hajcak et al. (2005) investigated the more general effect of being observed. They showed that ERN amplitude was larger on error trials in a condition where subjects were told that they were being evaluated by an observer sitting next to them compared to a solo condition performing the task alone. The authors concluded that the ERN was sensitive to affective and motivational factors, but the experiment is not able to provide further insight into co-representational effects on action monitoring. In the current study, we want to investigate whether and how differences in co-representation influence the action-monitoring processes of response inhibition and error detection.

1.3 Predictions

In the current study we investigated three different questions. First, although Sebanz and co-authors (2006) suggest that co-representation may affect response inhibition at a general level, it is unknown whether differences in co-representation within a joint-action setting affect response inhibition. In joint action, response inhibition as reflected in the NoGo P3 should be different in behavioural identical situations of one subject, dependent on the task of the second subject.

Second, no studies have examined whether differences in co-representation influence performance levels and error-detection processes. This was investigated by reaction times and response-locked ERN recording. If differences in co-representation affect performance levels and

error-detection, accuracy rates and the ERN would be different in behavioural identical situations of one subject, dependent on the task of the second subject.

Third, we investigated the role competitive response strategies may play in these processes. With respect to applied response strategies, there are two different basic modes of social cognition, which are possible when two or more people are working together on one task: cooperation among group members or competition between members of the group (Decety et al., 2004). In our experiment we wanted to look more closely to the modulatory effects within a competitive mode. This was reflected in situations where both participants had to be active and applied a competitive response strategy in order to be faster than the other. To optimise performance in a competitive setting it may be advantageous to concentrate on your own performance and disregard the other person to a maximum. If competitive response strategy affected co-representational differences in action monitoring, differences due to deviant co-representations within response inhibition, reaction times, and error detection should be modulated by the extent to which a participant adheres to a competitive strategy or not.

2. Methods

2.1 Participants

Fourteen pairs, each comprised of one EEG subject and one behavioural subject (see Figure 1B) participated in the experiment. All were right-handed and had normal or corrected-to-normal vision. Only the data from the EEG participants were analysed (13 females, 1 male; mean age 21.9

years SD 2.1 years). All participants were paid 6 euro per hour for participation.

2.2 Design and procedure

Participants sat next to each other and performed a joint Go-NoGo task in which they responded with their dominant index finger to the presentation of single letters. The stimuli were presented in white against a black background in the centre of a computer screen between two grey boxes, placed at a distance of roughly 70 cm from the subjects. The stimuli (the letters P, F, E, or T in an Arial uppercase font; font size 16) were presented for 100 ms. The left grey box coloured yellow when the left subject responded – the right grey box coloured yellow when the right subject responded (see Figure 1B.) The inter trial interval was random between 1000 and 2000 ms. Participants were instructed to press the response button “as fast as possible” on Go trials and to avoid errors, i.e. responding on NoGo trials. An experimental session was composed of eight blocks of 200 trials, during which both EEG and behavioural data was obtained from one participant (EEG participant) and only behavioural data from the other participant (RT participant). As we will only report the data obtained from the EEG participant, the naming of the different stimuli is done from the perspective of this participant. Both participants had to respond to Go stimuli that were presented in 70% of the trials. The remaining 30% were NoGo stimuli to which both participants had to withhold their response. The Go stimuli were comprised of ‘Both Go’ trials (55%; both participants need to respond) and of ‘Self Go’ trials (15%; EEG participant responds, while RT participant inhibits). Similarly, the NoGo stimuli were composed of ‘Self NoGo’ (15%; EEG

Condition	EEG-participant	RT-participant
BothGo (55%)	Go	Go
Self Go (15%)	Go	NoGo
Self NoGo (15%)	NoGo	Go
Both NoGo (15%)	NoGo	NoGo

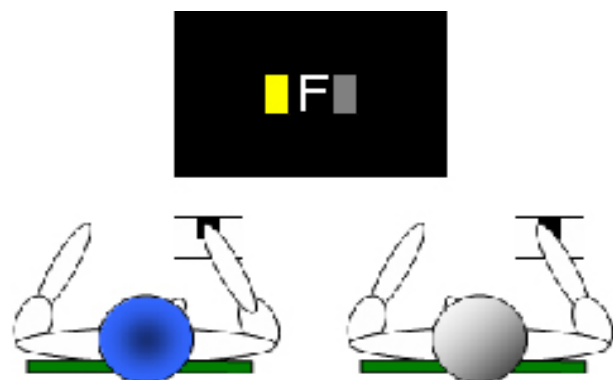


Figure 1. Left: Experimental paradigm and frequency distribution of the stimuli. Right: Experimental session with response of EEG participant (left; blue head) and no response of RT participant (right).

participant inhibits, while RT participant responds) and of ‘Both NoGo’ (15%; both participants need to inhibit their response). Half of the EEG participants were assigned to the left sitting-position and half of them to the right sitting-position. Reaction-time feedback (averaged over correct responses) per participant was presented after each block and at the end of the experiment (total average over all eight blocks). There was a short break between the blocks. The total experiment lasted 120 minutes, including preparation and breaks.

2.3 Electrophysiological Recording and Data Analysis

The EEG-signal was recorded from 27 locations on the scalp. Electrodes were placed at locations in accordance with the international 10-20 system. All signals were referenced to the left mastoid, but were later offline re-referenced to the average of both mastoids. The vertical electro-oculogram (EOG) was recorded bipolarly from electrodes placed above and below the right eye. The horizontal EOG was also recorded bipolarly from electrodes lateral to both eyes. All electrode impedances were kept below 5 k Ω . The EEG and EOG signals were amplified using a time-constant of 8 s and were filtered off-line low-pass at 15 Hz. All signals were digitised with a sampling rate of 200 Hz.

EOG artefact correction was carried out using the procedure by Gratton, Coles, and Donchin (1983). For both behavioural and ERP analyses all

responses with reaction times faster than 150 ms (1.1%) were removed from the data sets. Trials were averaged to ERPs separately for each condition and each subject, relative to a 200 ms pre-stimulus or pre-response baseline.

ERN amplitude was determined on incorrect response-locked subject ERP averages by subtracting the most negative peak in the 0-150 ms time-window after response onset from the most positive peak in the time-window starting 80 ms before and ending 80 ms after response onset at electrodes Fz, FCz, and Cz.

NoGo P3 amplitude was determined on correct stimulus-locked ERPs as the most positive peak in the 250 - 800 ms time window at electrode FCz, Cz, and Pz.

Individual averages for RTs, amplitudes, and number of responses were entered in a repeated measures General Linear Model (GLM) with inhibition (2 levels: Self NoGo vs. Both NoGo) as within-subject factor. The analyses on ERN and NoGo P3 amplitude also included the within-subject factor electrode (3 levels: Fz, FCz, and Cz for ERN – FCz, Cz, and Pz for NoGo P3).

To control for the influence of competitive response strategies, EEG participants were divided into two groups depending on the number of faster responses in the Both Go condition. The EEG participants who had more fast responses than their RT partners in the Both Go condition were assigned to the subgroup of “Fast Responders” (N = 7). Similarly, EEG participants who had more slow responses than their RT partners in the Both

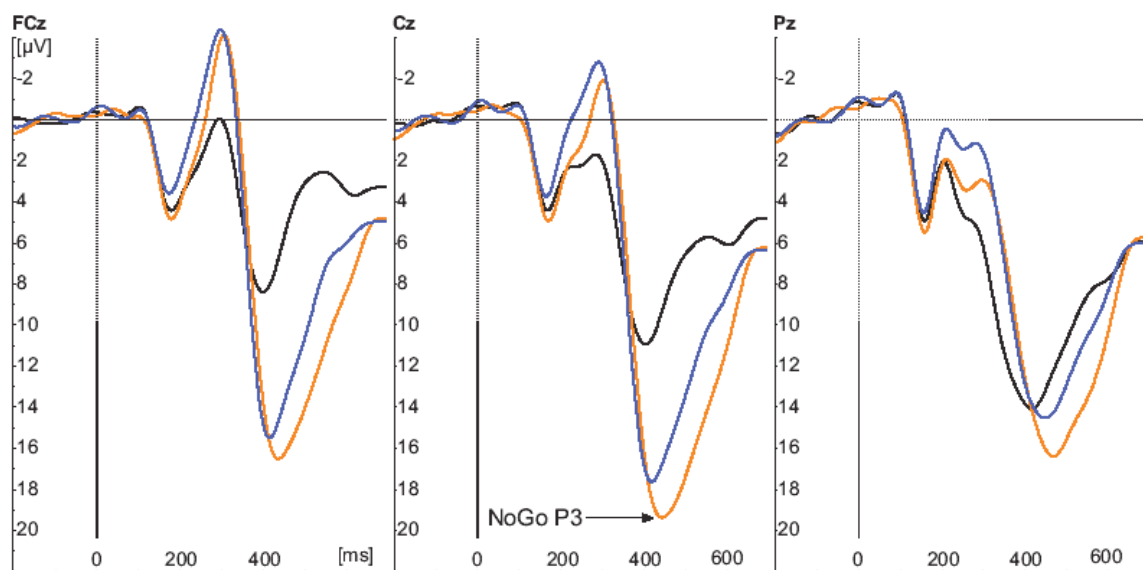


Figure 2. Grand average stimulus-locked NoGo P3 waveforms for correct Both Go, Self NoGo, and Both NoGo.

Go condition were assigned to the subgroup of “Slow Responders” ($N = 7$). Individual averages for RTs, amplitudes (electrode FCz for ERN and Cz for NoGo P3), and number of responses were entered in a repeated measures General Linear Model (GLM) with response strategy (2 levels: Fast Responders vs. Slow Responders) as between-subject factor and inhibition (2 levels: Self NoGo vs. Both NoGo) as a within-subject factor.

3. Results

3.1 Response inhibition: NoGo P3

Figure 2 depicts the grand-average of the stimulus-locked ERP. The analyses demonstrated that NoGo P3 amplitude for the Both NoGo condition (20.47 μ V) was significantly higher compared to the Self NoGo condition [18.87 μ V; $F(1,13) = 9.65$, $p = 0.008$]. There was also a main effect of electrode [$F(2,12) = 18.30$, $p < 0.001$]. Repeated contrasts showed that NoGo P3 amplitude was largest at electrode Cz [Figure 2 centre; Figure 4 centre; (FCz vs. Cz: $p < 0.001$; FCz vs. Pz: $p = 0.634$; Cz vs. Pz: $p = 0.027$)]. The interaction between electrode and inhibition (Self NoGo vs. Both NoGo) was not significant [$F(2,12) = 2.65$, $p = 0.112$].

3.2 Behavioural analyses

For an overview of mean reaction times and proportion of responses see Table 1. Reaction times were faster for incorrect responses (279 ms) than for correct responses [330 ms; $F(1,13) = 100.77$, $p < 0.001$]. More errors were made in the Self NoGo

condition (25.3%) compared to the Both NoGo condition [16.0%; $F(1,13) = 5.98$, $p = 0.030$].

3.3 Error monitoring: ERN

Figure 3 indicates that ERN amplitude was higher for incorrect Both NoGo (-12.63) than for incorrect Self NoGo [-11.03 μ V; $F(1,13) = 5.99$, $p = 0.029$]. There was a main effect of electrode [$F(2,12) = 14.09$, $p = 0.001$]. Repeated contrasts showed that ERN amplitude was largest at electrode FCz [Figure 3 centre; Figure 4 right; (Fz vs. Cz: $p = 0.889$; Fz vs. FCz: $p = 0.002$; FCz vs. Cz: $p < 0.001$)]. The interaction between electrode and inhibition (Incorrect Self NoGo vs. Incorrect Both NoGo) was not significant [$F(2,12) = 2.377$, $p = 0.135$].

3.4 Competitive strategy

The EEG participants who had more fast responses than their partner in the Both Go condition were assigned to the subgroup of “Fast Responders” ($N = 7$). Similarly, the EEG participants who had more slow responses than their partner in the Both Go condition were assigned to the subgroup of “Slow Responders” ($N = 7$). The subgroup of fast responders was on average in 62% of the Both Go trials faster than the behavioural subject. Slow responders were on average in 38% of the Both Go trials faster than the behavioural subject.

With respect to the analysis for error rate we found a main effect of inhibition [$F(1,12) = 7.78$, $p = 0.016$]. The factor response strategy did not reach significance [$F(1,12) = 1.658$, $p = 0.222$]. Crucially, the inhibition x response strategy interaction was significant [Figure 5 left; $F(1,12) = 4.912$, $p = 0.047$].

Type of response	Condition	Reaction time (proportion)
Correct	Both Go (Go / Go)	313 (96.4)
	Self Go (Go / NoGo)	348 (63.3)
Incorrect	Self NoGo (NoGo / Go)	276 (25.3)
	Both NoGo (NoGo / NoGo)	282 (16.0)

Table 1. Mean reaction times and proportions for correct and incorrect responses from the perspective of the EEG subject (“Self” corresponds to the EEG subject).

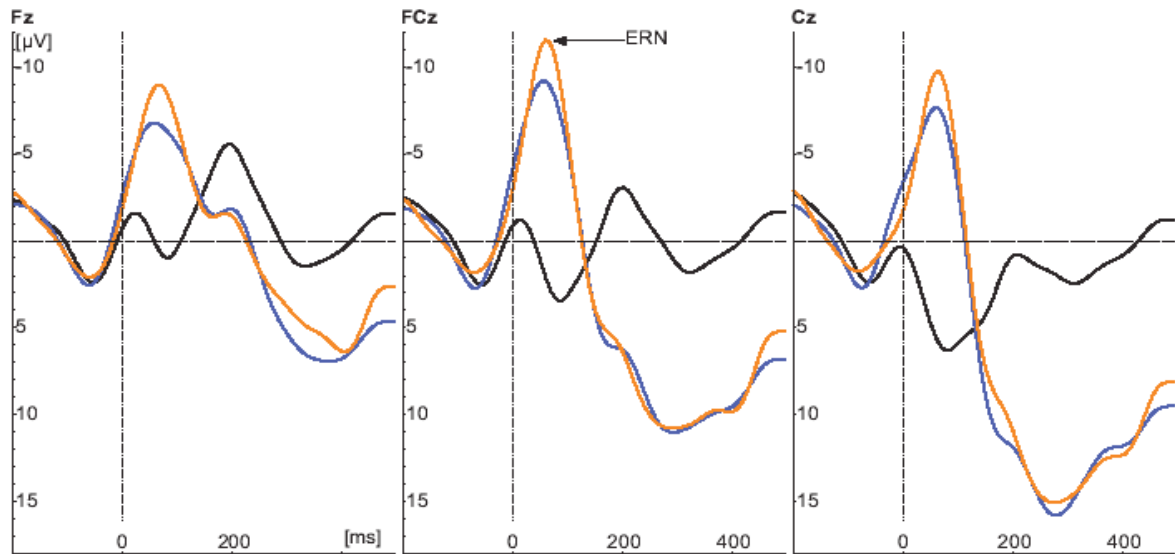


Figure 3. Grand average response-locked ERN waveforms for Correct Both Go, Incorrect Self NoGo, and Incorrect Both NoGo.

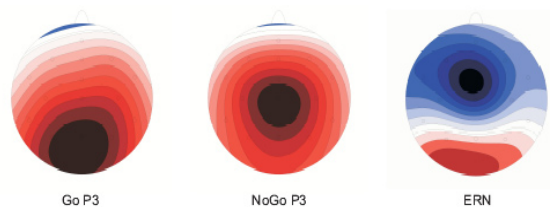


Figure 4. Topography of ERP components averaged over 14 subjects.

The subgroup of Slow Responders made more errors in the Self NoGo condition [75.86 errors (31.6%)] compared to the Both NoGo condition [35.86 errors (14.9%)], while Fast Responders did not differ in number of errors between the two conditions [46.71 errors (19.5%) in the Self NoGo condition vs. 42.14 errors (17.6%) in the Both NoGo condition].

Similarly, once more for the NoGo P3 analysis there was a main effect of inhibition [$F(1,12) = 18.04$, $p = 0.001$]. The factor response strategy was marginal significant [$F(1,12) = 4.65$, $p = 0.052$]. Fast Responders showed a higher amplitude of response inhibition (25.47 μV) than Slow Responders (17.92 μV). Importantly, the inhibition \times response strategy interaction was significant [Figure 5 right; $F(1,12) = 12.80$, $p = 0.004$]. The subgroup of Slow Responders had a lower NoGo P3 in the Self NoGo condition (16.27 μV) compared to the Both NoGo condition (19.58 μV), while Fast Responders did not differ in NoGo P3 between the two conditions (25.33 μV in the Self NoGo condition vs. 25.61 μV in the Both NoGo condition).

Apparently, again for the analysis of the ERN

we observed a main effect of inhibition [$F(1,12) = 8.45$, $p = 0.013$]. The main effect of response strategy was not significant [$F(1,12) = 0.004$, $p = 0.948$]. Interestingly, the ERN difference in response inhibition (Self NoGo vs. Both NoGo) was not modulated by response strategy (Fast vs. Slow Responders) [$F(1,12) = 1.85$, $p = 0.199$].

4. Discussion

In the present study we investigated how differences in co-representation influence the processes of response inhibition and error detection, as reflected in the NoGo P3, behavioural measures, and the ERN. The results showed a smaller NoGo P3 on Self NoGo stimuli, requiring only a response of the other participant compared to Both NoGo stimuli requiring withholding the response by both participants. Also, more errors and a reduced ERN were present on erroneous responses in situations, where only the other participant had to respond, compared to the situation, where both participants had to inhibit. Moreover, significant interactions with competitive response strategy revealed that response inhibition and the error rate of fast responders were least affected by shared action representations. We will first discuss these results separately and then later integrate them into an overall conclusion.

4.1 Response inhibition: NoGo P3

The smaller NoGo P3 on Self NoGo stimuli

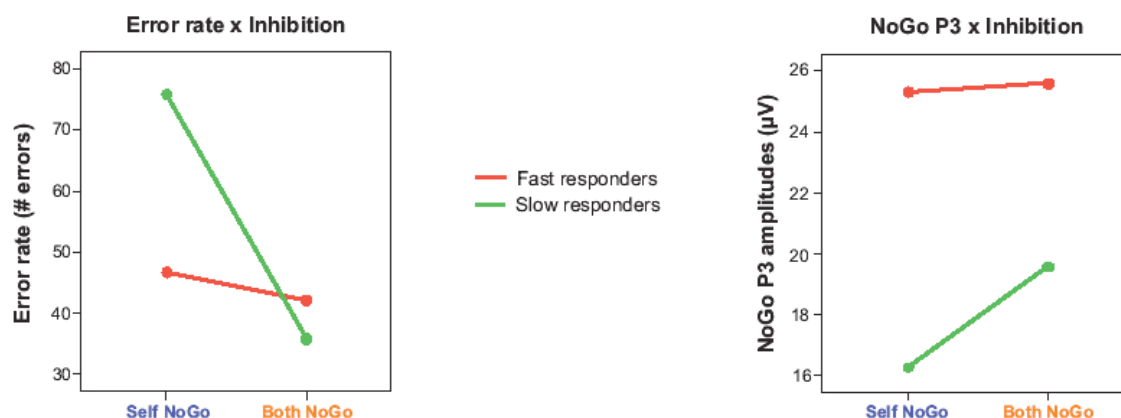


Figure 5. Left panel: Error rate x inhibition interaction effect, Right panel: NoGo P3 x inhibition interaction effect.

compared to Both NoGo stimuli provides evidence that differences in co-representation modulate the process of response inhibition. The NoGo P3 was maximal at central electrodes, which is in line with the more frontal orientation of the component (Pfefferbaum et al., 1984, Falkenstein et al., 1995). Apparently, participants issue less response inhibition on trials that require a response of the other person compared to trials that require an inhibition of both participants. Since the own task representation is the same in both conditions, viz. to inhibit a response, the current outcome can only be explained by the difference in task of the other person. This result indicates that along with the own task representation, the co-representation of the other participant's task affects the process of response inhibition, as reflected in the NoGo P3. This finding is in line with Sebanz et al. (2006) who recently showed a more general increase in NoGo P3 when comparing a joint condition to a single condition. The current study demonstrates that differences in co-representation even affect response-inhibition processes within a joint condition.

4.2 Error monitoring: behavioural results and ERN

The finding that participants make less errors on stimuli that require an inhibition of both participants is probably directly related to the higher amount of response inhibition that is issued in this condition, thus less frequently leading to incorrect responses. The finding of an increased ERN after an error on Both NoGo trials compared to an error on Self NoGo trials shows that co-representation also affects the process of error detection as

reflected in the ERN. Although Hajcak et al. (2005) demonstrated a more general ERN effect caused by observation, until now no studies have demonstrated influences of co-representational differences on error detection. Apparently, the impact of an error was higher when an error is made in the situation where both participants had to withhold their response. Two possible explanations exist for the higher impact of an error in the situation that requires the inhibition of both participants. First, according to the mismatch theory of the ERN (Coles, Scheffers, and Holroyd, 2001; Falkenstein et al., 1991; 1995; Gehring et al., 1993), making an erroneous response in the Both NoGo situation the error could reflect a mismatch to the own task representation (to inhibit) and a mismatch to the co-representation of the other person's task (other has to inhibit). An error in the Self NoGo situation mismatches only with the own task representation (to inhibit), but matches with the co-representation of the other person's task (the other has to respond). The higher amplitude of the ERN in the Both NoGo situation could thus reflect this larger mismatch between the representation of your own action and that of the other person. Second, our results are in line with an affective interpretation of the ERN (Gehring & Willoughby, 2002) stating that the ERN reflects an emotional response to an error. In the current experiment, inhibiting a response was obviously more difficult than responding. Thus, erroneous responding in the situation that required the inhibition of both participants could lead to a higher affective response associated with the committed error, because participants are aware that the other person did succeed in performing the same difficult job of inhibiting. An error in the condition that requires

only a response of the other participant may be associated with a lower emotional impact, due to the knowledge that the other participant had an easy task to perform. Responding erroneously while knowing that the other participant will probably succeed in a difficult situation may lead to an enhancement of the emotional response associated with the error, compared to committing an error while knowing that the other participant will probably do well in an easy situation.

We would like to point out that the higher amplitude of the ERN in the Both NoGo condition might be caused by the higher error rate in the Self NoGo condition compared to the Both NoGo condition. However, the significant interaction with competitive response strategies shows that only slow responders were responsible for the higher error rate in the Self NoGo condition. Therefore we would expect differences in ERN between the Self NoGo and Both NoGo condition also to be modulated by slow vs. fast responders – but this was not the case.

4.3 Competitive response strategies

The outcome that response inhibition and the accuracy of fast responders were least affected by shared action representations shows that employing a more competitive response strategy implies ignoring the other participant's task. This is also shown in a study of Georgiou et al. (2006), who found different action patterns for cooperative and competitive task settings. Kinematic patterns were different in tasks where two participants had to cooperate to join two objects in the middle of a working surface compared to tasks where participants had to compete to place the object first in the middle of a working surface. The authors argue that actions are planned differently depending on their underlying global intention, such as cooperation and competition. With respect to our study the argument that different sensory events in fast and slow responders related to response processing cause the inhibition x response strategy interaction can be ruled out because the NoGo P3 component was measured with respect to the moment of stimulus onset. This means that sensory events related to responses of subjects occur at different time points after stimulus onset and averaged to zero while calculating the NoGo P3 component.

Interestingly, in our experiment the error-detection process reflected by the ERN was not

modulated by the extent of competitive response strategy. This means that when an error was made fast responders and slow responders did not differ in the process of error detection. The current results strongly suggest that a clear dissociation exists between the influence of response strategies on error prevention, reflected in response inhibition, and error detection. The dissociation can be interpreted in the way that a level of competition is set as a goal and influence the process of error prevention but not the process of error detection. An explanation could be that only perfect behaviour was planned in terms of a response strategy, but making an error could have had disrupted such a global intention – the error was there, not expected and people, regardless of their response strategy, had to deal with it in the same way.

5. Conclusion

We conclude that different co-representations in a joint task lead to specific modulations of action-monitoring processes. Interestingly, due to the goal-directed nature of response strategies, the response strategies people employ in a competitive setting only affect the process of error prevention. In everyday life, co-representation of the co-actor's task provides an additional source of information that may be used to support human's decisions whether to act or to refrain from acting. Future research on joint action monitoring will be necessary to provide a deeper understanding of the neuronal correlates underlying the extent the faster one has blinkers on.

Acknowledgements

The authors would like to thank Mathieu Koppen for helpful advice.

References

- Bokura, H., Yamaguchi, S., Kobayashi, S. (2005). Event-related potentials for response inhibition in Parkinson's disease. *Neuropsychologia*, 43, 967-975.
- Botvinick, M.M., Cohen, J.D., & Carter, C. (2004). Conflict monitoring and anterior cingulate cortex: an update. *Trends in Cognitive Sciences*, 8, 539-546.
- Coles, M.G., Scheffers, M.K. & Holroyd, C.B. (2001). Why is there an ERN/Ne on correct trials? Response

- representations, stimulus-related components, and the theory of error-processing. *Biological Psychology*, 56, 173-189.
- Decety, J., Jackson, P.L., Sommerville, J.A., Chaminade, T., & Meltzoff, A.N. (2004). The neural bases of cooperation and competition: an fMRI investigation. *NeuroImage*, 23, 744-751.
- Donkers, F.C.L., & Boxtel, G.J.M. (2004). The N2 in go/no-go tasks reflects conflict monitoring not response inhibition. *Brain and Cognition*, 56, 165-176.
- Falkenstein, M., Hohnsbein, J., Hoormann, J., & Blanke, L. (1991). Effects of cross-modal divided attention on late ERP components: II. *Electroencephalography and clinical Neurophysiology*, 78, 447-455.
- Falkenstein, M., Koshlykova, N.A., Kiroj, V.N., Hoormann, K.J., & Hohnsbein, J. (1995). Late ERP components in visual and auditory Go/Nogo tasks. *Electroencephalography and clinical Neurophysiology*, 96, 36-43.
- Gehring, W.J., Goss, B., Coles, M.G.H., Meyer, D.E., & Donchin, E. (1993). A neural system for error detection and compensation. *Psychological Science*, 4, 385-390.
- Georgiou, I., Becchio, C., Glover, S., & Castiello, U. (in press). Different action patterns for cooperative and competitive behaviour. *Cognition*.
- Gratton, G., Coles, M.G., & Donchin, E. (1983). A new method for off-line removal of ocular artifact. *Electroencephalography and clinical Neurophysiology*, 55, 468-484.
- Hajcak, G., Moser, J.S., Yeung, N., & Simons, R.F. (2005). On the ERN and the significance of errors. *Psychophysiology*, 42, 151-160.
- Nieuwenhuis, S., & Yeung, N. (2003). Electrophysiological correlates of anterior cingulate function in a go/no-go task: Effects of response conflict and trial type frequency. *Cognitive, Affective, & Behavioral Neuroscience*, 3 (1), 17-26.
- Pfefferbaum, A., Ford, J.M., Weller, B.J., Kopell, B.S. (1984). ERPs to Response Production and Inhibition. *Electroencephalography and clinical Neurophysiology*, 60, 423-434.
- Prinz, W. (1997). Perception and Action Planning. *European Journal of Cognitive Psychology* 9 (2), 129-154.
- Ramnani, N. & Miall, R.C. (2004). A system in the human brain for predicting the actions of others. *Nature Neuroscience*, 7, 85-90.
- Ridderinkhof, K.R., Ullsperger, M., Crone, E., & Nieuwenhuis, S. (2004). The Role of the Medial Frontal Cortex in Cognitive Control. *Science*, 306, 443-447.
- Sebanz, N., Knoblich, G., & Prinz, W. (2003). Representing others' actions: just like one's own? *Cognition*, 88, B11-B21.
- Sebanz, N., Bekkering, H., & Knoblich, G. (2006). Joint action: Bodies and minds moving together. *Trends in Cognitive Science*, 10 (2), 70-76.
- Sebanz, N., Knoblich, G., & Prinz, W. (2005). How Two Share a Task: Corepresenting Stimulus-Response Mappings. *Journal of Experimental Psychology: Human Perception and Performance* 31 (6), 1234-1246.
- Sebanz, N., Knoblich, G., Prinz, W., & Wascher, E. (in press). Twin Peaks: An ERP study of action planning and control in co-acting individuals. *Journal of Cognitive Neuroscience*.
- van Schie, H.T., Mars, R.B., Coles, M.G.H., & Bekkering, H. (2004). Modulation of activity in medial frontal and motor cortices during error observation. *Nature Neuroscience* 7, 549-554.

Abstracts

Nijmegen CNS committed to publish all submitted thesis. However, due to the number of submissions, we make a selection based on the recommendations by the editors. Submissions that are not part of the print version can be found on the website (<http://www.cns.ru.nl/nijmegencns>). Below, as a special service to the interested reader, we provide the abstracts of the theses that are published only in the online version.

What the electrocorticogram can tell us about the electroencephalogram

Denise van Barneveld, Supervisors: Stan Gielen, Thom Oostendorp, Peter Desain

Although brain signals measured under the skull (electrocorticogram, ECoG) and signals measured on top of the scalp (electroencephalogram, EEG) stem from the same brain activity, they are different. We investigated how we can produce EEG when we know ECoG (“forward problem”) and how we can produce ECoG when we know EEG (“inverse problem”). We modeled the head as three concentric spheres, representing the brain, skull and scalp. Brain activity is simulated by a dipole.

The forward method links the ECoG potentials on the inner sphere to the EEG potentials on the outer sphere via a transfer matrix, based on the geometries and the conductivities of tissues involved. Results showed that the error between analytically computed EEG and EEG produced from analytically produced ECoG with the forward method, is smaller at electrodes close to the source, compared to electrodes far away from the source. The higher the resolution of an ECoG electrode grid, the better the forward model works. Another finding was that the forward model is more accurate for surface sources, compared to deep sources. This result is of practical importance, since most cognitive interesting sources stem from the cortex (the outermost layer of the brain).

In the inverse model, the transfer matrix is inverted and additional regularization constraints are applied to compute ECoG from simulated EEG. We showed that the inverse model gives good results.

The forward method is tested with data measured from an epileptic patient at the University of Freiburg. Results show that the forward model gives better results at the EEG electrode overlying the ECoG grid compared to the electrode posterior to the grid.

Further research is needed to make errors smaller.

The Interplay of Prosody and Syntax in Sentence Processing: Two ERP-studies

Sara Bögels, Supervisors: Herbert Schriefers, Dorothee Chwilla, Roel Kerkhofs

In earlier studies, which were mostly reading studies, it has become clear that not only syntax but also other factors such as semantics and discourse context play an important role in sentence processing. Much less research has been done to investigate auditory sentence comprehension, although this is by far the most common way of human communication. The focus of the present study, prosody, is unique to *auditory* sentence processing. ERPs are presumably the best method to investigate auditory sentence comprehension, because they are the only straightforward, online method available. In this thesis, two experiments are described that used two different types of locally ambiguous sentences to investigate the role of prosody in sentence processing.

In Experiment 1, as a follow-up on Kerkhofs et al. (submitted-a), sentences with an NP/S-coordination ambiguity with and without a prosodic break (PB) were used (see sentences 1 and 2).

1. The mannequin kissed the designer (PB) and the photographer on the party. (NP)
2. The mannequin kissed the designer (PB) and the photographer opened a bottle of Champaign. (S)

According to late closure, the NP-coordination sentence should be preferred. However, we hypothesized that the PB could reverse this preference. At the PB, a Closure Positive Shift (CPS) was found, replicating Kerkhofs et al. Comparing the S-coordination sentences with and without a PB at the disambiguation point (*opened*), a mid-frontal P600 effect, which indicated processing difficulty, was found throughout the

experiment. This result was different from Kerkhofs et al., who found a LAN-effect in the first half of their experiment. This difference could have been caused by a different ratio of items in the different conditions in the two studies. Comparing the NP-coordination sentences with and without a PB at the disambiguation point (*on the party*), a comparison that was not included in Kerkhofs et al., a mid-posterior P600 effect was found for the sentences with a PB, but only in the first half of the experiment. This asymmetrical pattern of effects is difficult to interpret. One possible explanation is that participants came to regard sentences with a PB in a special way in the course of the experiment.

In Experiment 2, as a follow-up on Steinhauer et al. (1999), sentences with another type of late closure ambiguity with and without a PB were used (see sentences 3 and 4).

3. De verpleegster hielp (PB) de zieke te lopen...
The nurse helped the patient to walk...
4. De verpleegster hielp (PB) de zieke te vervoeren...
The nurse helped to transport the patient...

According to late closure, sentence 3 should be preferred because *de zieke* (the patient) is the object of the previous verb *hielp* (helped). However, we hypothesized that a PB after *hielp* could reverse this preference. At the PB, the ERPs showed a CPS, which replicates Steinhauer et al. Comparing the sentences with a PB at the disambiguation point, an N400 effect was found for the condition with a mismatch between prosody and syntax (3). This contrasts with Steinhauer et al. who found a biphasic N400/P600 response in a similar comparison in German. The fact that we only find an N400 effect (without a P600) suggests that here, the PB is such a strong cue for a certain syntactic parse, that - in case of a mismatch - the disambiguating verb is picked up as a semantic anomaly, without triggering a revision of the incorrect syntactic analysis. Comparing the sentences without a PB at the disambiguation point, a LAN-like effect for the mismatch condition (4) was found, but only in the first half of the experiment. This suggests that listeners can use the absence of a PB in a strategic way while this appears to be impossible for the presence of a PB.

Overall the results suggest that the CPS is a reliable indicator of a PB. At the disambiguation point, the results of the two experiments are quite different. Both experiments show that prosody can influence the decision to analyze the sentence in a certain way, at least initially. Furthermore, the differences between the results of the two experiments make clear that the nature of processing difficulty in late closure sentences depends on the precise nature of the structures themselves.

Language lateralization in healthy people with Auditory Verbal Hallucinations: A pilot study

Kelly Diederer, Supervisors: Iris Sommer, Indira Tendolkar

Language lateralization in schizophrenia has been reported to be decreased, which is due to increased language activity of the right hemisphere. Furthermore increased right hemisphere language activity is correlated to the severity of auditory verbal hallucinations (AVH) in schizophrenia, and could possibly be a predisposing factor for AVH. However, schizophrenia is a complex syndrome consisting of psychotic, cognitive and negative symptoms. In order to learn whether decreased lateralization plays a causal role in the pathophysiology of AVH, the isolated form of AVH should be investigated, which can be found in healthy subjects with AVH. Language lateralization was measured in 10 healthy subjects with AVH and compared to 10 schizophrenia patients and 10 healthy controls matched for age, handedness and education. Subjects were scanned while covertly performing a paced letter fluency task. A significant main effect for group was revealed with respect to the right hemisphere. This was due to increased activation in the right hemisphere of the schizophrenia patients relative to the healthy controls. Differences in language lateralization between schizophrenia patients, healthy subjects with AVH and healthy controls did not reach significance. However, mean lateralization indices were lower in both hallucinating groups. This difference is likely to become significant when sample size increases.

Localisation Techniques to improve Analysis for BCI

Rianne Hupse, Supervisors: Peter Desain and Stan Gielen

An experiment is described to explore the possibility to elaborate a new type of brain computer interface (BCI) system: a system in which selective attention to rhythmic tactile stimuli is used to control an external device. It is known that temporal rhythmic tactile stimuli induce a steady-state somatosensory evoked potential oscillating at the same temporal frequency as the driving stimulus. The amplitude of this oscillation increases when the subject is attending to the stimulus. This attention induced power gain can be detected in the EEG (electroencephalogram) and might be translated into commands for a computer or other device. Because EEG data has a small signal to noise ratio, it is investigated if a beamformer spatial filter improves the classification success rates. To be sure that the beamformer filter allocates activity to the correct anatomical locations, a new method is proposed to construct realistic head models. During the experiment, tactile stimuli with different temporal frequencies are presented to the left and right index finger of a subject. The subject is instructed to attend to one finger and to ignore the sensations of the other finger. Perception conditions, in which only one finger was stimulated, were included as a baseline. Single trial EEG and voxel data was used in a classification algorithm to detect which finger was attended. Classification rates are relatively high ($\pm 90\%$) for perception conditions, while selective attention conditions give success rates below chance level. An explanation for this can be that the attention induced power gain is too small to be detected in single trials. Results show that beamforming allocates the frequencies presented to left and right index finger to separate areas of the brain. This is in contrast to electrode data, in which the two frequencies reach electrodes at both sides of the scalp. Therefore, by using the beamformer filter the power of a single stimulus is focused to a single area which will increase the signal to noise ratio. However, classification success rates show no improvements when the beamformer filter is used. A suggestion for further research is to include a discrimination task in the experiment which

might increase the attention level of the subject and therefore the attention induced power gain. The amount of trials can be increased that is used as a training set in the cross validation procedure of the classification algorithm. Furthermore, the amount of trials used for estimating the covariance between the sensors, which is necessary for building the beamformer filter, might improve the results. More experiments are necessary to investigate if the results described here are representative to sessions with other subjects.

Auditory Selective Attention as a method for a Brain Computer Interface

Michiel Kallenberg, Supervisors: Peter Desain, Stan Gielen

The object of this study was to design a Brain Computer Interface (BCI) based on auditory selective attention (ASA). ASA is a promising paradigm for a BCI, as focusing attention does not require a lot of training, whereas the possibility of offering a large number of possible targets facilitates a high bit rate. In this study subjects focused attention on one tone out of two. The two tones were separated in space and pitch, and each tone was frequency tagged by means of amplitude modulation (AM). AM tones are known to evoke an auditory steady state response (ASSR) at the am frequency, and previous research has demonstrated that the power of this ASSR is increased by selective attention.

To detect the direction of the subject's attention, features were calculated that characterized the ASSR. Subsequently, a classifier was trained based on linear discriminant analysis.

The best results were obtained with a feature that consisted of the real and imaginary parts of the Fourier transformed signal at the am-frequency. Electrodes above the auditory cortices yielded the best results. On perception data, single trial classification reached a classification rate of 80%. On attention data, the best classification rate was 68%.

The current BCI achieved a bit rate of 3.78 bits/min, which is moderate compared to other BCI-systems. We will discuss several procedures for improvement.

Contextual memory in patients remitted from their first episode of depression: An fMRI study

Sara Pieters, Supervisors: Indira Tendolkar, Philip van Eijndhoven, Guillen Fernandez

Background: Memory problems are a well known symptom of major depressive disorder (MDD). Recollection of past experiences is thought to be more impaired than familiarity in MDD. We investigated whether these memory problems are still persistent in remission. Furthermore, we tried to delineate the neural correlates of memory processing in remission.

Methods: 13 remitted patients (non medicated, remitted from first episode) and 13 matched controls participated in a contextual memory task while lying in a fMRI scanner.

Results: Behavioural performance did not differ between remitted patients and controls. We did find a difference between remitted patients and controls in brain activation during encoding.

Conclusions: Although the sample size is small, there is striking evidence that MDD patients even when being in remission from their first episode already form declarative memories differently.

Neural Correlates of Masking

Martijn Schippers, Supervisors: Jens Schwarzbach, Peter Hagoort

This study looks at the phenomenon of visual masking. When two stimuli are presented in rapid succession the perception of one can be blocked by the perception of the other, depending on the timing and features of the stimuli used. There is currently an open discussion as to whether this effect is neurally limited to brain activity in the primary visual areas or whether it also extends to higher parts of the brain. We try to determine the neural correlates of visual masking by showing where in the brain there is a significant difference between consciously (unmasked) and not consciously (masked) perceived stimuli.

Two behavioral experiments were performed to determine the optimal stimulus-setup and stimulus-timing for masking effects. The optimal settings found were used in an fMRI experiment. The stimulus visibility was measured while manipulating the time between the start of the stimulus and the start of the mask. This Stimulus Onset Asynchrony (SOA) influences the visibility of the stimulus in a manner that looks like a U-shape (high visibility at short and long SOAs, low visibility in between). We added a control condition where we replaced the mask with a non-masking, but physically almost identical shape. As this control shape does not mask, the SOA should not influence visibility, and hence a U-shape should not occur when plotting visibility versus SOA. These two differently shaped masking functions make it possible to attribute differences in brain activity (as measured by fMRI) to a difference in visibility.

As our behavioural data in the scanner did not lead to such opposing masking functions, the found brain activity differences could not be attributed to an effect of masking. We did find activity in the primary visual cortex, the left angular gyrus and extrastriate cortex and the left superior temporal gyrus, but this data can only be taken as an indication where activity might be found in a study where the behavioural data is significantly different. As we present this study as a pretest for such a more elaborately controlled experiment, we present some suggestions as to how this level of control over the masking effect can be achieved.

The effect of fame as a context: An fMRI study

Gitty Smit, Supervisors: Guillen Fernandez, Vasily Klucharev, Ale Smidts

Over the past decades there has been an increase of celebrities in advertising, but there is still a huge variance in the effectiveness of celebrities in advertising. Previous studies (Klucharev et al., 2006; Rossiter and Smidts, 2006) have shown that memory and attitudes of a product increases when the famous presenter is an expert on the presented product. To study the mechanisms of effective use of famous presenters in advertising we simulated advertising and studied the modulation of memory and attitudes for products with fame as a context. We presented 24 female subjects with photos of products (shoes) coupled to famous and non-famous faces. To contrast effects of presenters' attractiveness and expertise as well as

specific item characteristics, we equated attractiveness and used only shoes as stimuli. During this task we recorded brain activity via fMRI. We found a substantial behavioural effect of fame on memory for the products; more products coupled to famous faces were remembered. Turning to the neural underpinnings of this behavioural effect, we found a subsequent memory effect x fame interaction in the thalamus. Moreover, we found a main effect of fame in left frontal and temporal regions, which are commonly seen during semantic processing and a positive emotional encoding context. Celebrities trigger semantic knowledge and can be seen as a positive emotional encoding context. Behaviourally they increase memory for the products presented. It seems that using a celebrity in advertising increases brand awareness and memory of the advertised product by increasing elaboration and positive emotional processing of the advertised product such that brand awareness increases.

Institutes associated with the Master's Programme in Cognitive Neuroscience



F.C. Donders Centre for Cognitive Neuroimaging
Kapittelweg 29
6525 EN Nijmegen

P.O. Box 9101
6500 HB Nijmegen
<http://www.ru.nl/fcdonders>



MAX-PLANCK-GESELLSCHAFT

Max Planck Institute for Psycholinguistics
Wundtlaan 1
6525 XD Nijmegen

P.O. Box 310
6500 AH Nijmegen
<http://www.mpi.nl>



Radboud Universiteit Nijmegen
Comeniuslaan 4
6525 HP Nijmegen

P.O. Box 9102
6500 HC Nijmegen
<http://www.ru.nl>



Nijmegen Institute for Cognition and Information
Montessorilaan 3
6525 HR Nijmegen

P.O. Box 9104
6500 HE Nijmegen
<http://www.nici.ru.nl>



Universitair Medisch Centrum St Radboud
Geert Grooteplein-Zuid 10
6525 GA Nijmegen

P.O. Box 9101
6500 HB Nijmegen
<http://www.umcn.nl>

